

# Using Generalised Dissimilarity Modelling to assess potential impacts of climate change on biodiversity composition in Australia, and on the representativeness of the National Reserve System

Climate Adaptation Flagship Working Paper #13E

Simon Ferrier, Tom Harwood, Kristen J Williams and Michael Dunlop

September 2012



## National Library of Australia Cataloguing-in-Publication entry

Title:	Using Generalised Dissimilarity Modelling to assess potential impacts of climate change on biodiversity composition in Australia, and on the representativeness of the National Reserve System / Simon Ferrier
ISBN:	978-1-4863-0217-8 (pdf)
Series:	CSIRO Climate Adaptation Flagship working paper series; 13E.
Other Authors/Contributors:	Climate Adaptation Flagship, Tom Harwood, Kristen J Williams and Mike Dunlop

### Enquiries

Enquiries regarding this document should be addressed to:

Simon Ferrier

CSIRO Ecosystem Sciences

Black Mountain Laboratories, Clunies Ross Street, Black Mountain ACT 2601, Australia

[Simon.Ferrier@csiro.au](mailto:Simon.Ferrier@csiro.au)

Enquiries about the Climate Adaptation Flagship or the Working Paper series should be addressed to:

Working Paper Coordinator

CSIRO Climate Adaptation Flagship

[CAFworkingpapers@csiro.au](mailto:CAFworkingpapers@csiro.au)

### Citation

Ferrier S, Harwood T, Williams KJ and Dunlop M (2012) *Using Generalised Dissimilarity Modelling to assess potential impacts of climate change on biodiversity composition in Australia, and on the representativeness of the National Reserve System*. CSIRO Climate Adaptation Flagship Working Paper No. 13E.

[www.csiro.au/resources/CAF-working-papers](http://www.csiro.au/resources/CAF-working-papers)

### Copyright and disclaimer

© 2012 CSIRO To the extent permitted by law, all rights are reserved and no part of this publication covered by copyright may be reproduced or copied in any form or by any means except with the written permission of CSIRO.

### Important disclaimer

CSIRO advises that the information contained in this publication comprises general statements based on scientific research. The reader is advised and needs to be aware that such information may be incomplete or unable to be used in any specific situation. No reliance or actions must therefore be made on that information without seeking prior expert professional, scientific and technical advice. To the extent permitted by law, CSIRO (including its employees and consultants) excludes all liability to any person for any consequences, including but not limited to all losses, damages, costs, expenses and any other compensation, arising directly or indirectly from using this publication (in part or in whole) and any information or material contained in it.

## **The Climate Adaptation Flagship Working Paper series**

The CSIRO Climate Adaptation National Research Flagship has been created to address the urgent national challenge of enabling Australia to adapt more effectively to the impacts of climate change and variability.

This working paper series aims to:

- provide a quick and simple avenue to disseminate high-quality original research, based on work in progress
- generate discussion by distributing work for comment prior to formal publication.

The series is open to researchers working with the Climate Adaptation Flagship on any topic relevant to the Flagship's goals and scope.

Copies of Climate Adaptation Flagship Working Papers can be downloaded at:

[www.csiro.au/resources/CAF-working-papers](http://www.csiro.au/resources/CAF-working-papers)

*CSIRO initiated the National Research Flagships to provide science-based solutions in response to Australia's major research challenges and opportunities. Flagships form multidisciplinary teams with industry and the research community to deliver impact and benefits for Australia.*



# Contents

Acknowledgements .....	vi
Executive summary.....	vii
1 Introduction .....	1
2 Derivation of GDM models.....	4
3 Selection and downscaling of climate scenarios.....	5
4 Whole-landscape analysis of biotically scaled environmental stress .....	6
4.1 Potential change on a cell-by-cell basis .....	6
4.2 Disappearing and novel environments .....	28
4.3 Potential for landscape buffering .....	31
4.4 Potential change in ‘effective habitat area’ .....	37
4.5 Added effects of habitat loss and fragmentation .....	42
5 Analysis of NRS representativeness under climate change .....	46
6 Conclusion .....	50
References .....	51
Appendix A GDM models used in the NRS2 project .....	53

# Figures

Figure 1 Major steps in the GDM-modelling component of the NRS2 project .....	2
Figure 2 Illustration of how the GDM model is constructed with current environmental layers and observed species compositional patterns, and how it is then used to project biotically scaled environmental stress.....	3
Figure 3a Predicted dissimilarity between the current composition of each 1 km <sup>2</sup> grid cell and its potential composition under each of the 2030 climate scenarios, for vascular plants .....	7
Figure 3b Predicted dissimilarity between the current composition of each 1 km <sup>2</sup> grid cell and its potential composition under each of the 2070 climate scenarios, for vascular plants .....	8
Figure 4a Predicted dissimilarity between the current composition of each 1 km <sup>2</sup> grid cell and its potential composition under each of the 2030 climate scenarios, for land snails .....	9
Figure 4b Predicted dissimilarity between the current composition of each 1 km <sup>2</sup> grid cell and its potential composition under each of the 2070 climate scenarios, for land snails .....	10
Figure 5a Predicted dissimilarity between the current composition of each 1 km <sup>2</sup> grid cell and its potential composition under each of the 2030 climate scenarios, for amphibians .....	11
Figure 5b Predicted dissimilarity between the current composition of each 1 km <sup>2</sup> grid cell and its potential composition under each of the 2070 climate scenarios, for amphibians .....	12
Figure 6a Predicted dissimilarity between the current composition of each 1 km <sup>2</sup> grid cell and its potential composition under each of the 2030 climate scenarios, for reptiles .....	13
Figure 6b Predicted dissimilarity between the current composition of each 1 km <sup>2</sup> grid cell and its potential composition under each of the 2070 climate scenarios, for reptiles.....	14
Figure 7a Predicted dissimilarity between the current composition of each 1 km <sup>2</sup> grid cell and its potential composition under each of the 2030 climate scenarios, for birds .....	15
Figure 7b Predicted dissimilarity between the current composition of each 1 km <sup>2</sup> grid cell and its potential composition under each of the 2070 climate scenarios, for birds .....	16
Figure 8a Predicted dissimilarity between the current composition of each 1 km <sup>2</sup> grid cell and its potential composition under each of the 2030 climate scenarios, for mammals .....	17
Figure 8b Predicted dissimilarity between the current composition of each 1 km <sup>2</sup> grid cell and its potential composition under each of the 2070 climate scenarios, for mammals .....	18
Figure 9a Predicted dissimilarity between the current composition of each 1 km <sup>2</sup> grid cell and its potential composition under each of the 2030 climate scenarios – weighted average of the results for all six biological groups, where each group is weighted according to the total amount of spatial turnover exhibited by the group under current climate conditions .....	19
Figure 9b Predicted dissimilarity between the current composition of each 1 km <sup>2</sup> grid cell and its potential composition under each of the 2070 climate scenarios – weighted average of the results for all six biological groups, where each group is weighted according to the total amount of spatial turnover exhibited by the group under current climate conditions .....	20
Figure 10 Location of the IBRA bioregions used in this analysis .....	21
Figure 11a Mean predicted dissimilarity between the current composition of each 1 km <sup>2</sup> grid cell and its potential composition under each of 2030 scenarios, as an average for each of the IBRA bioregions – for vascular plants.....	23
Figure 11b Mean predicted dissimilarity between the current composition of each 1 km <sup>2</sup> grid cell and its potential composition under each of 2070 scenarios, as an average for each of the IBRA bioregions – for vascular plants.....	24

Figure 12a Mean predicted dissimilarity between the current composition of each 1 km <sup>2</sup> grid cell and its potential composition under each of 2030 scenarios, as an average for each of the IBRA bioregions – weighted average of the results for all six biological groups, where each group is weighted according to the total amount of spatial turnover exhibited by the group under current climate conditions .....	25
Figure 12b Mean predicted dissimilarity between the current composition of each 1 km <sup>2</sup> grid cell and its potential composition under each of 2070 scenarios, as an average for each of the IBRA bioregions – weighted average of the results for all six biological groups, where each group is weighted according to the total amount of spatial turnover exhibited by the group under current climate conditions .....	26
Figure 13 Disappearing biotically scaled environments under 2070 medium-impact and high-impact scenarios, based on the vascular plant GDM. The colours depict different levels of minimum predicted dissimilarity between the current composition of each cell and the potential future composition of all cells on the continent for this scenario .....	29
Figure 14 Novel biotically scaled environments under 2070 medium-impact and high-impact scenarios, based on the vascular plant GDM. The colours depict different levels of minimum predicted dissimilarity between the potential future composition of each cell and the current composition of all cells on the continent for this scenario .....	30
Figure 15 Potential buffering of environmental heterogeneity in the landscape within 6.25 km under 2070 medium-impact and high-impact scenarios, based on the vascular plant GDM .....	32
Figure 16 Potential buffering of environmental heterogeneity in the landscape within 12.5 km under 2070 medium-impact and high-impact scenarios, based on the vascular plant GDM .....	33
Figure 17 Potential buffering of environmental heterogeneity in the landscape within 50 km under 2070 medium-impact and high-impact scenarios, based on the vascular plant GDM .....	34
Figure 18 Potential buffering of environmental heterogeneity in the landscape within 100 km under 2070 medium-impact and high-impact scenarios, based on the vascular plant GDM .....	35
Figure 19 Potential buffering effects of environmental heterogeneity in the landscape within 6.25 km and 25 km under 2070 high-impact scenario based on the vascular plant GDM. Close up of the south-eastern corner of Australia and of Tasmania, illustrating topographic buffering effects .....	36
Figure 20 Change in the effective habitat area within 6.25 km for both 2070 medium-impact and high-impact scenarios based on the vascular plants GDM. Browns indicate a reduction, pale green (value of 1 in the legend) indicates no change, and darker greens an increase in effective habitat area.....	38
Figure 21 Change in the effective habitat area within 12.5 km for both 2070 medium-impact and high-impact scenarios based on the vascular plants GDM. Browns indicate a reduction, pale green (value of 1 in the legend) indicates no change, and darker greens an increase in effective habitat area.....	39
Figure 22 Change in the effective habitat area within 100 km for both 2070 medium-impact and high-impact scenarios based on the vascular plants GDM. Browns indicate a reduction, pale green (value of 1 in the legend) indicates no change, and darker greens an increase in effective habitat area.....	40
Figure 23 Change in effective habitat area in the landscape within 6.25 km and 25 km under 2070 high-impact scenario based on the vascular plants GDM. Close up of the south-eastern corner of Australia and of Tasmania, illustrating topographic buffering effects .....	41
Figure 24 Current (extant) distribution of native vegetation in Australia derived from the National Vegetation Information System (NVIS) version 3.1 (Williams et al. 2010) as used in subsequent analyses ...	42
Figure 25 Change in effective habitat area within a 50 km radius under 2070 medium-impact scenario, based on the vascular plant GDM, with (top) and without (bottom) the effects of habitat loss applied .....	43
Figure 26 Change in effective habitat area within a 50 km radius under 2070 high-impact scenario, based on the vascular plant GDM, with (top) and without (bottom) the effects of habitat loss applied .....	44

Figure 27 Areas where restoration would enhance the effective habitat area of present biotically scaled environments under future climate for the vascular plant GDM. Greens indicate little benefit to restoration, and largely show land in good condition. Pinks indicate maximum benefit. Note that these are fewer in the high-impact scenario, due to the generally less suitable habitat.....	45
Figure 28 The extent to which the reserve system (CAPAD 2006) is representative of the present environment based on the vascular plant GDM. The index shows the proportion of the present continental distribution of each biotically scaled environment which is covered by the reserve system. Orange colours indicate poor representation, and blues better representation .....	47
Figure 29 The extent to which the NRS under future climate scenarios is representative of the present environment based on the vascular plant GDM. The index shows the proportion of the present continental distribution of each biotically scaled environment that is covered by the NRS under future climate .....	48
Figure 30 The extent to which the NRS under future climate scenarios is representative of the future environment based on the vascular plant GDM. The index shows the proportion of the future continental distribution of each biotically scaled environment that is covered by the NRS under future climate .....	49
Apx Figure A.1 Location of vascular plant sites (0.01° grids) used for GDM analysis showing bioregion boundaries (IBRA 6.1).....	55
Apx Figure A.2: Location of mammal sites (0.01° grids) used for GDM analysis showing bioregion boundaries (IBRA 6.1).....	55
Apx Figure A.3 Location of birds sites (0.01° grids) used for GDM analysis showing bioregion boundaries (IBRA 6.1) .....	56
Apx Figure A.4 Location of reptile sites (0.01° grids) used for GDM analysis showing bioregion boundaries (IBRA 6.1).....	56
Apx Figure A.5 Location of frog sites (0.01° grids) used for GDM analysis showing bioregion boundaries (IBRA 6.1).....	57

## Tables

Table 1 Mean predicted dissimilarity between the current composition of each 1 km <sup>2</sup> grid cell and its potential composition under each of the four climate scenarios, as an average for the whole continent – summary of all groups .....	6
Table 2 Mean predicted dissimilarity between the current composition of each 1 km <sup>2</sup> grid cell and its potential composition under each of the four climate scenarios (years 2030, 2070 and change rates M, A1B medium climate sensitivity and H, A1FI high climate sensitivity) as an average for the whole continent (Mean) and for each of the IBRA bioregions – for vascular plants .....	22
Table 3 Mean predicted dissimilarity between the current composition of each 1 km <sup>2</sup> grid cell and its potential composition under each of the four climate scenarios (years 2030, 2070 and change rates M, A1B medium climate sensitivity and H, A1FI high climate sensitivity), as an average for the whole continent (Mean) and for each of the IBRA bioregions – weighted average of the results for all six biological groups, where each group is weighted according to the total amount of spatial turnover exhibited by the group under current climate conditions .....	27
Apx Table A.1 Summary of ANHAT data available for the biological groups used in the NRS2 project .....	54
Apx Table A.2 Filters used to customise queries by spatial precision and IBRA region for each biological group .....	54
Apx Table A.3 Substrate and terrain attributes.....	58
Apx Table A.4 Climate attributes.....	59
Apx Table A.5 Vegetation attributes .....	60
Apx Table A.6 Predictor variables and summed fitted coefficients for final models for each taxa group.....	61

# Acknowledgements

We thank Janet Stein, ANU Fenner School for Environment and Society, for providing spatial layers for a number of the environmental predictors employed in this study. We also thank Mike Hutchinson and Tingbao Xu of ANU Fenner School for Environment and Society for providing the ANUCLIM 6 software in its pre-release format and for expert advice.

The project was supported by all Australian governments through the Climate Change in Agriculture and NRM (CLAN) Working Group of the Natural Resource Management Ministerial Council, the Australian Government Department of Sustainability, Environment, Water, Population and Communities (DSEWPaC), and the Department of Climate Change and Energy Efficiency (DCCEE). The project was co-funded by CSIRO Climate Adaptation Flagship.

We thank Ruth Davies of centrEditing for editing this report.

## Executive summary

This report describes the use of generalised dissimilarity modelling (GDM) to assess the potential impact of climate change on biodiversity composition across Australia, and on the representativeness of the National Reserve System (NRS).

GDM is a statistical technique for modelling the compositional dissimilarity between pairs of geographical locations for a given biological group, that is, the proportion of species occurring at one location that do not occur at the other location as a function of the environmental characteristics of different locations. By linking GDM models to scenarios of climatically driven environmental change, it was possible to estimate the potential for change in biodiversity composition due to climate change, providing an index of 'environmental stress' that is scaled for the biological group being modelled. It should be noted that this index reflects only *potential* change. The actual change in biological composition resulting from climate change will be shaped by many factors, and associated sources of uncertainty, beyond those considered in this modelling. A similar technique, combining environmental variation in space and time, was used to assess changes in the representativeness of the NRS under climate change.

The GDM models were derived using continent-wide biological data fitted at 1 km<sup>2</sup> grid resolution<sup>1</sup> across the entire continent. Models were derived for 12 different biological groups, six of which are described in this report: vascular plants, land snails, frogs, reptiles, birds and mammals.

Two scenarios were considered: a *medium* impact scenario, using the A1B emissions scenario; and a *high* impact scenario, using the A1FI emissions scenario. The main future date considered was 2070, although an intermediate 2030 scenario was also developed.

### Potential change on a cell-by-cell basis

Modelled environmental stress varied between biological groups and across the continent. This reflects the different sensitivities to climate change, the coverage and quality of the available biological data, and the variation in natural niche breadth and range size between groups. The vascular plant dataset was the most spatially and environmentally extensive and had the greatest number of species. Since plants provide habitat for many animals, change in plant communities can also be thought of as an additional indirect driver of ecological change in the other groups.

Modelled environmental stress based on vascular plants, and the weighted average of the six groups, provided very strong indication that ecologically significant environmental stress, due to climate change, may begin to be apparent by 2030 and that high levels of stress could be widespread by 2070. The modelling also showed the stress would be greater at 2070 under higher emissions climate scenarios.

The impact on biodiversity of significant environmental change in any given location may be mitigated by environments at new locations becoming more similar to those of the original location, resulting in a shifting of the habitat as the climate changes. The study explored various aspects of this phenomenon with analyses of environmental analogues (disappearing and novel environments) and landscape buffering.

### Disappearing and novel environments

Using the GDM of vascular plants and the 2070 climate change scenarios, the study looked at the extent to which current environments at each location might be found somewhere on the continent in the future – where the match was poor, this indicated locations with environments or habitat types that may disappear from the continent due to the effects of climate change. A similar analysis looked back from the future

---

<sup>1</sup> The models were fitted to data based on 0.01° by 0.01° grids, which are approximately 1 km by 1 km, but their exact dimensions vary with latitude.

environment at each location to assess the extent to which future environments are currently occurring in Australia. Novel environments are those that are found in the future that have no current analogues.

The study found very high levels of disappearing and novel environments across Australia by 2070. Notably, areas with greater topographic variability tended to show lower levels of disappearing and novel environments. The levels of analogue were much lower in higher emissions climate scenarios.

### **Potential for landscape buffering, effective habitat area, habitat loss and fragmentation**

Landscape buffering describes the phenomenon where local environmental variation potentially leads to future habitats at some places near a given location being more similar to the current habitat than the future habitat there, which buffers the impact of climate change on plants and animals that may be able to disperse to these more-suitable nearby locations. The study found that buffering, at the scale of the analysis, was moderate relative to the magnitude of change expected at each location and very strongly associated with landscapes that had significant variation in elevation. Analysis of effective habitat area assesses the change in the area that has similar environment to a given location: only the elevated regions of south-eastern Australia show areas where the effective habitat area is relatively unchanged under the medium-impact scenario for 2070. The study was further extended to consider the added effect of past habitat loss (and fragmentation), highlighting areas in the south-east and south-west of the continent where restoration might have maximum benefit in terms of reducing the impact on effective habitat area. These benefits are not as strong in the 2070 high impact scenario as they are for the 2070 medium impact scenario.

### **Analysis of NRS representativeness under climate change**

The potential effects of climate change on the representativeness of the NRS have not been modelled before. We compared the extent to which present and projected future environments might be represented within the current boundaries of the NRS. Current environments are likely to be very poorly represented in the NRS under climate change by 2070 because of the high levels of disappearing and novel environments. However, the level of representation of the continent's future environments, in the NRS in the future, shows a remarkably similar pattern to the current representation of today's environments, which suggests that the NRS will continue to include about the same amount of diversity of the continent's habitats of the day in the future as it does now.

# 1 Introduction

This report describes the application of generalised dissimilarity modelling (GDM) to assess the potential impact of climate change on biodiversity composition across the Australian continent, and on the representativeness of the National Reserve System (NRS). This work was conducted as part of a consultancy performed by CSIRO for the (then) Department of Environment, Water, Heritage and the Arts (DEWHA) – ‘Impacts of climate change for the development and management of the National Reserve System: Phase 2’, hereafter referred to as the ‘NRS2 project’. Other components of this broader consultancy are described in a series of separate reports. This particular report focuses on the methods and raw results of the GDM modelling component, and avoids drawing conclusions concerning the broader ecological or policy implications of these results. Readers interested in discussion of these implications should access the four biome reports (House et al. 2012; Liedloff 2012; Prober et al. 2012; Smyth et al. 2012) and the overall ‘synthesis report’ (Dunlop et al. 2012) from this consultancy, all of which consider the GDM modelling results as one source of information alongside the results of other modelling approaches, and various sources of expert knowledge and opinion.

GDM is a statistical technique for modelling the compositional dissimilarity between pairs of geographical locations for a given biological group (e.g. reptiles), as a function of environmental differences between these locations (Ferrier 2002; Ferrier et al. 2002, 2007). The measure of compositional dissimilarity ( $d$ ) employed in this project is the Sorenson, or Bray–Curtis, index:

$$d_{ij} = 1 - \frac{2A}{2A + B + C}$$

where  $A$  is the number of species common to both locations  $i$  and  $j$

$B$  is the number of species present only at location  $i$

$C$  is the number of species present only at location  $j$

In other words, based on this measure, the compositional dissimilarity between a given pair of locations is the proportion of species occurring at one location that do not occur at the other location (averaged across the two locations) – ranging from 0 if the two locations have exactly the same species through to 1 if they have no species in common.

GDM uses data on species recorded at a sample of locations across the region of interest to fit a model predicting the compositional dissimilarity between pairs of locations as a non-linear multivariate function of the environmental attributes of these locations. Another way of viewing this is that GDM effectively weights and transforms the environmental variables of interest such that distances between locations in this transformed multidimensional environmental space now correlate, as closely as possible, with observed compositional dissimilarities between these same locations (see Ferrier et al. 2007 for full explanation).

The major steps involved in implementing the GDM modelling component of the NRS2 project are depicted in Figure 1.

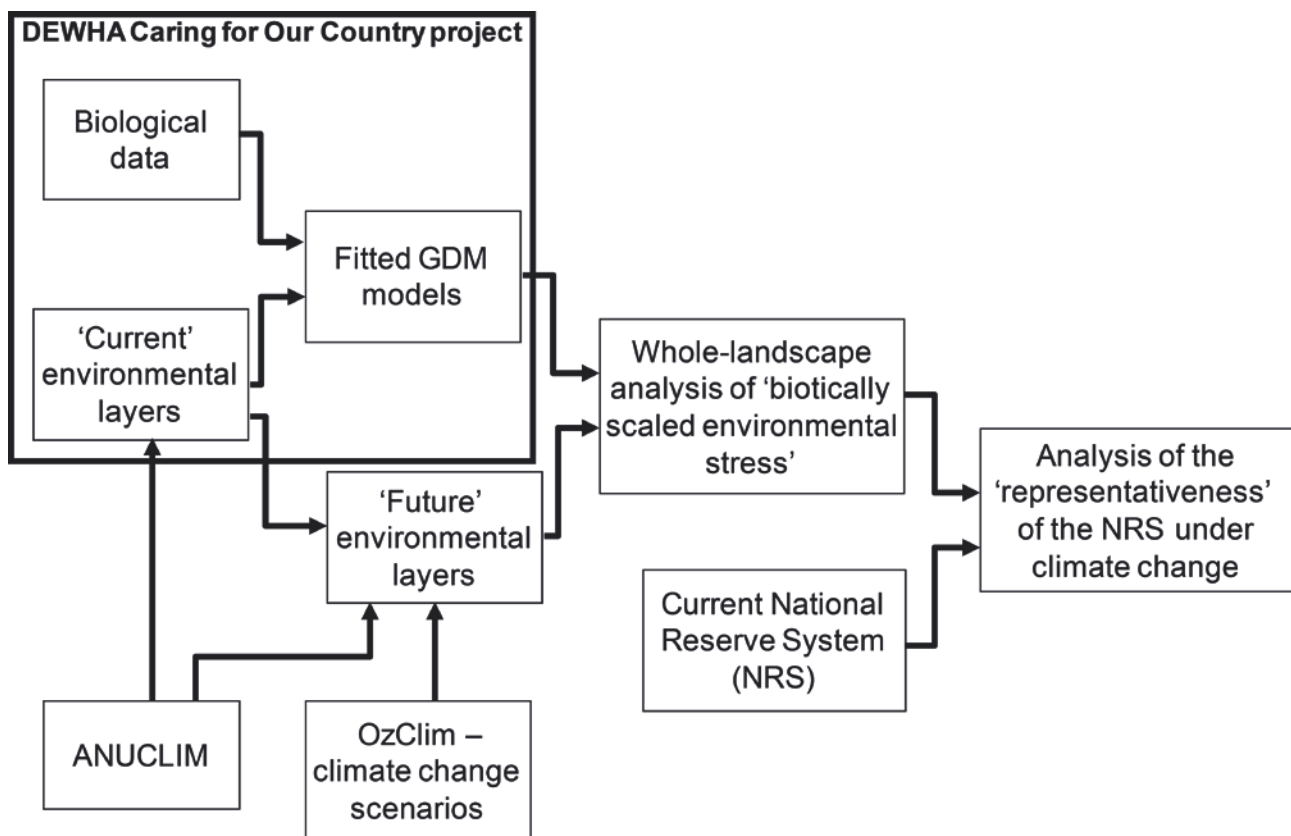


Figure 1 Major steps in the GDM-modelling component of the NRS2 project

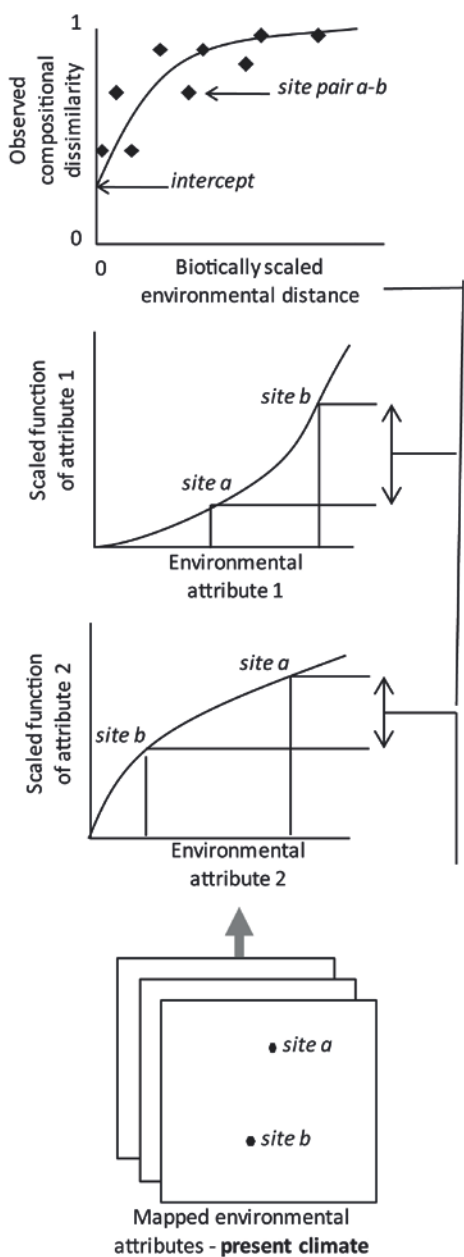
The approach is illustrated diagrammatically in Figure 2. On the left-hand side, a GDM model is fitted to compositional dissimilarities observed between pairs of surveyed locations (sites). The model-fitting process automatically identifies non-linear transformations of the original environmental variables (attributes) such that the summed environmental difference (distance) between each pair of sites (say 'a' and 'b') correlates, as closely as possible, with the observed compositional dissimilarity between these sites.

The curved line in the top-left graph represents the so-called link function used in GDM to account for the well-known asymptotic relationship between increasing environmental difference and observed compositional dissimilarity (the latter cannot exceed 1 once sites share no species).

The 'intercept' in this graph represents the observed compositional dissimilarity expected between two sites with identical environmental conditions. This baseline dissimilarity summarises the effects of ecological factors other than those modelled and the effects of sampling error. Under a changing climate, the intercept remains constant, and was consequently excluded from the change analyses, such that they model only the component of compositional turnover driven by the changing climate.

On the right-hand side of Figure 2, the GDM model fitted to compositional dissimilarities observed between pairs of sites under present environmental conditions is used to estimate (project) the level of environmental stress expected under a given climate scenario. Here the non-linear transformations of environmental variables from the fitted model are used to calculate the biotically scaled environmental difference, and thereby potential stress, associated with any particular site (say 'x') given the environmental attributes of this site under present and future climatic conditions.

**Model fitted to compositional dissimilarities observed between pairs of sites (grid cells) under present environmental conditions**



**This model then used to project level of environmental stress expected under climate change for any given site (grid cell)**

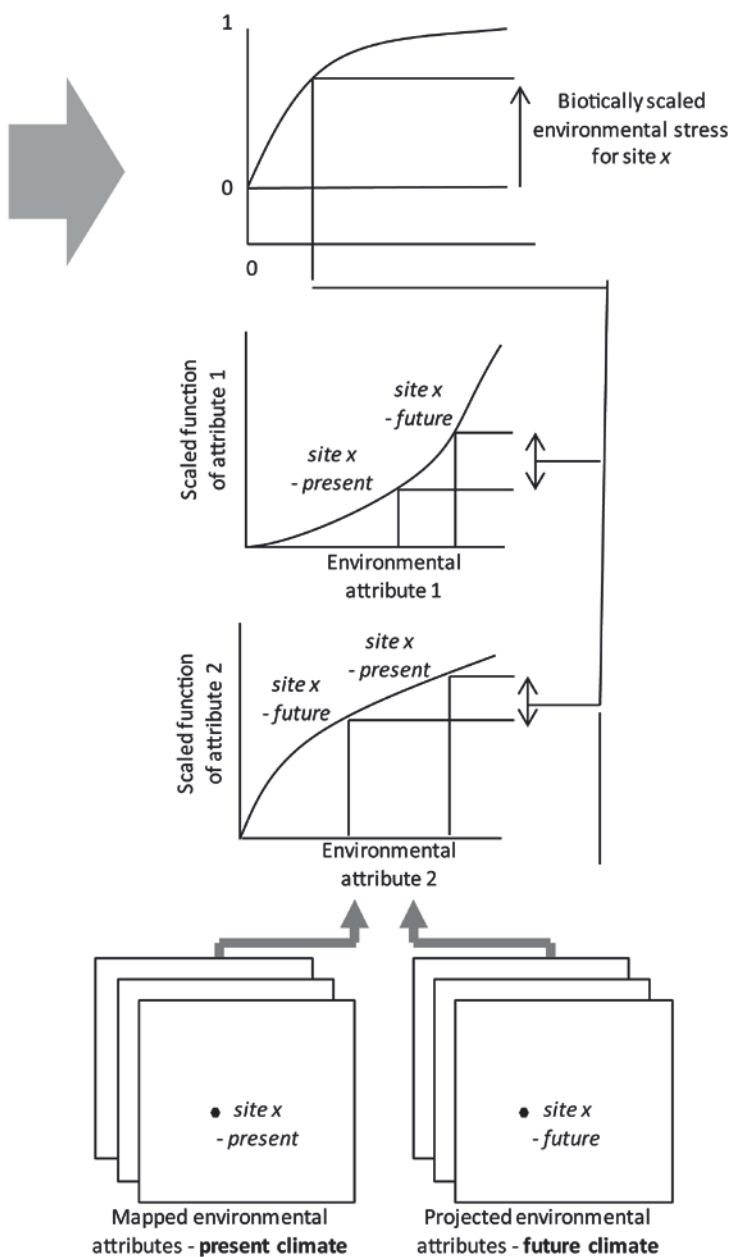


**Figure 2 Illustration of how the GDM model is constructed with current environmental layers and observed species compositional patterns, and how it is then used to project biotically scaled environmental stress**

This project employed a set of GDM models already derived for the Australian continent by a separate (then) DEWHA-funded Caring for Our Country Open Grants project performed by CSIRO in collaboration with DEWHA and the ANU Fenner School of Environment and Society (Williams et al. 2010). These models are described in Section 2 below and in Appendix A. The NRS2 project linked these models to downscaled climate scenarios for the Australian continent (described in Section 3) to assess potential changes in biodiversity composition as an indicator of 'environmental stress' (described in Section 4), and to assess changes in the representativeness of the NRS under climate change (described in Section 5).

## 2 Derivation of GDM models

The GDM models generated by the Caring for Our Country project were derived using continent-wide biological data collated within DEWHA's Australian Natural Heritage Assessment Tool (ANHAT) database, a compilation of species-location records from a large number of herbaria, museums, State and Commonwealth departments, and private individuals. The models were fitted at 1 km<sup>2</sup> grid resolution<sup>2</sup> across the entire continent using best-available environmental layers for 76 climate (1990-centred ANUCLIM sourced data), terrain and substrate variables (Williams et al. 2010). Models were derived for 12 different biological groups, six of which were employed in the work described in this current report:

- vascular plants (model based on data for 12,881 species at 374,640 locations – i.e. 1 km<sup>2</sup> grid cells)
- land snails (model based on 2,774 species at 19,118 locations)
- frogs (model based on 218 species at 100,143 locations)
- reptiles (model based on 819 species at 83,661 locations)
- birds (model based on 690 species at 242,814 locations)
- mammals (model based on 298 species at 100,369 locations)

These models are described further in Appendix A. For further detail on the data and model-fitting procedures used to derive these models, see Williams et al. (2010).

Environmental stress resulting from climate change was calculated by deriving new climatic predictor variables (as listed in Appendix A; Table A.4) for a range of climate change scenarios (next section). The last 10% of the linear trend from each end of the fitted function was extrapolated, where necessary, to accommodate novel climates for each predictor. The future climate predictors were then used, along with the existing substrate and terrain predictors, to develop GDM projections of each fitted model. The fitted and projected GDM models were used to estimate dissimilarity or environmental stress between 1960 and the future 2030 and 2070 climate scenarios.

---

<sup>2</sup> The models were fitted to data based on 0.01° by 0.01° grids, which are approximately 1 km by 1 km, but their exact dimensions vary with latitude.

### 3 Selection and downscaling of climate scenarios

Two scenarios were considered, both using outputs from the CSIRO Mk3.5 Global Climate Model (GCM) downloaded from OzClim (CSIRO 2012): a *medium* impact scenario, using the A1B emissions scenario; and a *high* impact scenario, using the A1FI emissions scenario (IPCC 2000). The main future date considered was 2070, although an intermediate 2030 scenario was also developed.

The CSIRO Mk3.5 model was selected from the two GCMs that met the requirements of our downscaling approach within the limited time frame of the project in that they were immediately available as 0.25° grids for the required climate change input parameters for ANUCLIM beta. While a direct comparison of the newly released CSIRO Mk3.5 model was not available, it offered improved skill for Australia relative to CSIRO Mk3.0 (Gordon et al. 2010) which had the same skill rating as Miroc-m in Suppiah et al. (2007). Further to this we sought expert opinion to confirm our selection. Another reason for choosing the CSIRO Mk3.5 model over other GCMs was its superior representation of hydrological processes as revealed when measuring model skill of the individual components of water balance. Other GCMs could be expected to demonstrate climatic differences, and would provide an avenue for future investigation.

The first step was to download monthly climate change grids at 0.25° resolution for maximum temperature, minimum temperature, rainfall and evaporation, by specifying the above scenarios in OzClim. Spatial downscaling was carried out using the ANUCLIM software (Houlder et al. 2000; Fenner School of Environment and Society 2012), which incorporates three submodels: ESOCLIM, which outputs raw climate variable grids; BIOCLIM (Busby 1986), which outputs grids of bioclimatic parameters; and GROCLIM, which can output gridded indices from simple growth models. The beta release of ANUCLIM version 6.0 was used, which allows climate change grids to be applied relative to historical 1990-centred climate surfaces to create grids of 2030 and 2070 climate variable for each scenario. Software (Harwood and Williams 2009) was written to interpolate the raw 0.25° CSIRO grids to cover the whole Australian landmass, and relate evaporation change to the date range used in ANUCLIM 6. Following this interpolation, monthly maximum temperature, minimum temperature, rainfall, and evaporation change grids were input into ANUCLIM 6 with a 0.01° digital elevation model. The result was a suite of monthly 0.01° ( $\approx 1 \text{ km}^2$ ) resolution future climate surfaces for maximum temperature, minimum temperature, rainfall, evaporation and radiation, with 35 BIOCLIM variables and four plant growth indices for each scenario.

For a full description of the preparation of climate scenarios for use in this project, see Harwood et al. (2012).

## 4 Whole-landscape analysis of biotically scaled environmental stress

The current project used the GDM models fitted to current biological and environmental data (see Section 2 and Appendix A) to infer potential changes in biological composition across the continent as a function of projected changes in climate, from 1960 to 2030 and 2070. This is based on the assumption that the amount of change in species composition expected for location *A* as a result of climate change will be equivalent to the compositional dissimilarity currently observed between location *A* and another location *B* with a current climate matching that projected for location *A* (Ferrier and Guisan 2006; Ferrier et al. 2007). It is likely that the actual change in biological composition resulting from climate change will be shaped by many factors, and associated sources of uncertainty, beyond those considered in this modelling – for example, biotic interactions, indirect effects of changed fire regimes, dispersal ability, lag effects, adaptation capacity and plasticity. The level of compositional change predicted by the GDM approach is therefore best interpreted as no more than a relative indicator of potential ‘environmental stress’ expected to be experienced by species in a given biological group under a given climate scenario.

### 4.1 Potential change on a cell-by-cell basis

The predicted dissimilarity between the current (1960) composition of each grid cell and its composition under a given climate scenario is a general indicator of potential environmental stress on a cell-by-cell basis. This was estimated and mapped separately for each of the six biological groups, for each of the four downscaled climate scenarios (Figures 3 to 8). A weighted average of these six sets of maps was also derived (Figure 9), in which each biological group was weighted according to the total amount of spatial turnover exhibited by the group under current climate conditions (see Williams et al. 2010 for further explanation of this weighting). Green colours show areas where the predicted dissimilarity is less than 0.5. In the pink areas, the predicted dissimilarity is between 0.5 and 0.95, indicating very different biotically scaled environments, and therefore the areas of greatest scaled environmental change. Results for different biological groups vary both spatially and quantitatively. This is a consequence of the coverage and quality of the available biological data (see Section 2 and Appendix A), but also of the variation in natural range size and dispersal capacity between groups.

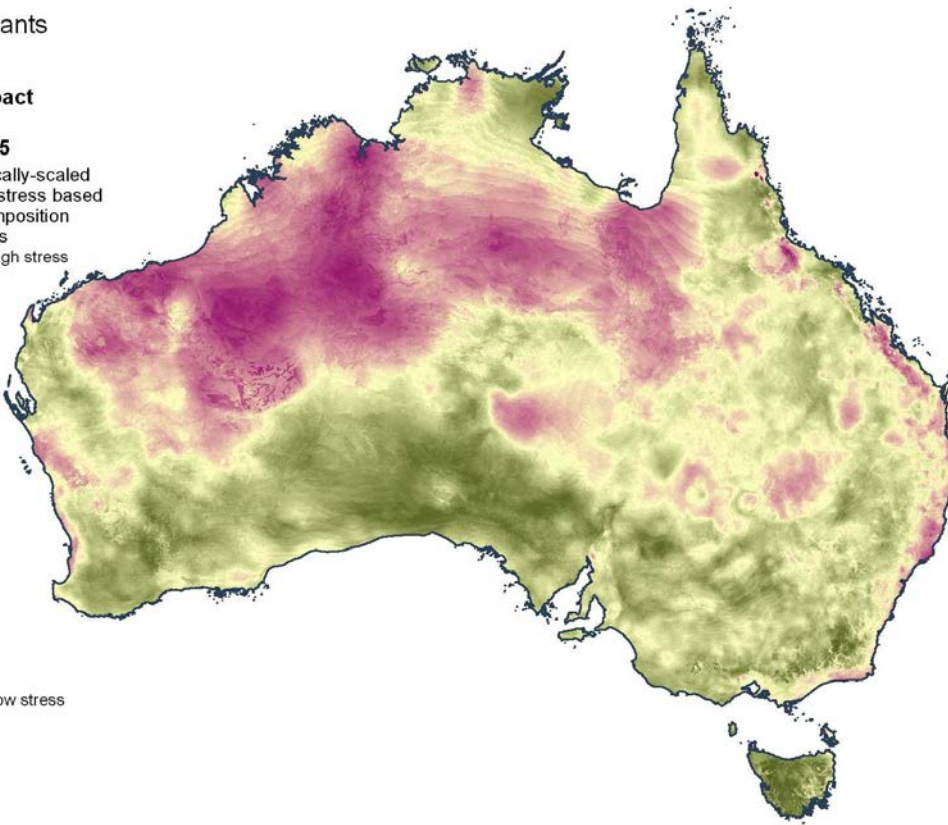
This statistic was further analysed as an average for each Interim Biogeographic Regionalisation for Australia (IBRA) bioregion and as continental mean potential dissimilarity. Table 1 below summarises continental-scale results for all groups. Figure 10 shows the location of the IBRA bioregions. Tables 2 and 3 and Figures 11 and 12 show results by bioregion for vascular plants and the weighted mean respectively.

**Table 1 Mean predicted dissimilarity between the current composition of each 1 km<sup>2</sup> grid cell and its potential composition under each of the four climate scenarios, as an average for the whole continent – summary of all groups**

	MEDIUM IMPACT		HIGH IMPACT	
	2030	2070	2030	2070
Vascular plants	0.496	0.709	0.537	0.853
Land snails	0.542	0.745	0.577	0.867
Amphibians	0.206	0.277	0.217	0.376
Reptiles	0.501	0.610	0.520	0.702
Birds	0.116	0.176	0.126	0.257
Mammals	0.193	0.354	0.217	0.510
Average	0.404	0.561	0.432	0.682

Vascular plants

**2030**  
**medium impact**  
**A1B**  
**CSIRO mk3.5**  
Predicted biotically-scaled  
environmental stress based  
on GDM of composition  
in 1km grid cells



Vascular plants

**2030**  
**high impact**  
**A1FI**  
**CSIRO mk3.5**  
Predicted biotically-scaled  
environmental stress based  
on GDM of composition  
in 1km grid cells

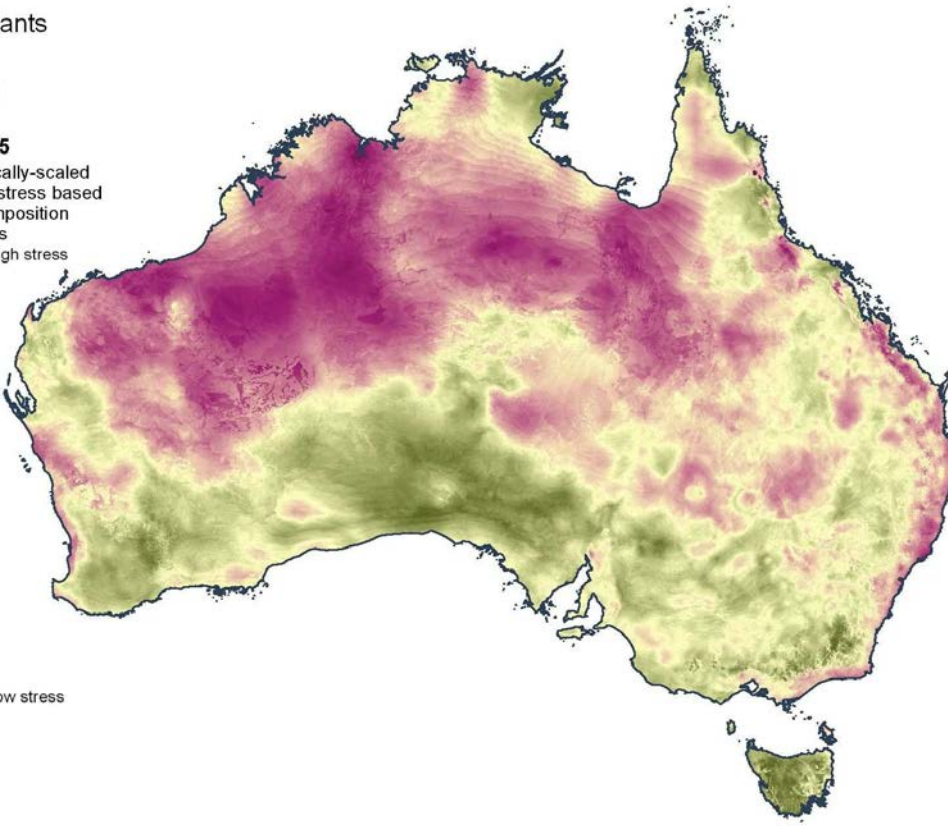
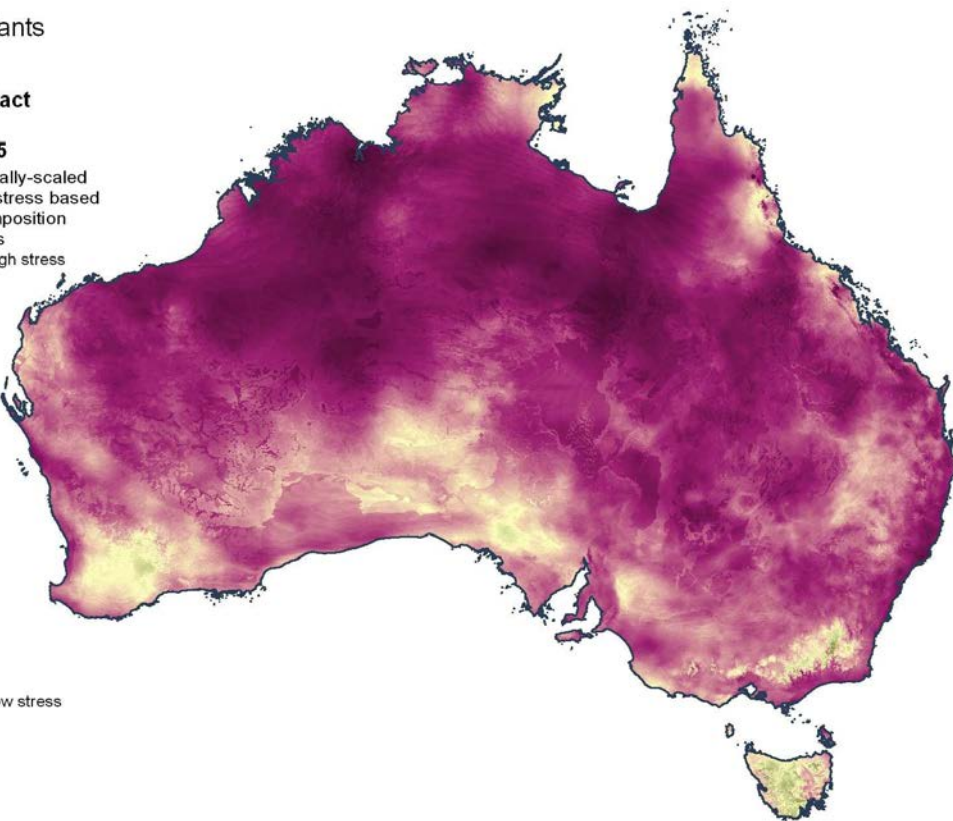


Figure 3a Predicted dissimilarity between the current composition of each 1 km<sup>2</sup> grid cell and its potential composition under each of the 2030 climate scenarios, for vascular plants

Vascular plants

**2070  
medium impact  
A1B  
CSIRO mk3.5**  
Predicted biotically-scaled  
environmental stress based  
on GDM of composition  
in 1km grid cells

0.95 - 1	High stress
0.9 - 0.95	
0.85 - 0.9	
0.8 - 0.85	
0.75 - 0.8	
0.7 - 0.75	
0.65 - 0.7	
0.6 - 0.65	
0.55 - 0.6	
0.5 - 0.55	
0.45 - 0.5	
0.4 - 0.45	
0.35 - 0.4	
0.3 - 0.35	
0.25 - 0.3	
0.2 - 0.25	
0.15 - 0.2	
0.1 - 0.15	
0.05 - 0.1	
0 - 0.05	Low stress



Vascular plants

**2070  
high impact  
A1FI  
CSIRO mk3.5**  
Predicted biotically-scaled  
environmental stress based  
on GDM of composition  
in 1km grid cells

0.95 - 1	High stress
0.9 - 0.95	
0.85 - 0.9	
0.8 - 0.85	
0.75 - 0.8	
0.7 - 0.75	
0.65 - 0.7	
0.6 - 0.65	
0.55 - 0.6	
0.5 - 0.55	
0.45 - 0.5	
0.4 - 0.45	
0.35 - 0.4	
0.3 - 0.35	
0.25 - 0.3	
0.2 - 0.25	
0.15 - 0.2	
0.1 - 0.15	
0.05 - 0.1	
0 - 0.05	Low stress

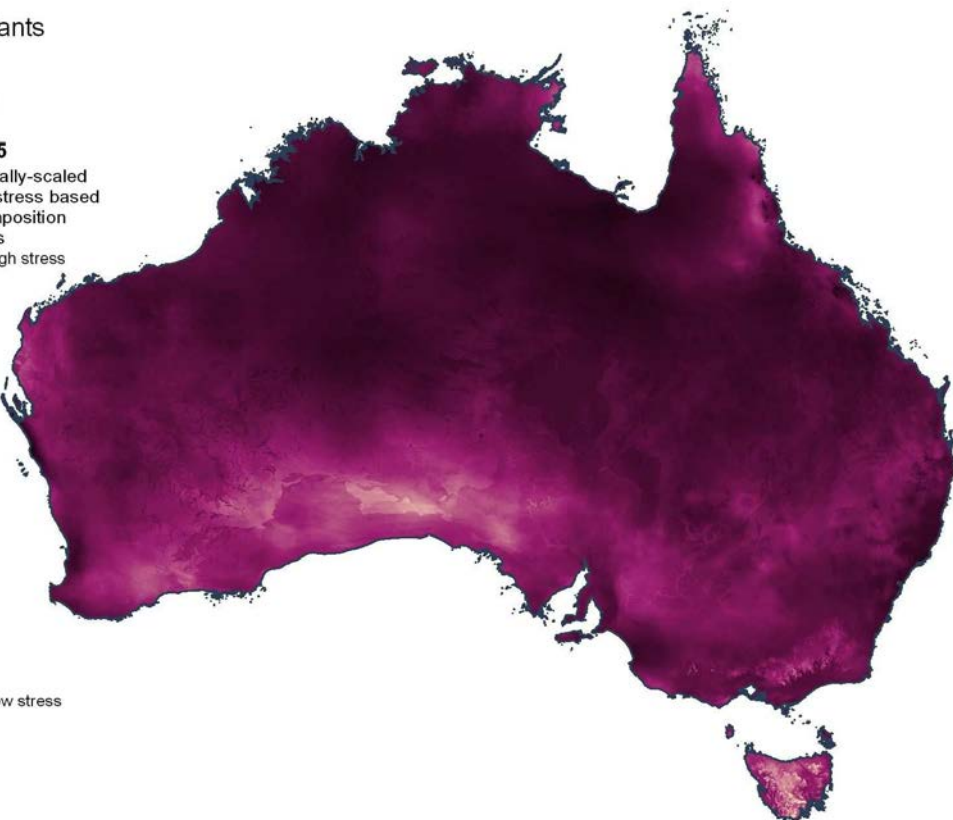
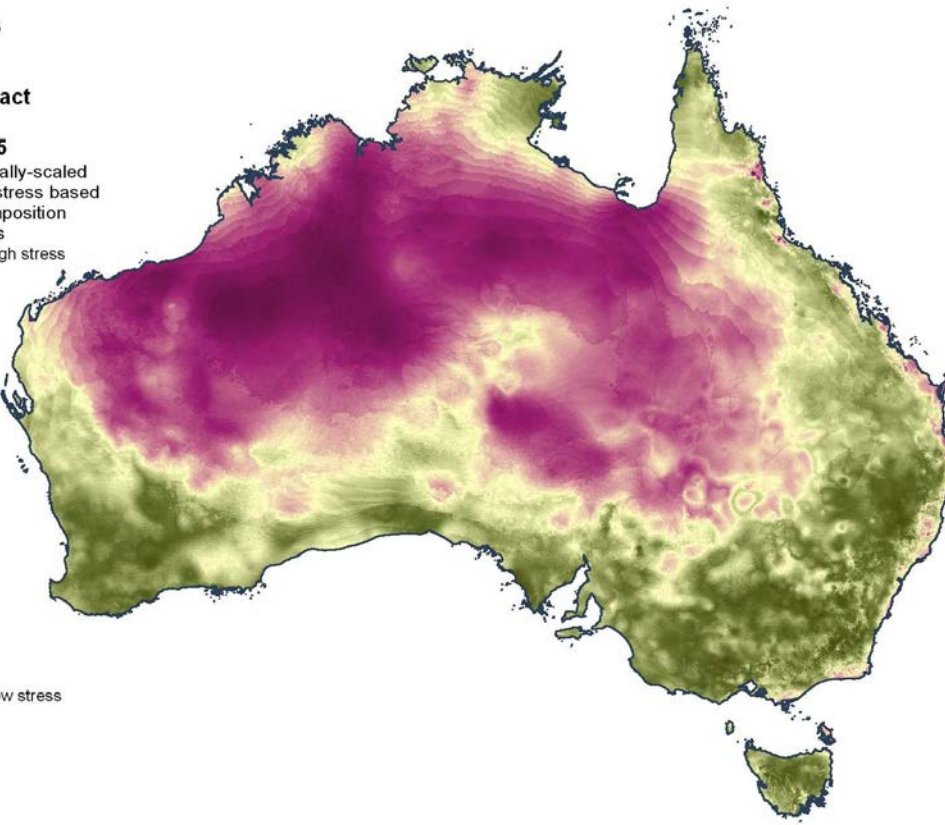
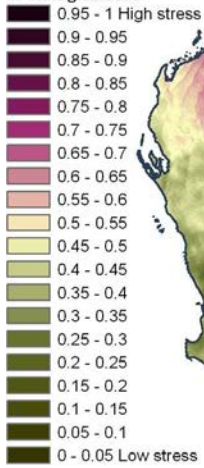


**Figure 3b Predicted dissimilarity between the current composition of each 1 km<sup>2</sup> grid cell and its potential composition under each of the 2070 climate scenarios, for vascular plants**

Land snails

**2030  
medium impact  
A1B  
CSIRO mk3.5**  
Predicted biotically-scaled  
environmental stress based  
on GDM of composition  
in 1km grid cells



Land snails

**2030  
high impact  
A1FI  
CSIRO mk3.5**  
Predicted biotically-scaled  
environmental stress based  
on GDM of composition  
in 1km grid cells

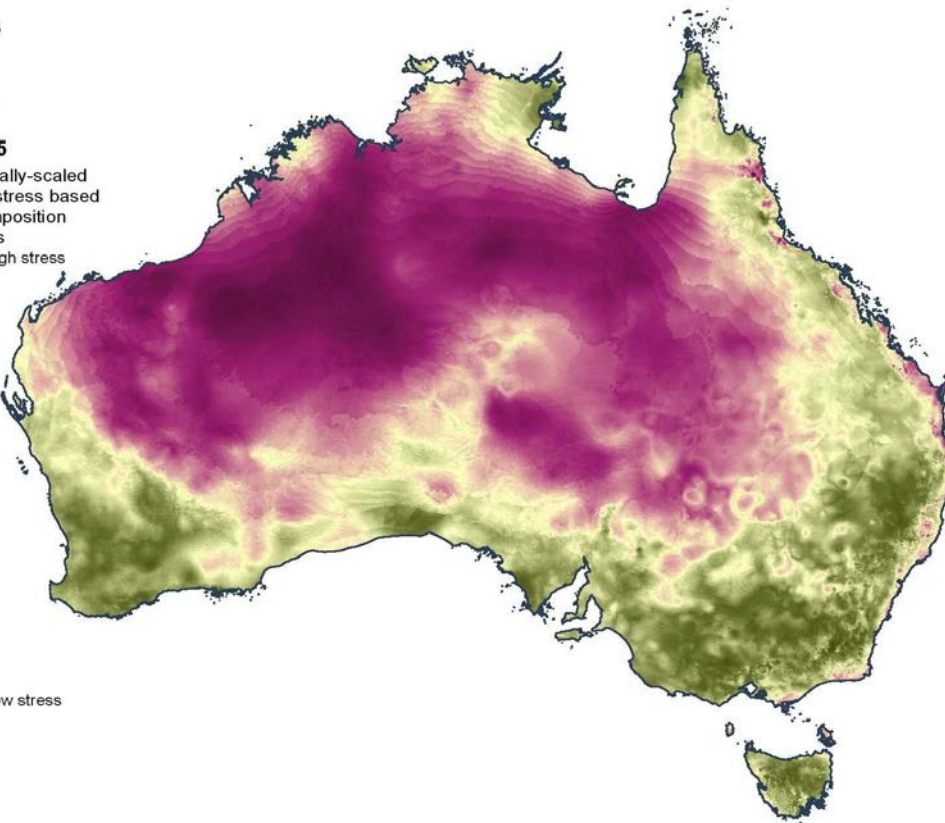
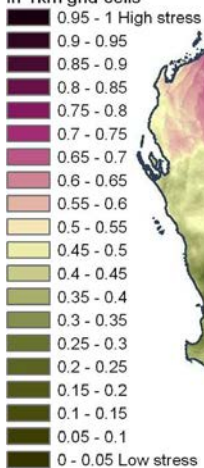
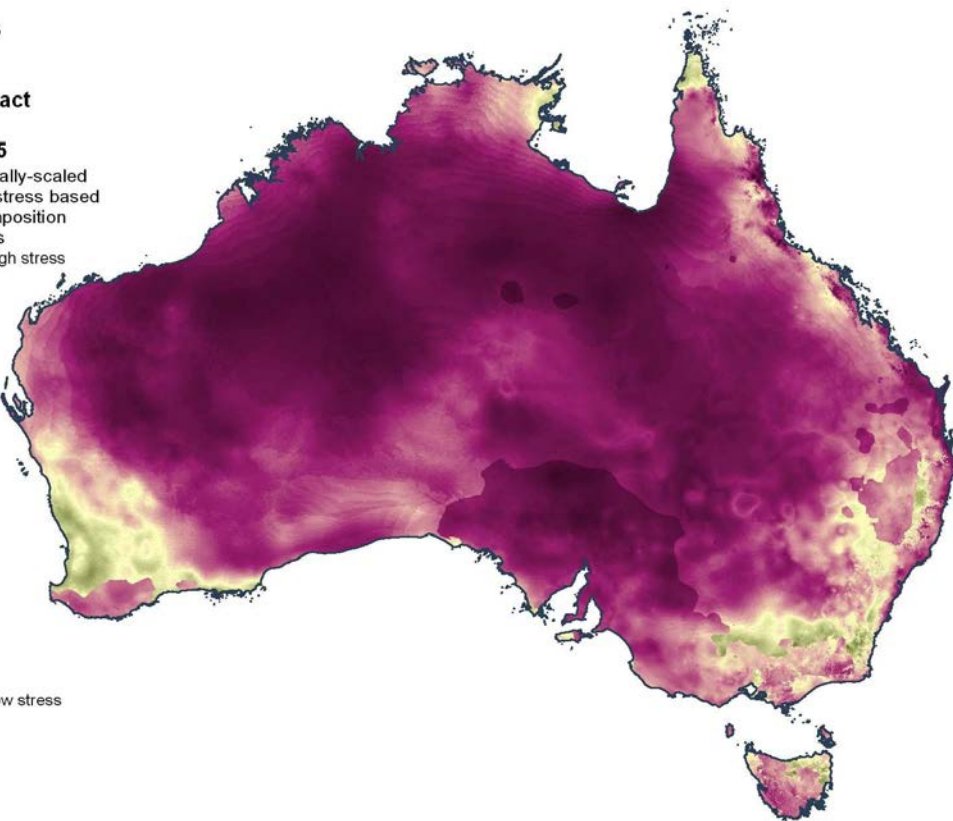
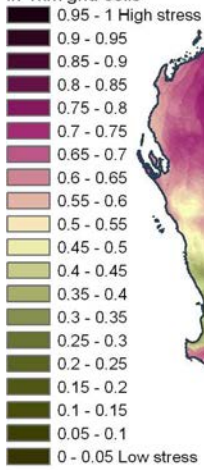


Figure 4a Predicted dissimilarity between the current composition of each 1 km<sup>2</sup> grid cell and its potential composition under each of the 2030 climate scenarios, for land snails

Land snails

**2070  
medium impact  
A1B  
CSIRO mk3.5**  
Predicted biotically-scaled  
environmental stress based  
on GDM of composition  
in 1km grid cells



Land snails

**2070  
high impact  
A1FI  
CSIRO mk3.5**  
Predicted biotically-scaled  
environmental stress based  
on GDM of composition  
in 1km grid cells

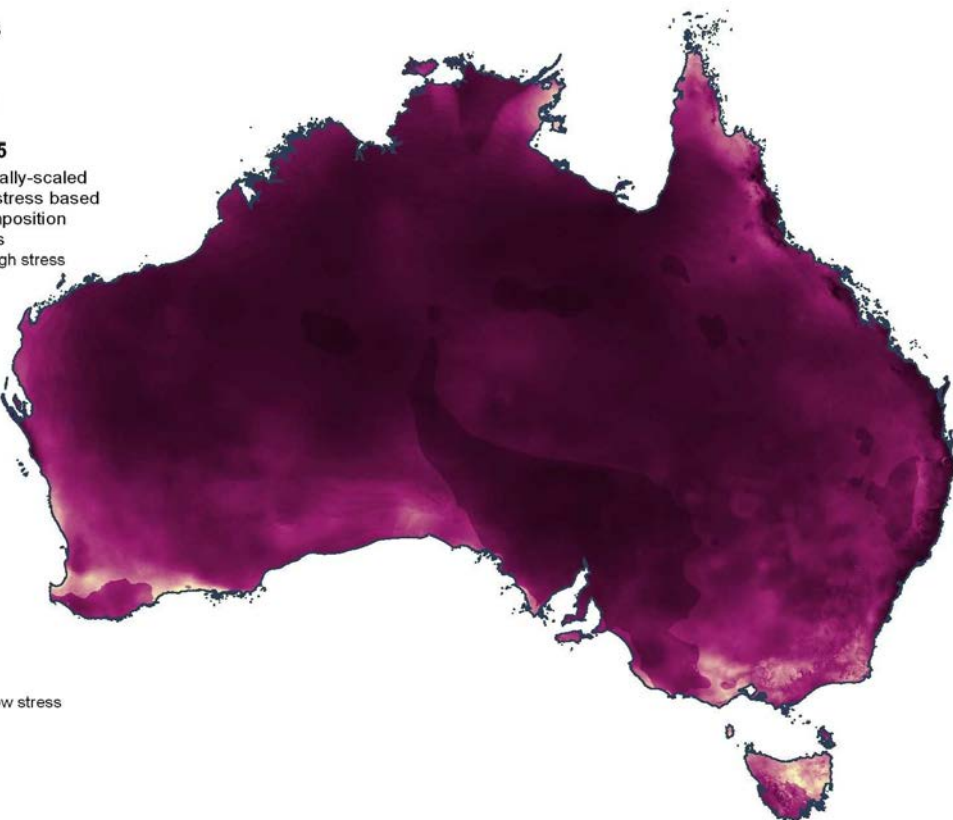
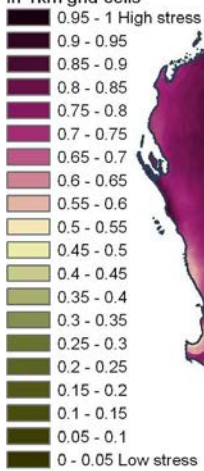
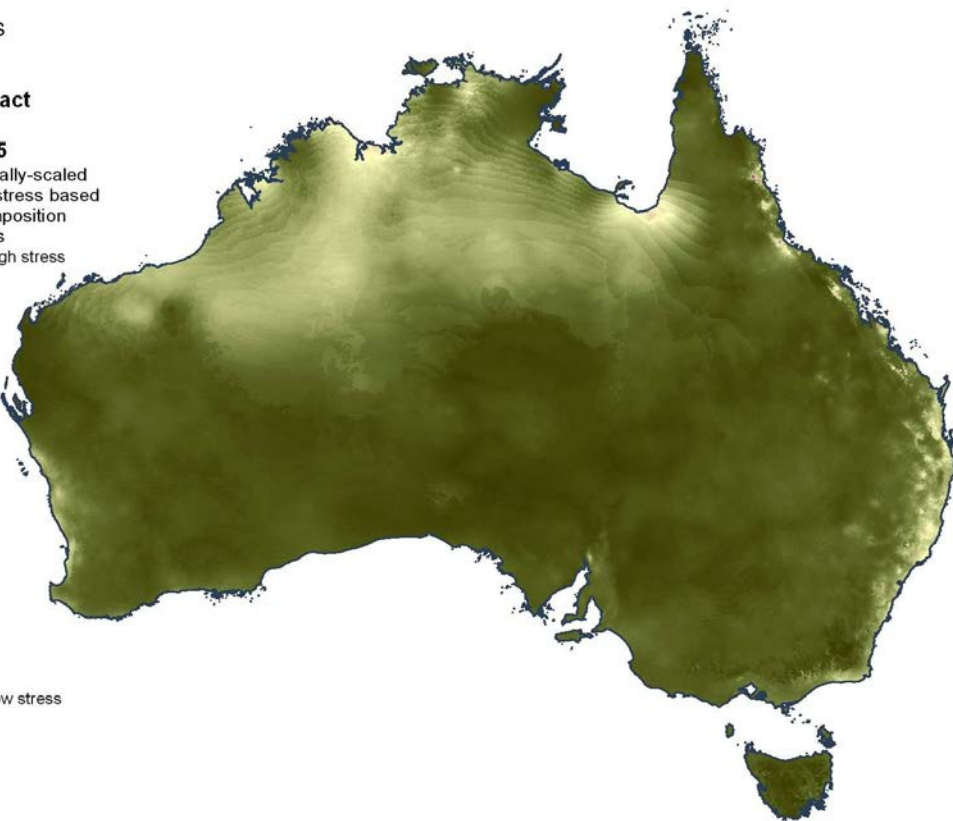
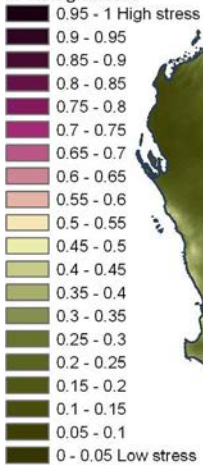


**Figure 4b Predicted dissimilarity between the current composition of each 1 km<sup>2</sup> grid cell and its potential composition under each of the 2070 climate scenarios, for land snails**

Amphibians

**2030  
medium impact  
A1B  
CSIRO mk3.5**  
Predicted biotically-scaled  
environmental stress based  
on GDM of composition  
in 1km grid cells



Amphibians

**2030  
high impact  
A1FI  
CSIRO mk3.5**  
Predicted biotically-scaled  
environmental stress based  
on GDM of composition  
in 1km grid cells

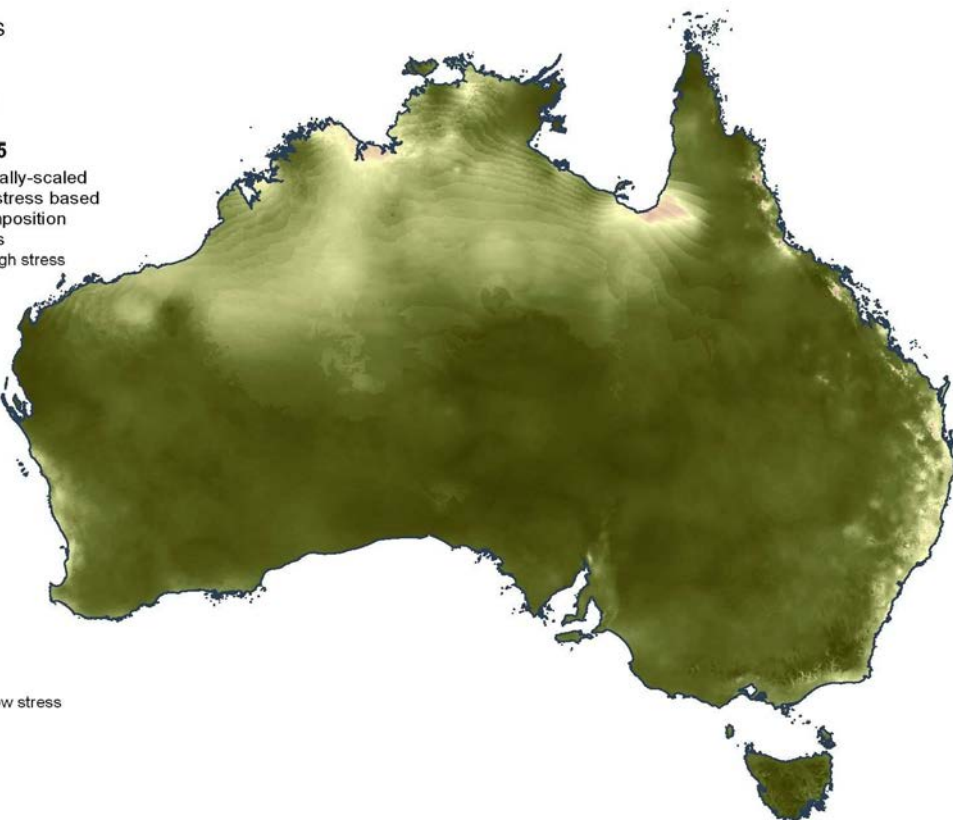
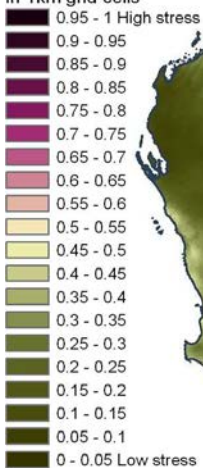
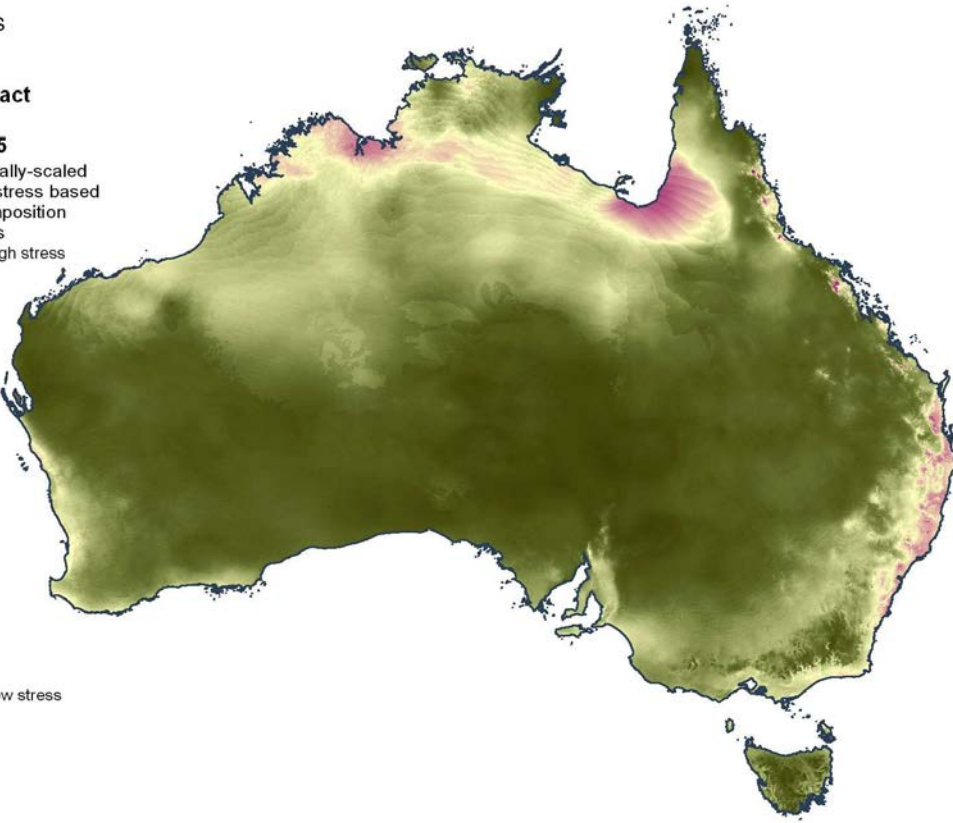
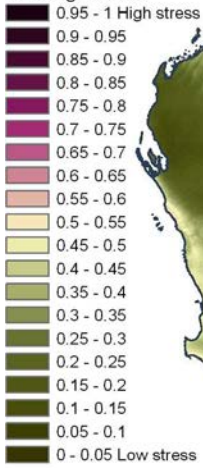


Figure 5a Predicted dissimilarity between the current composition of each 1 km<sup>2</sup> grid cell and its potential composition under each of the 2030 climate scenarios, for amphibians

Amphibians

**2070  
medium impact  
A1B  
CSIRO mk3.5**  
Predicted biotically-scaled  
environmental stress based  
on GDM of composition  
in 1km grid cells



Amphibians

**2070  
high impact  
A1FI  
CSIRO mk3.5**  
Predicted biotically-scaled  
environmental stress based  
on GDM of composition  
in 1km grid cells

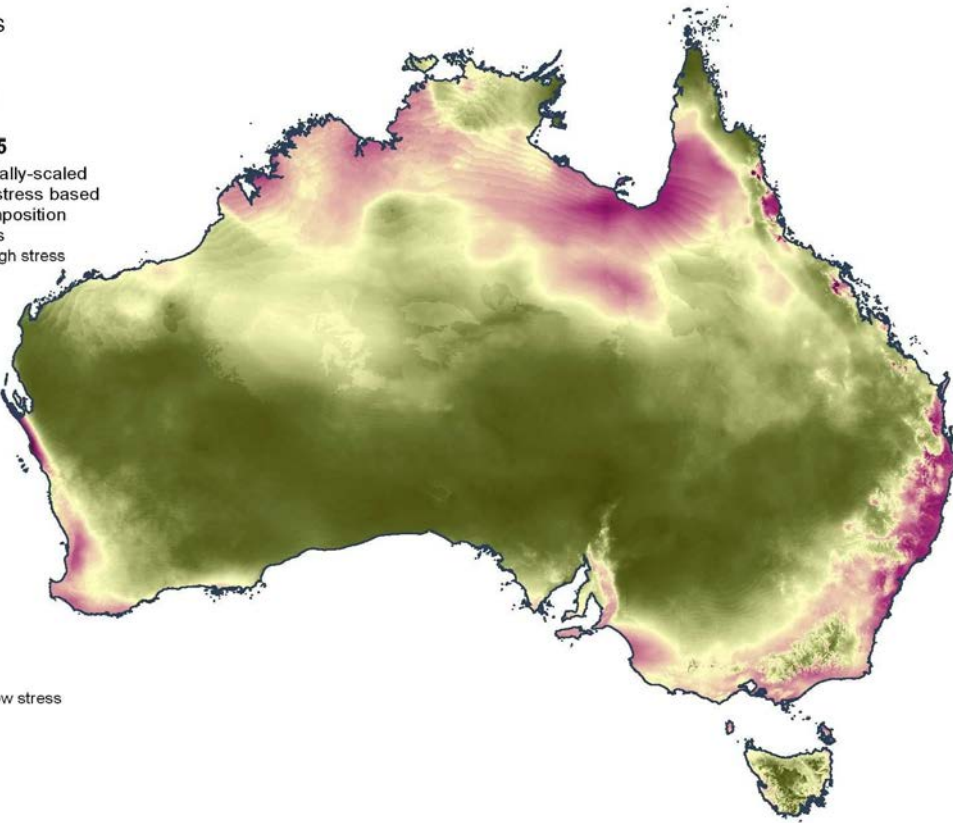
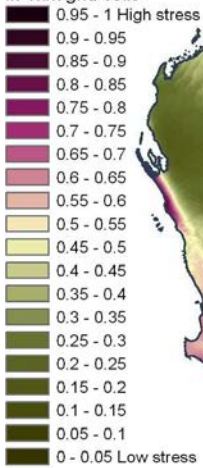
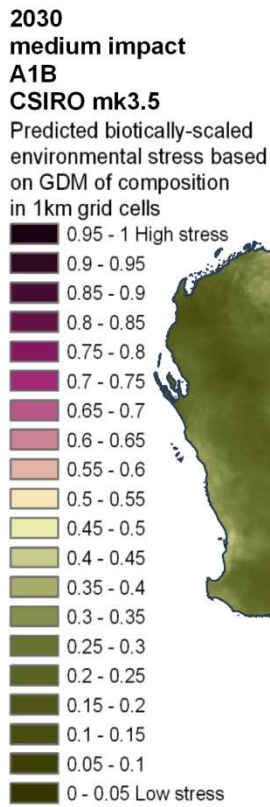
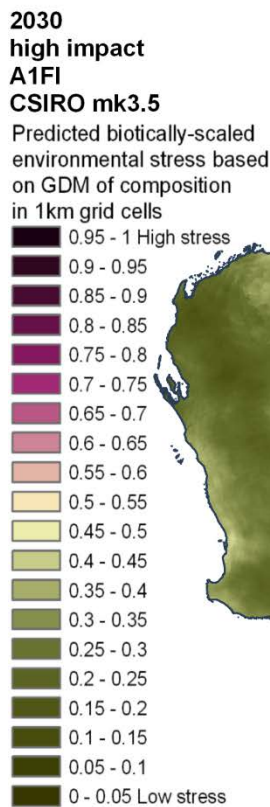


Figure 5b Predicted dissimilarity between the current composition of each 1 km<sup>2</sup> grid cell and its potential composition under each of the 2070 climate scenarios, for amphibians

## Reptiles



## Reptiles



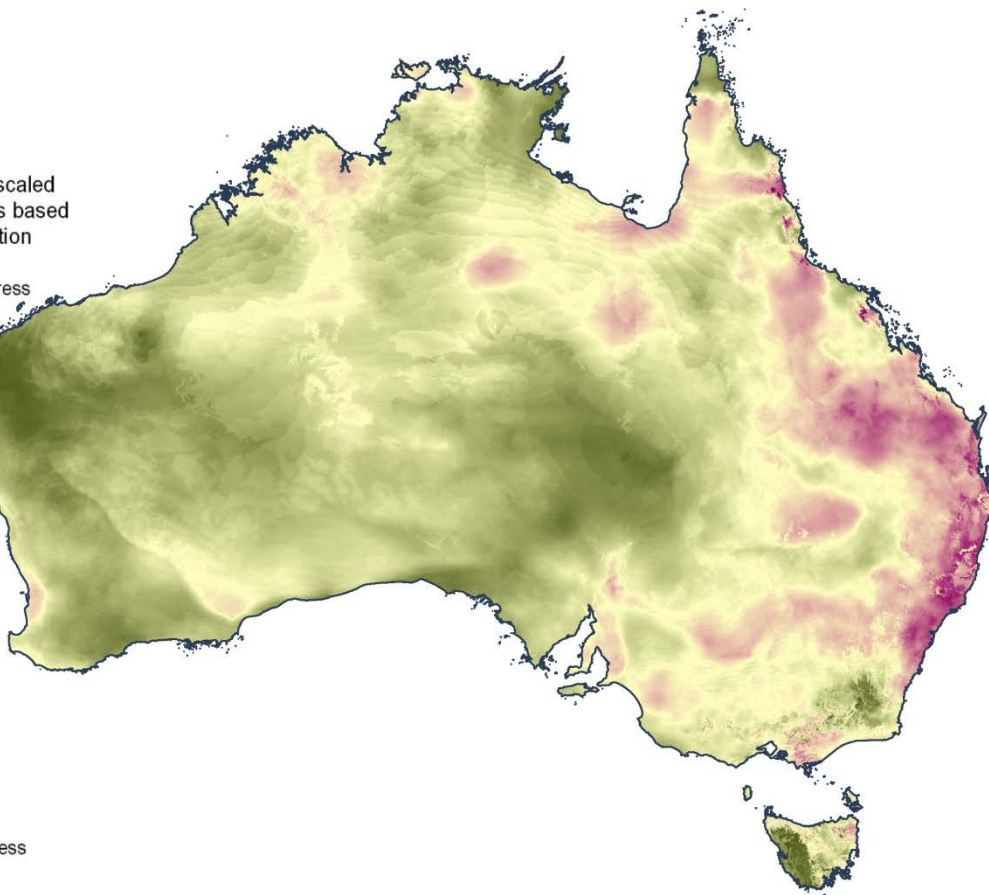
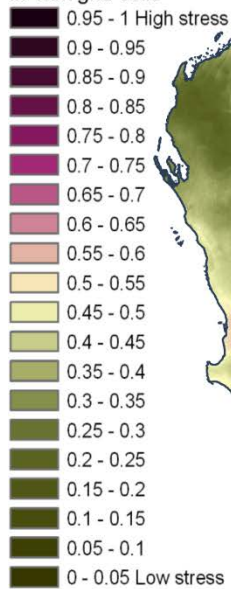
**Figure 6a Predicted dissimilarity between the current composition of each 1 km<sup>2</sup> grid cell and its potential composition under each of the 2030 climate scenarios, for reptiles**

## Reptiles

2070  
medium impact  
A1B

CSIRO mk3.5

Predicted biotically-scaled  
environmental stress based  
on GDM of composition  
in 1km grid cells



## Reptiles

2070  
high impact  
A1FI

CSIRO mk3.5

Predicted biotically-scaled  
environmental stress based  
on GDM of composition  
in 1km grid cells

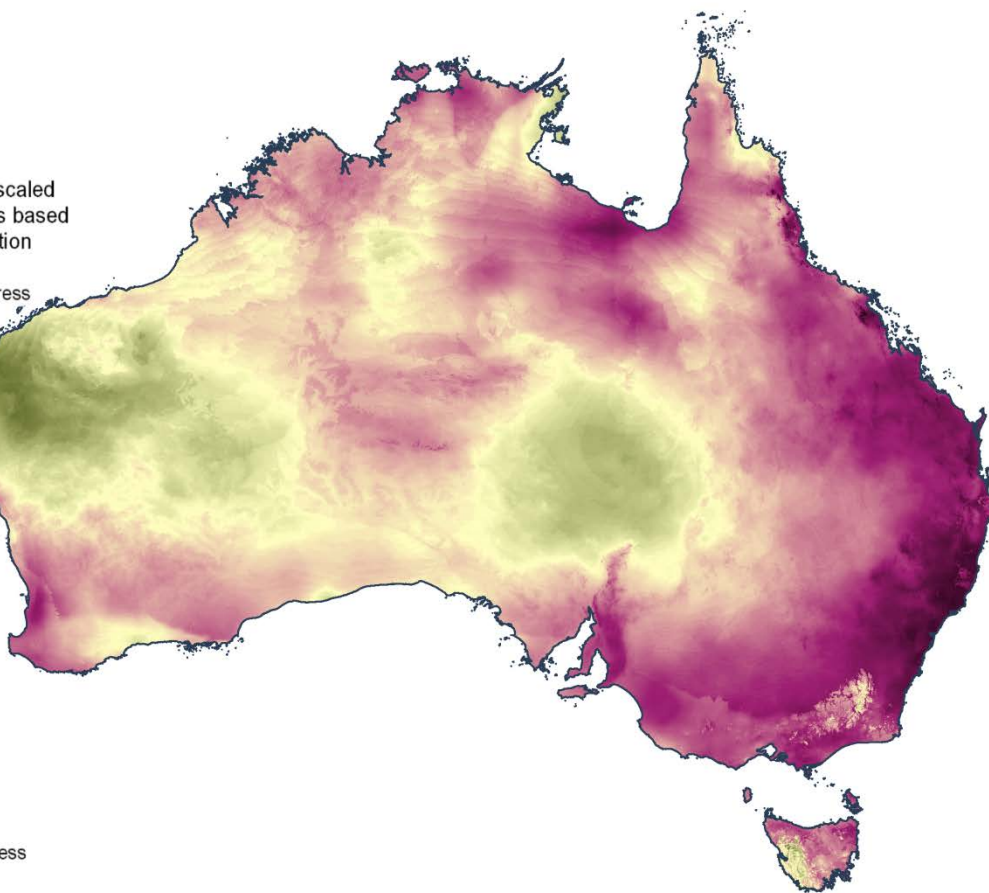
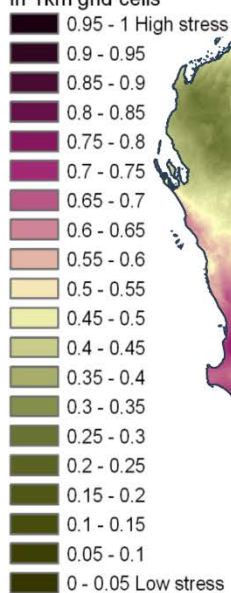


Figure 6b Predicted dissimilarity between the current composition of each 1 km<sup>2</sup> grid cell and its potential composition under each of the 2070 climate scenarios, for reptiles

Birds

2030  
medium impact  
A1B  
CSIRO mk3.5

Predicted biotically-scaled  
environmental stress based  
on GDM of composition  
in 1km grid cells



Birds

2030  
high impact  
A1FI  
CSIRO mk3.5

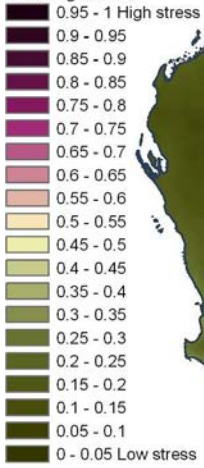
Predicted biotically-scaled  
environmental stress based  
on GDM of composition  
in 1km grid cells



Figure 7a Predicted dissimilarity between the current composition of each 1 km<sup>2</sup> grid cell and its potential composition under each of the 2030 climate scenarios, for birds

Birds

**2070  
medium impact  
A1B  
CSIRO mk3.5**  
Predicted biotically-scaled  
environmental stress based  
on GDM of composition  
in 1km grid cells



Birds

**2070  
high impact  
A1FI  
CSIRO mk3.5**  
Predicted biotically-scaled  
environmental stress based  
on GDM of composition  
in 1km grid cells

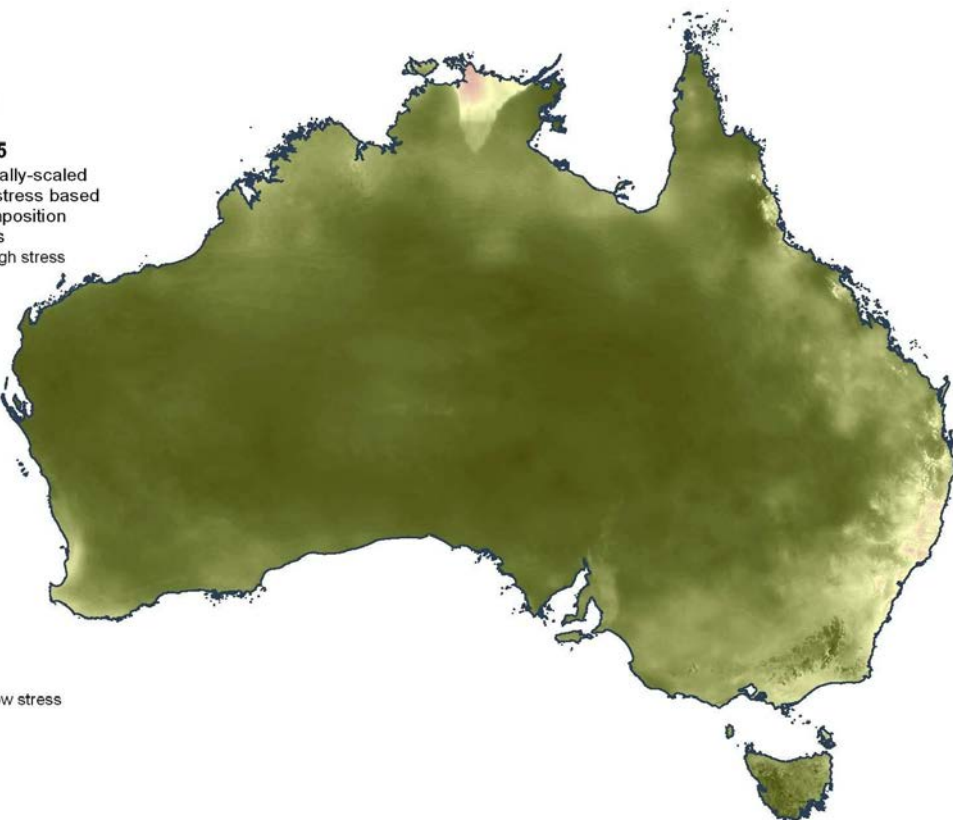
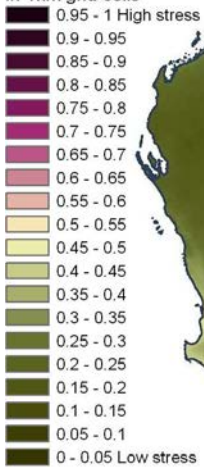
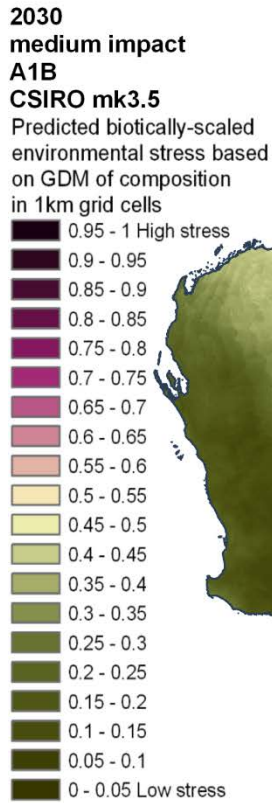


**Figure 7b Predicted dissimilarity between the current composition of each 1 km<sup>2</sup> grid cell and its potential composition under each of the 2070 climate scenarios, for birds**

## Mammals



## Mammals

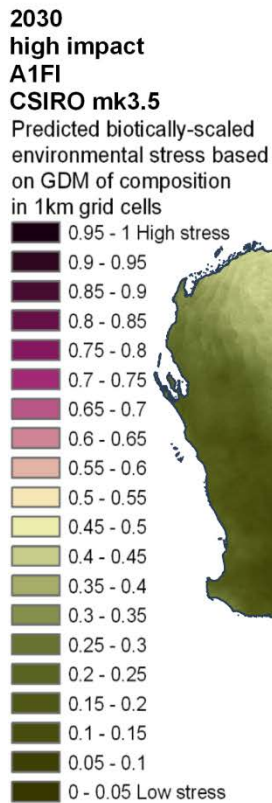
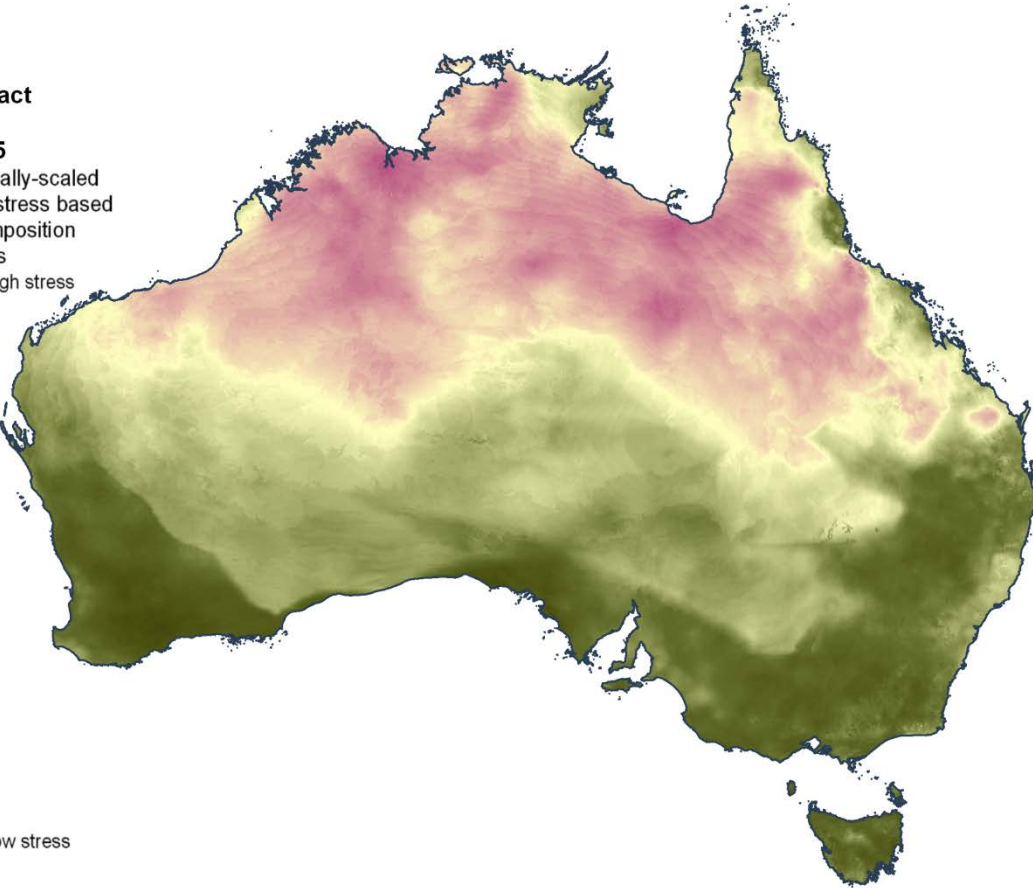
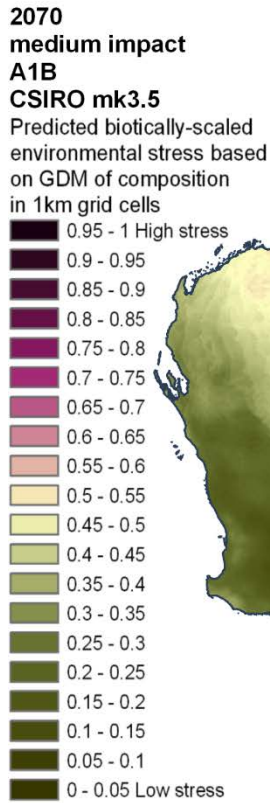


**Figure 8a Predicted dissimilarity between the current composition of each 1 km<sup>2</sup> grid cell and its potential composition under each of the 2030 climate scenarios, for mammals**

## Mammals



## Mammals

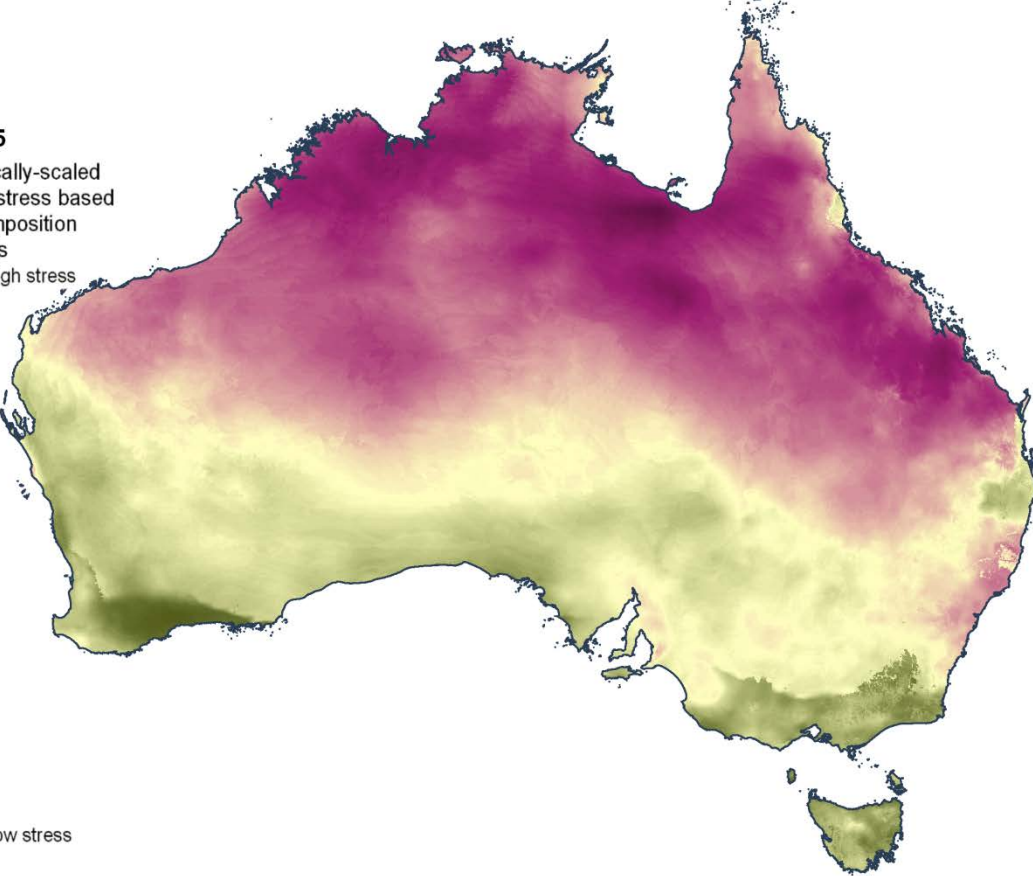
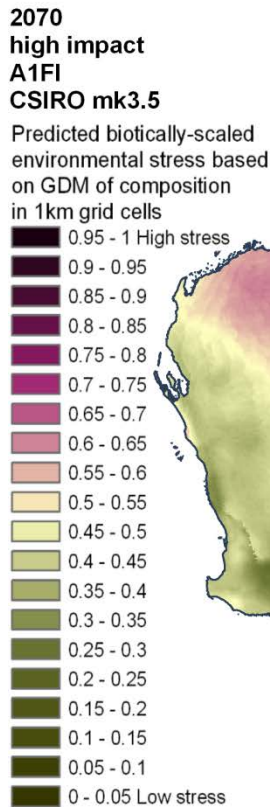
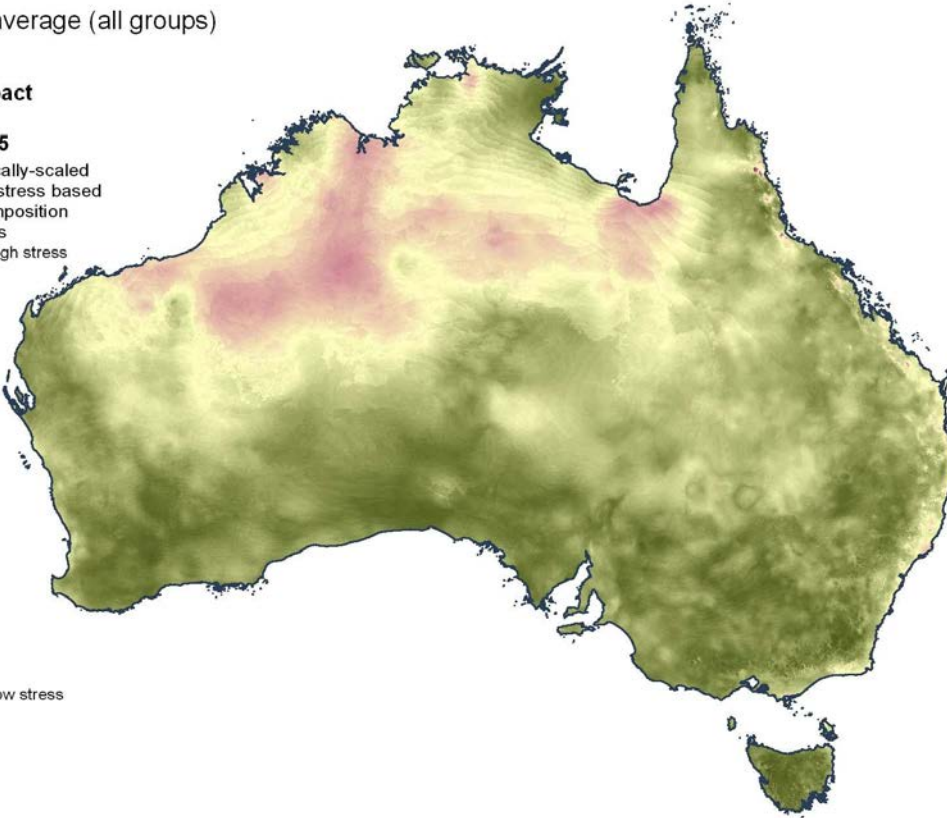
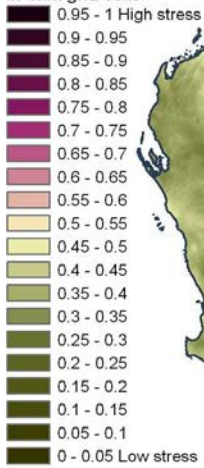


**Figure 8b Predicted dissimilarity between the current composition of each 1 km<sup>2</sup> grid cell and its potential composition under each of the 2070 climate scenarios, for mammals**

Weighted average (all groups)

**2030  
medium impact  
A1B  
CSIRO mk3.5**

Predicted biotically-scaled  
environmental stress based  
on GDM of composition  
in 1km grid cells



Weighted average (all groups)

**2030  
high impact  
A1F1  
CSIRO mk3.5**

Predicted biotically-scaled  
environmental stress based  
on GDM of composition  
in 1km grid cells

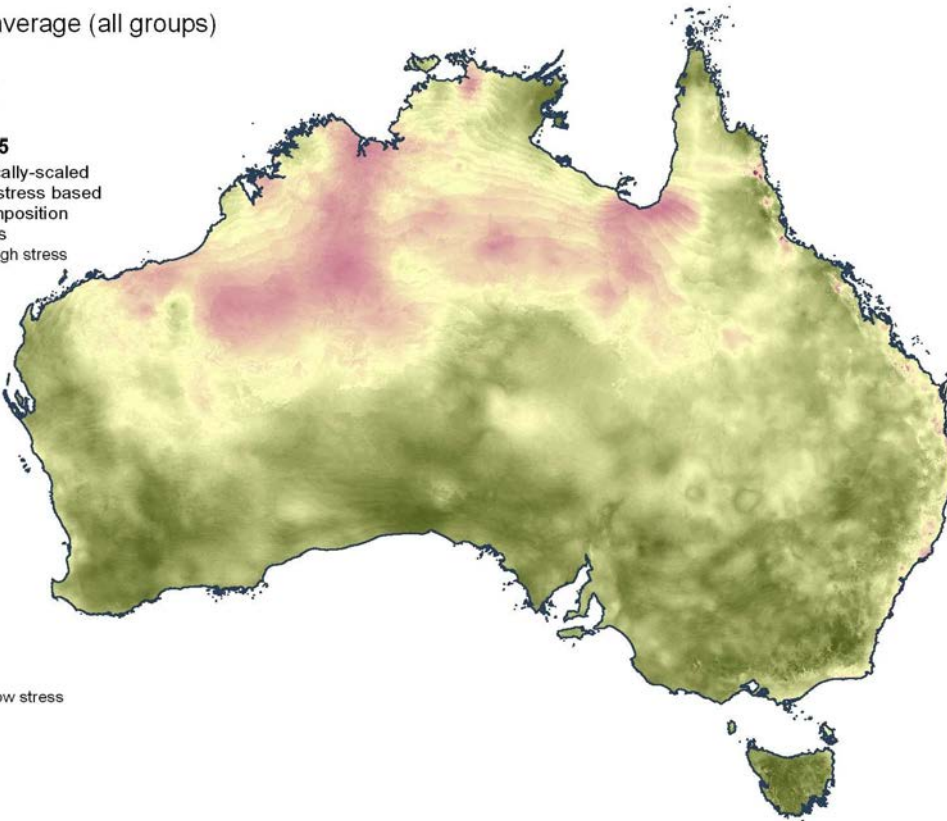
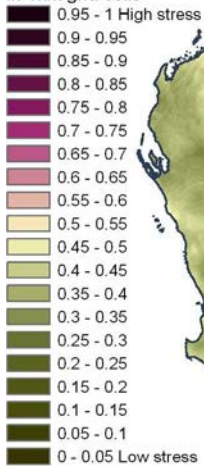
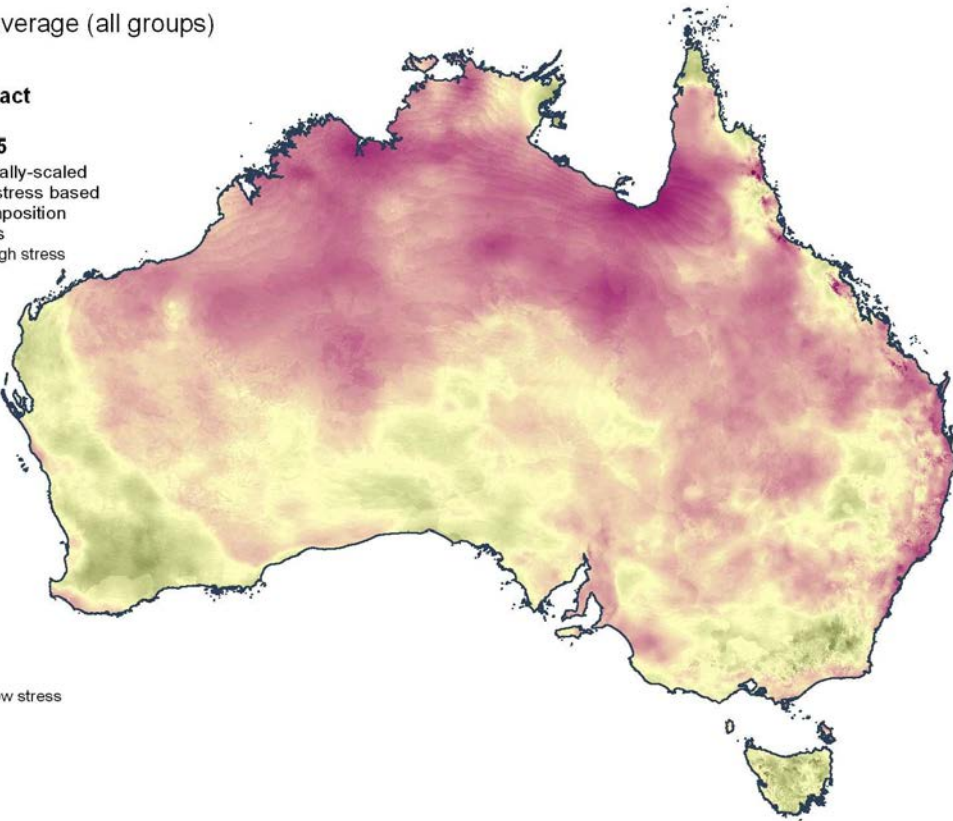
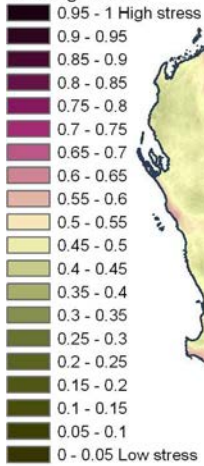


**Figure 9a Predicted dissimilarity between the current composition of each 1 km<sup>2</sup> grid cell and its potential composition under each of the 2030 climate scenarios – weighted average of the results for all six biological groups, where each group is weighted according to the total amount of spatial turnover exhibited by the group under current climate conditions**

Weighted average (all groups)

**2070  
medium impact  
A1B  
CSIRO mk3.5**

Predicted biotically-scaled  
environmental stress based  
on GDM of composition  
in 1km grid cells



Weighted average (all groups)

**2070  
high impact  
A1FI  
CSIRO mk3.5**

Predicted biotically-scaled  
environmental stress based  
on GDM of composition  
in 1km grid cells

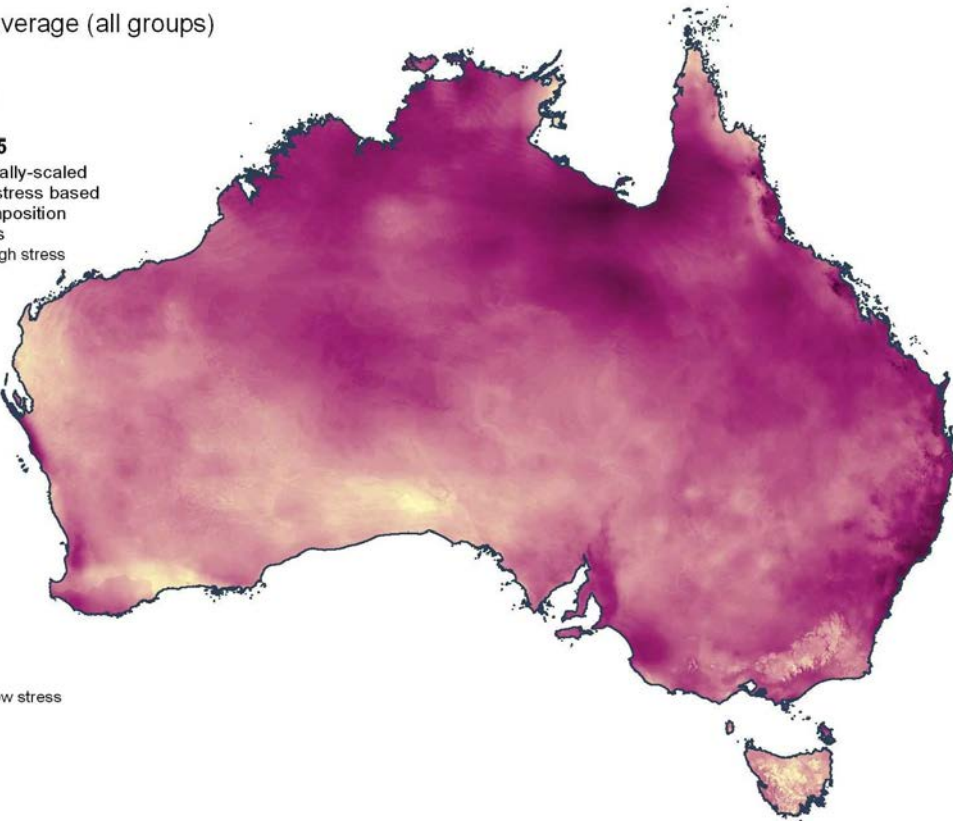
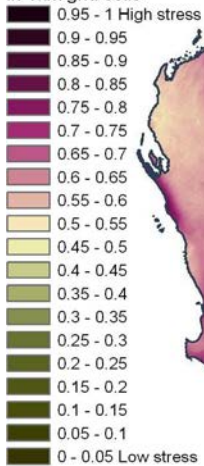


**Figure 9b Predicted dissimilarity between the current composition of each 1 km<sup>2</sup> grid cell and its potential composition under each of the 2070 climate scenarios – weighted average of the results for all six biological groups, where each group is weighted according to the total amount of spatial turnover exhibited by the group under current climate conditions**

## IBRA Bioregions

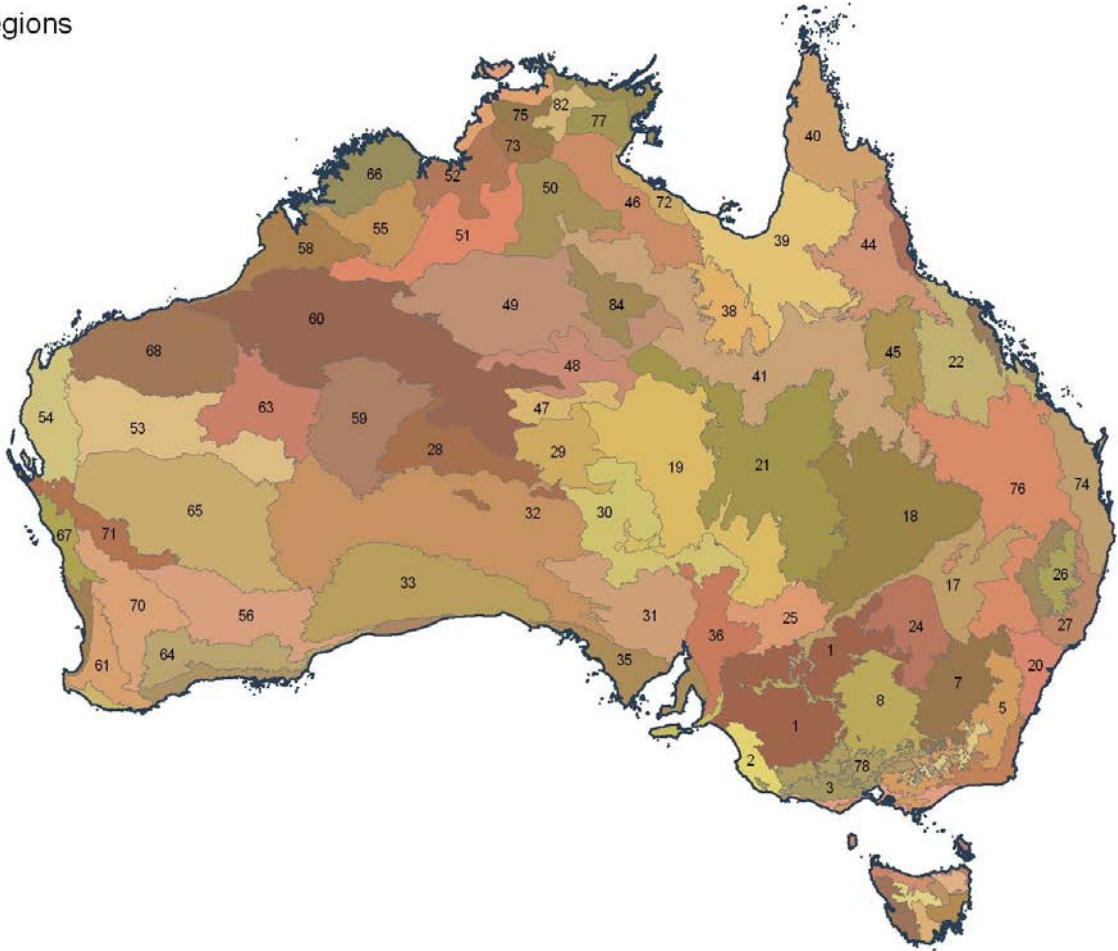


**Figure 10** Location of the IBRA bioregions used in this analysis

The larger bioregions are numbered according to the index in Tables 2 and 3

**Table 2 Mean predicted dissimilarity between the current composition of each 1 km<sup>2</sup> grid cell and its potential composition under each of the four climate scenarios (years 2030, 2070 and change rates M, A1B medium climate sensitivity and H, A1FI high climate sensitivity) as an average for the whole continent (Mean) and for each of the IBRA bioregions – for vascular plants**

IBRA BIOREGION	2030	2030	2070	2070	IBRA BIOREGION	2030	2030	2070	2070
	M	H	M	H		M	H	M	H
Mean	0.496	0.537	0.709	0.853	43 Central Mackay Coast	0.451	0.488	0.646	0.868
1 Murray Darling Depression	0.412	0.455	0.658	0.811	44 Einasleigh Uplands	0.462	0.501	0.666	0.839
2 Naracoorte Coastal Plain	0.420	0.460	0.648	0.857	45 Desert Uplands	0.489	0.550	0.791	0.921
3 Victorian Volcanic Plain	0.408	0.453	0.636	0.840	46 Gulf Fall and Uplands	0.521	0.579	0.771	0.930
4 South East Coastal Plain	0.478	0.522	0.683	0.853	47 MacDonnell Ranges	0.459	0.498	0.717	0.898
5 South Eastern Highlands	0.410	0.453	0.632	0.837	48 Burt Plain	0.503	0.536	0.742	0.898
6 Australian Alps	0.306	0.333	0.473	0.753	49 Tanami	0.629	0.655	0.792	0.907
7 NSW South Western Slopes	0.427	0.482	0.693	0.856	50 Sturt Plateau	0.570	0.616	0.784	0.923
8 Riverina	0.410	0.453	0.664	0.813	51 Ord Victoria Plain	0.628	0.661	0.789	0.911
9 Flinders	0.471	0.502	0.640	0.816	52 Victoria Bonaparte	0.600	0.641	0.800	0.926
10 South East Corner	0.501	0.542	0.689	0.844	53 Gascoyne	0.577	0.619	0.734	0.851
11 Ben Lomond	0.337	0.365	0.513	0.713	54 Carnarvon	0.433	0.475	0.628	0.776
12 Tasmanian Northern Midlands	0.359	0.397	0.567	0.756	55 Central Kimberley	0.670	0.706	0.823	0.930
13 Tasmanian South East	0.385	0.414	0.556	0.748	56 Coolgardie	0.387	0.430	0.630	0.770
14 Tasmanian West	0.297	0.335	0.510	0.728	57 Esperance Plains	0.426	0.461	0.597	0.752
15 Tasmanian Southern Ranges	0.283	0.307	0.437	0.644	58 Dampierland	0.587	0.627	0.772	0.893
16 Tasmanian Central Highlands	0.283	0.307	0.441	0.644	59 Gibson Desert	0.575	0.631	0.772	0.899
17 Darling Riverine Plains	0.473	0.511	0.679	0.826	60 Great Sandy Desert	0.659	0.690	0.801	0.909
18 Mulga Lands	0.501	0.541	0.739	0.874	61 Jarrah Forest	0.400	0.435	0.590	0.820
19 Simpson Strzelecki Dunefields	0.496	0.535	0.742	0.887	62 Warren	0.455	0.497	0.664	0.854
20 Sydney Basin	0.491	0.541	0.722	0.882	63 Little Sandy Desert	0.661	0.685	0.760	0.876
21 Channel Country	0.517	0.567	0.755	0.892	64 Mallee	0.404	0.432	0.559	0.739
22 Brigalow Belt North	0.456	0.497	0.702	0.895	65 Murchison	0.488	0.538	0.690	0.822
23 Nandewar	0.435	0.477	0.643	0.817	66 Northern Kimberley	0.584	0.624	0.780	0.905
24 Cobar Penepplain	0.445	0.492	0.696	0.815	67 Geraldton Sandplains	0.555	0.586	0.703	0.843
25 Broken Hill Complex	0.397	0.440	0.705	0.820	68 Pilbara	0.626	0.656	0.764	0.876
26 New England Tablelands	0.470	0.519	0.694	0.859	69 Swan Coastal Plain	0.536	0.570	0.691	0.854
27 NSW North Coast	0.563	0.605	0.760	0.903	70 Avon Wheatbelt	0.424	0.454	0.601	0.798
28 Central Ranges	0.460	0.493	0.704	0.874	71 Yalgoo	0.504	0.530	0.656	0.828
29 Finke	0.447	0.466	0.650	0.852	72 Gulf Coastal	0.481	0.536	0.750	0.917
30 Stony Plains	0.467	0.497	0.685	0.815	73 Daly Basin	0.481	0.534	0.728	0.908
31 Gawler	0.327	0.358	0.577	0.758	74 South Eastern Queensland	0.540	0.581	0.724	0.855
32 Great Victoria Desert	0.365	0.402	0.604	0.759	75 Pine Creek	0.500	0.549	0.726	0.892
33 Nullarbor	0.347	0.395	0.628	0.711	76 Brigalow Belt South	0.467	0.511	0.694	0.865
34 Hampton	0.436	0.462	0.695	0.745	77 Central Arnhem	0.368	0.427	0.621	0.839
35 Eyre Yorke Block	0.415	0.461	0.645	0.807	78 Victorian Midlands	0.399	0.440	0.618	0.837
36 Flinders Lofty Block	0.408	0.451	0.683	0.812	79 Darwin Coastal	0.505	0.553	0.721	0.886
37 Kanmantoo	0.439	0.483	0.673	0.866	80 Tasmanian Northern Slopes	0.289	0.318	0.477	0.695
38 Mount Isa Inlier	0.635	0.698	0.836	0.950	81 Arnhem Coast	0.384	0.421	0.589	0.799
39 Gulf Plains	0.558	0.607	0.780	0.918	82 Arnhem Plateau	0.503	0.550	0.699	0.864
40 Cape York Peninsula	0.453	0.502	0.657	0.813	83 Tiwi Cobourg	0.451	0.502	0.678	0.830
41 Mitchell Grass Downs	0.561	0.623	0.800	0.925	84 Davenport Murchison Ranges	0.666	0.698	0.826	0.931
42 Wet Tropics	0.458	0.487	0.654	0.860	85 King	0.358	0.392	0.546	0.744

Potential change by bioregion : Vascular plants

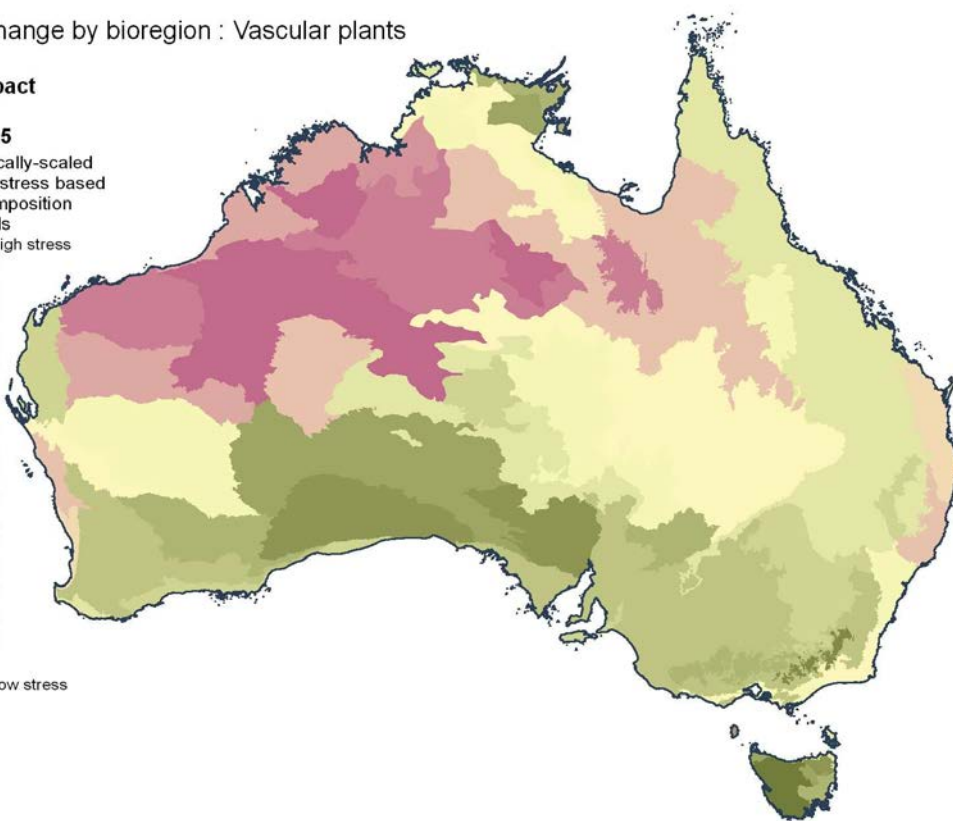
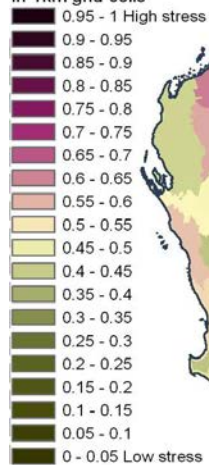
2030

medium impact

A1B

CSIRO mk3.5

Predicted biotically-scaled environmental stress based on GDM of composition in 1km grid cells



Potential change by bioregion : Vascular plants

2030

high impact

A1F1

CSIRO mk3.5

Predicted biotically-scaled environmental stress based on GDM of composition in 1km grid cells

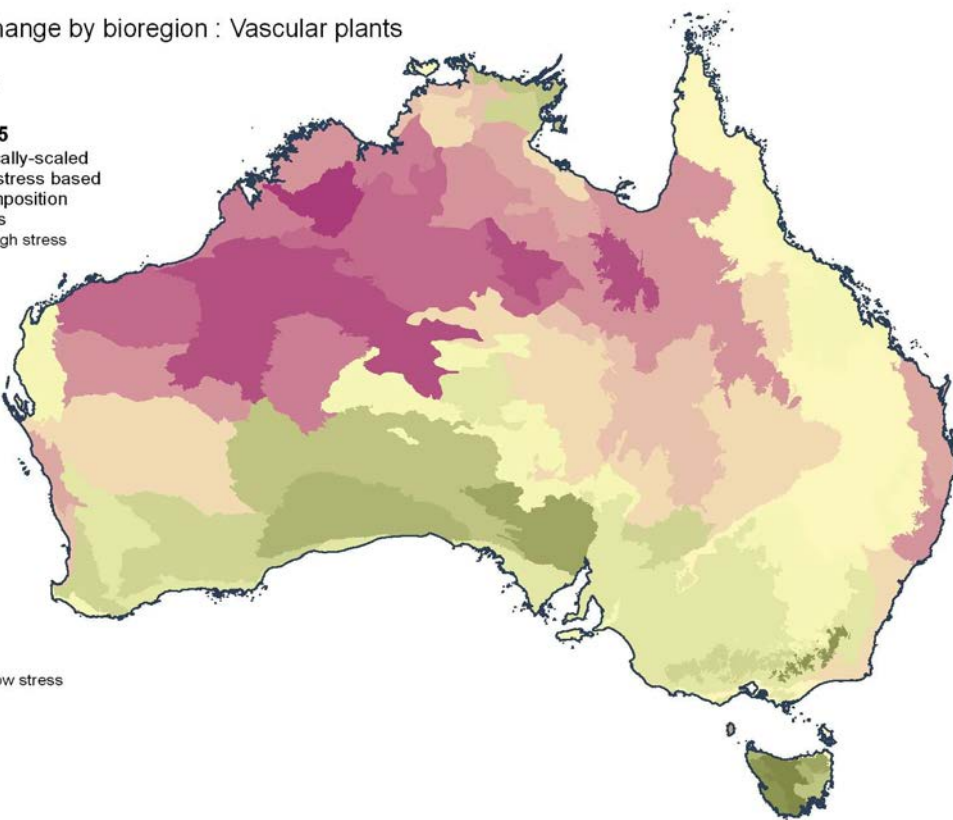
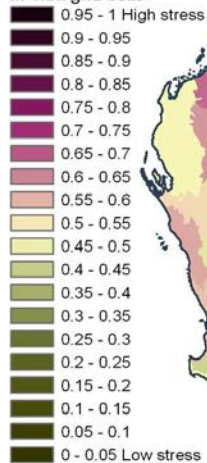
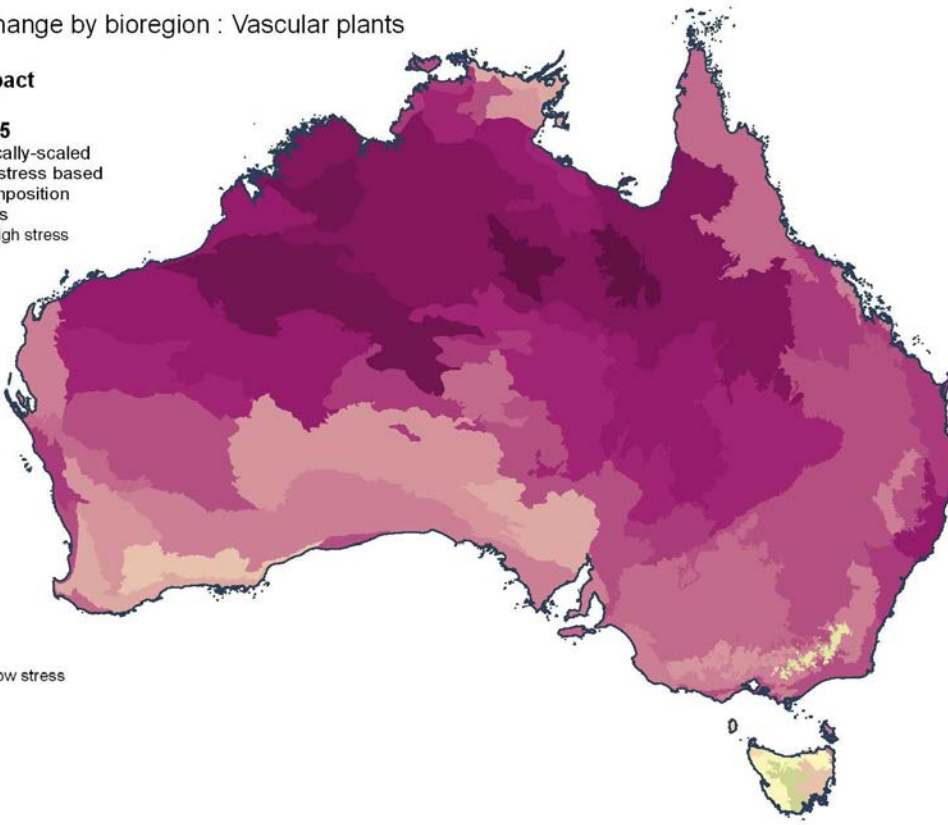
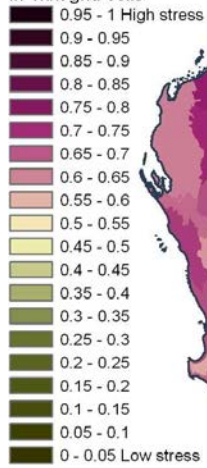


Figure 11a Mean predicted dissimilarity between the current composition of each 1 km<sup>2</sup> grid cell and its potential composition under each of 2030 scenarios, as an average for each of the IBRA bioregions – for vascular plants

Potential change by bioregion : Vascular plants  
 2070  
 medium impact  
 A1B

CSIRO mk3.5  
 Predicted biotically-scaled  
 environmental stress based  
 on GDM of composition  
 in 1km grid cells



Potential change by bioregion : Vascular plants  
 2070  
 high impact  
 A1F1

CSIRO mk3.5  
 Predicted biotically-scaled  
 environmental stress based  
 on GDM of composition  
 in 1km grid cells

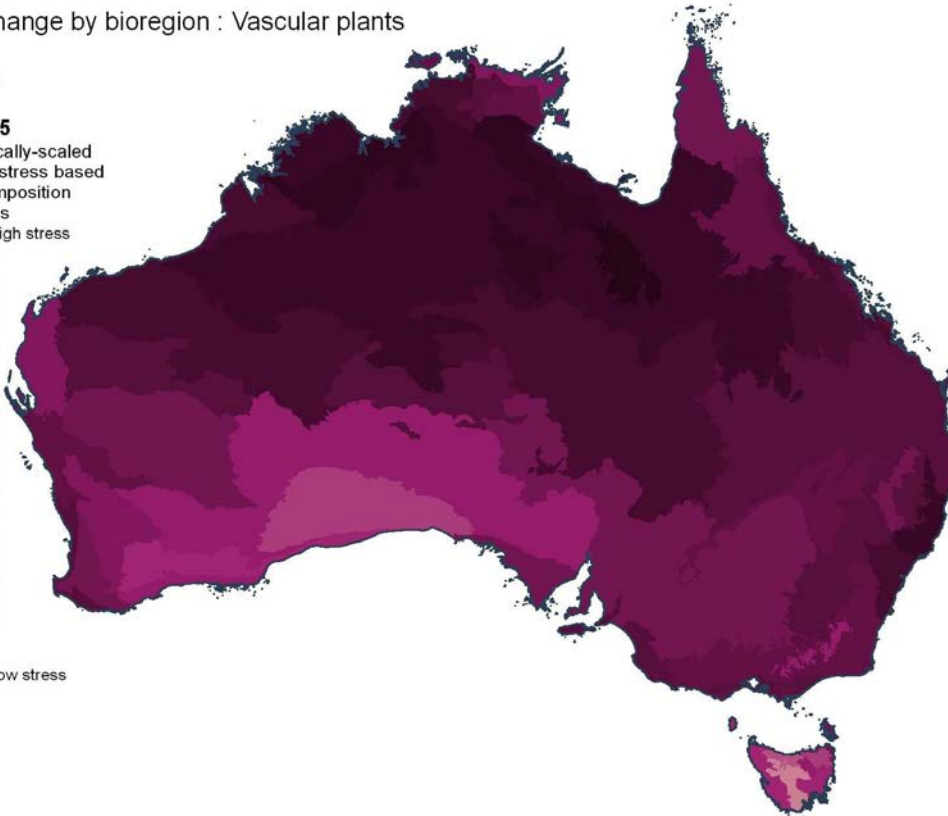
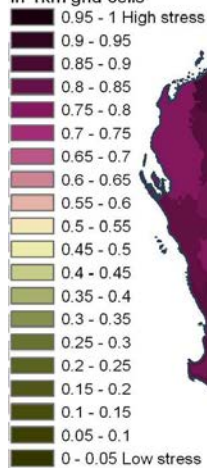


Figure 11b Mean predicted dissimilarity between the current composition of each 1 km<sup>2</sup> grid cell and its potential composition under each of 2070 scenarios, as an average for each of the IBRA bioregions – for vascular plants

Potential change by bioregion : Weighted average (all groups)

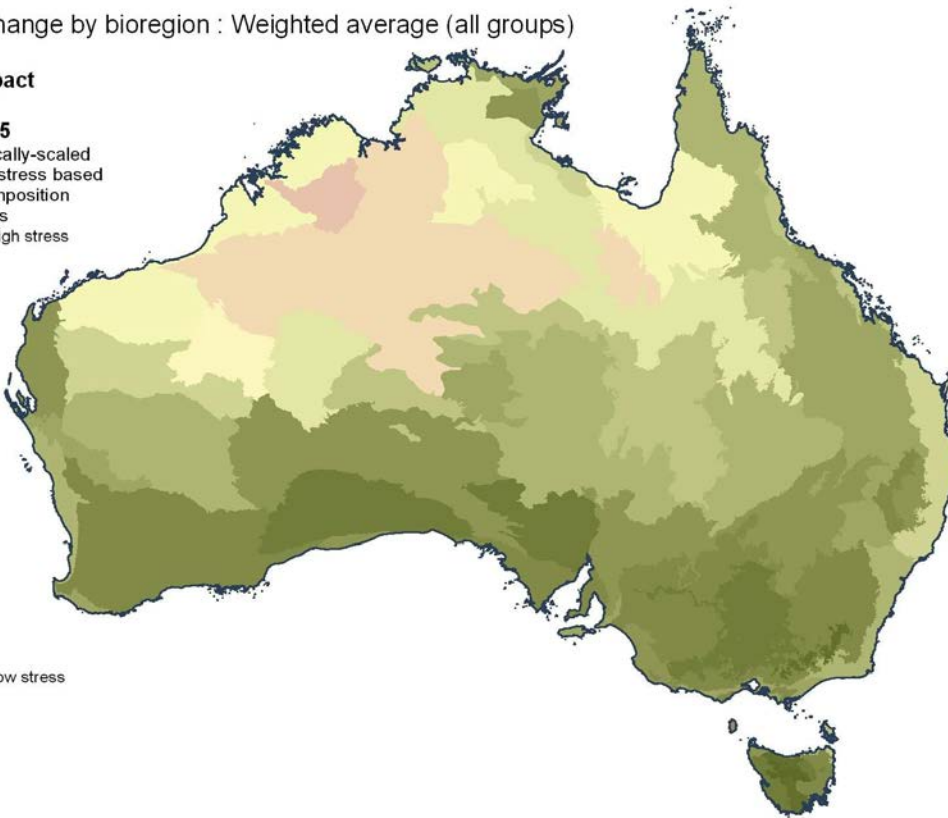
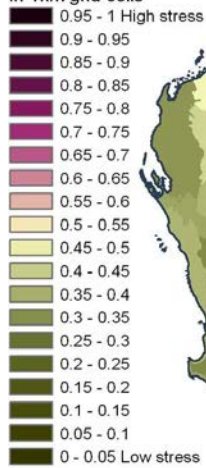
2030

medium impact

A1B

CSIRO mk3.5

Predicted biotically-scaled environmental stress based on GDM of composition in 1km grid cells



Potential change by bioregion : Weighted average (all groups)

2030

high impact

A1F1

CSIRO mk3.5

Predicted biotically-scaled environmental stress based on GDM of composition in 1km grid cells

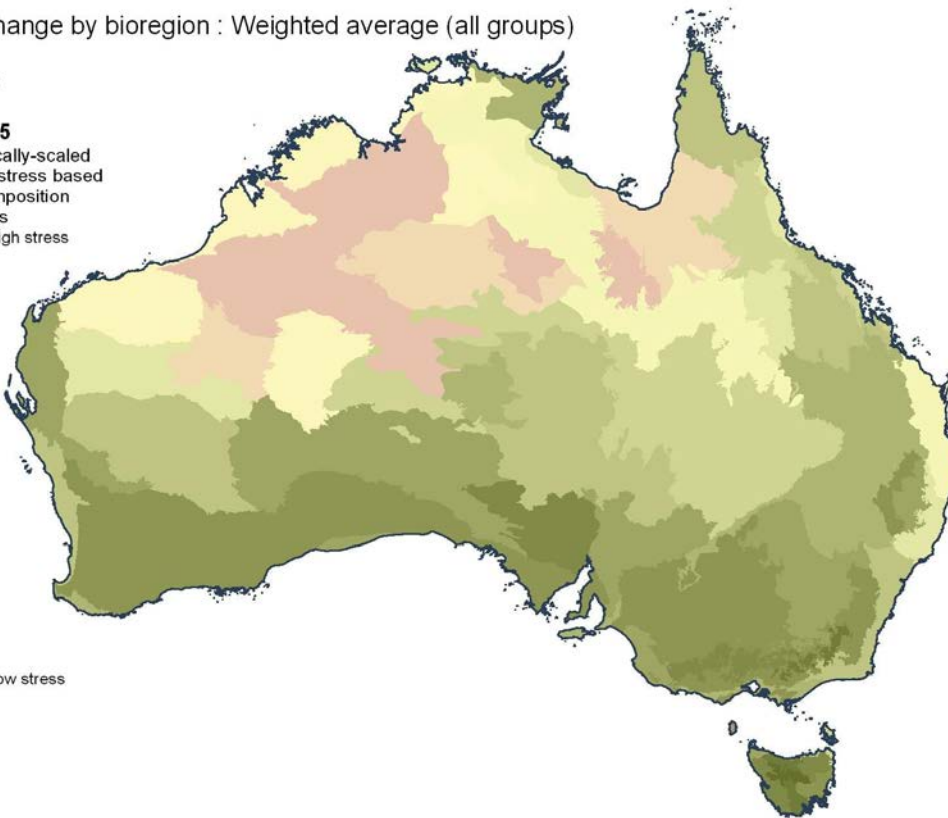
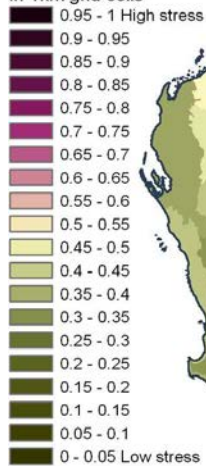
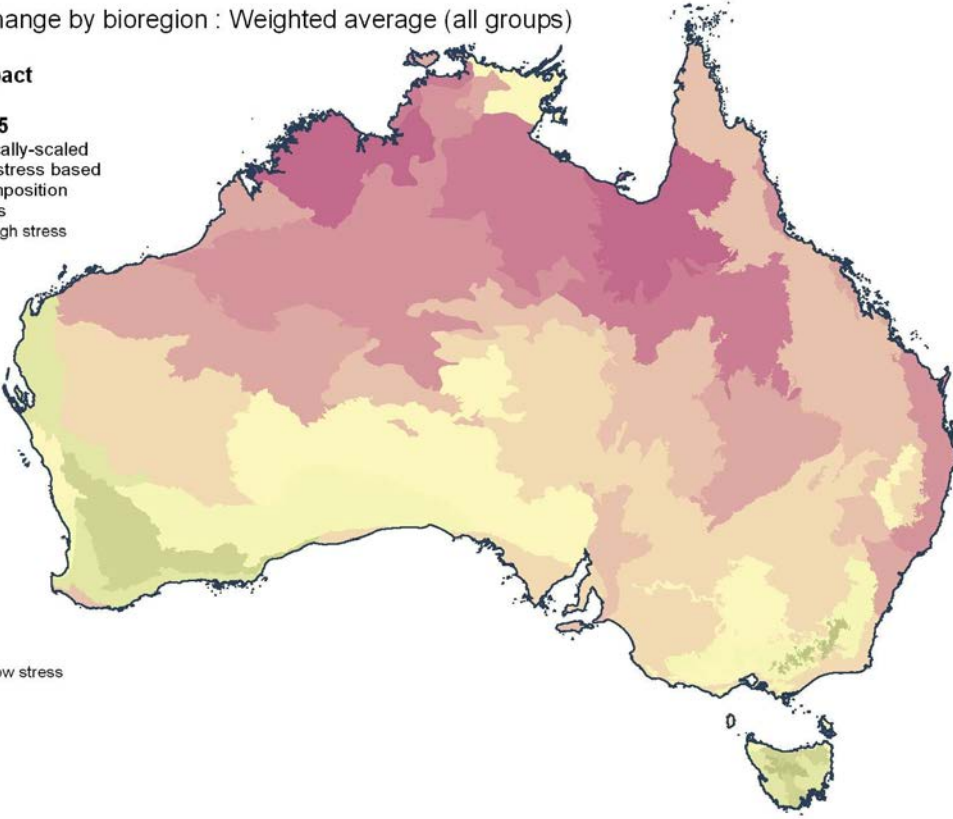


Figure 12a Mean predicted dissimilarity between the current composition of each 1 km<sup>2</sup> grid cell and its potential composition under each of 2030 scenarios, as an average for each of the IBRA bioregions – weighted average of the results for all six biological groups, where each group is weighted according to the total amount of spatial turnover exhibited by the group under current climate conditions

Potential change by bioregion : Weighted average (all groups)  
**2070**  
**medium impact**  
**A1B**

**CSIRO mk3.5**  
 Predicted biotically-scaled  
 environmental stress based  
 on GDM of composition  
 in 1km grid cells

- 0.95 - 1 High stress
- 0.9 - 0.95
- 0.85 - 0.9
- 0.8 - 0.85
- 0.75 - 0.8
- 0.7 - 0.75
- 0.65 - 0.7
- 0.6 - 0.65
- 0.55 - 0.6
- 0.5 - 0.55
- 0.45 - 0.5
- 0.4 - 0.45
- 0.35 - 0.4
- 0.3 - 0.35
- 0.25 - 0.3
- 0.2 - 0.25
- 0.15 - 0.2
- 0.1 - 0.15
- 0.05 - 0.1
- 0 - 0.05 Low stress



Potential change by bioregion : Weighted average (all groups)  
**2070**  
**high impact**  
**A1F1**

**CSIRO mk3.5**  
 Predicted biotically-scaled  
 environmental stress based  
 on GDM of composition  
 in 1km grid cells

- 0.95 - 1 High stress
- 0.9 - 0.95
- 0.85 - 0.9
- 0.8 - 0.85
- 0.75 - 0.8
- 0.7 - 0.75
- 0.65 - 0.7
- 0.6 - 0.65
- 0.55 - 0.6
- 0.5 - 0.55
- 0.45 - 0.5
- 0.4 - 0.45
- 0.35 - 0.4
- 0.3 - 0.35
- 0.25 - 0.3
- 0.2 - 0.25
- 0.15 - 0.2
- 0.1 - 0.15
- 0.05 - 0.1
- 0 - 0.05 Low stress

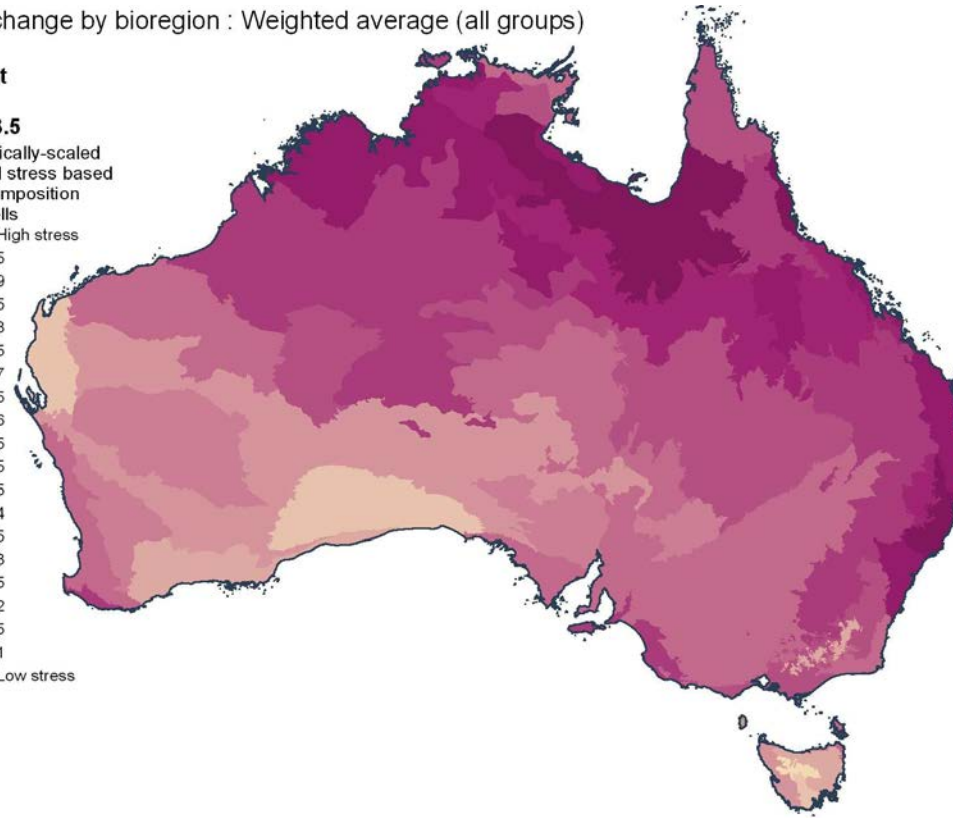


**Figure 12b** Mean predicted dissimilarity between the current composition of each 1 km<sup>2</sup> grid cell and its potential composition under each of 2070 scenarios, as an average for each of the IBRA bioregions – weighted average of the results for all six biological groups, where each group is weighted according to the total amount of spatial turnover exhibited by the group under current climate conditions

**Table 3 Mean predicted dissimilarity between the current composition of each 1 km<sup>2</sup> grid cell and its potential composition under each of the four climate scenarios (years 2030, 2070 and change rates M, A1B medium climate sensitivity and H, A1FI high climate sensitivity), as an average for the whole continent (Mean) and for each of the IBRA bioregions – weighted average of the results for all six biological groups, where each group is weighted according to the total amount of spatial turnover exhibited by the group under current climate conditions**

IBRA BIOREGION		2030	2030	2070	2070	IBRA BIOREGION		2030	2030	2070	2070
		M	H	M	H			M	H	M	H
Mean		<b>0.404</b>	<b>0.432</b>	<b>0.561</b>	<b>0.682</b>	43	Central Mackay Coast	0.414	0.449	0.585	0.769
1	Murray Darling Depression	0.312	0.341	0.534	0.662	44	Einasleigh Uplands	0.389	0.426	0.571	0.714
2	Naracoorte Coastal Plain	0.335	0.361	0.546	0.717	45	Desert Uplands	0.415	0.457	0.632	0.762
3	Victorian Volcanic Plain	0.303	0.329	0.510	0.670	46	Gulf Fall and Uplands	0.456	0.495	0.642	0.775
4	South East Coastal Plain	0.363	0.392	0.534	0.694	47	MacDonnell Ranges	0.379	0.406	0.547	0.693
5	South Eastern Highlands	0.319	0.347	0.495	0.683	48	Burt Plain	0.415	0.439	0.571	0.697
6	Australian Alps	0.262	0.277	0.414	0.599	49	Tanami	0.525	0.538	0.615	0.712
7	NSW South Western Slopes	0.316	0.354	0.531	0.716	50	Sturt Plateau	0.496	0.523	0.643	0.755
8	Riverina	0.299	0.326	0.508	0.667	51	Ord Victoria Plain	0.539	0.554	0.622	0.723
9	Flinders	0.411	0.429	0.515	0.660	52	Victoria Bonaparte	0.532	0.559	0.670	0.770
10	South East Corner	0.392	0.417	0.529	0.675	53	Gascoyne	0.443	0.468	0.542	0.623
11	Ben Lomond	0.303	0.322	0.435	0.583	54	Carnarvon	0.340	0.367	0.464	0.570
12	Tasmanian Northern Midlands	0.286	0.307	0.467	0.589	55	Central Kimberley	0.554	0.574	0.656	0.760
13	Tasmanian South East	0.312	0.328	0.461	0.595	56	Coolgardie	0.300	0.333	0.495	0.617
14	Tasmanian West	0.281	0.308	0.462	0.620	57	Esperance Plains	0.316	0.338	0.457	0.583
15	Tasmanian Southern Ranges	0.266	0.282	0.430	0.573	58	Dampierland	0.491	0.510	0.596	0.714
16	Tasmanian Central Highlands	0.246	0.262	0.408	0.539	59	Gibson Desert	0.474	0.503	0.593	0.700
17	Darling Riverine Plains	0.348	0.375	0.527	0.663	60	Great Sandy Desert	0.542	0.557	0.619	0.707
18	Mulga Lands	0.398	0.426	0.584	0.691	61	Jarrah Forest	0.314	0.339	0.469	0.662
19	Simpson Strzelecki Dunefields	0.389	0.411	0.534	0.650	62	Warren	0.358	0.389	0.558	0.718
20	Sydney Basin	0.383	0.420	0.577	0.768	63	Little Sandy Desert	0.514	0.528	0.578	0.662
21	Channel Country	0.416	0.443	0.568	0.680	64	Mallee	0.309	0.331	0.441	0.593
22	Brigalow Belt North	0.370	0.404	0.564	0.744	65	Murchison	0.388	0.419	0.530	0.626
23	Nandewar	0.314	0.343	0.524	0.702	66	Northern Kimberley	0.490	0.522	0.665	0.758
24	Cobar Penepplain	0.332	0.364	0.544	0.661	67	Geraldton Sandplains	0.393	0.415	0.505	0.660
25	Broken Hill Complex	0.326	0.353	0.548	0.638	68	Pilbara	0.498	0.515	0.584	0.670
26	New England Tablelands	0.336	0.370	0.548	0.732	69	Swan Coastal Plain	0.384	0.406	0.489	0.657
27	NSW North Coast	0.433	0.464	0.608	0.794	70	Avon Wheatbelt	0.311	0.332	0.445	0.626
28	Central Ranges	0.408	0.433	0.567	0.702	71	Yalgoo	0.355	0.373	0.470	0.625
29	Finke	0.373	0.388	0.506	0.655	72	Gulf Coastal	0.426	0.465	0.635	0.763
30	Stony Plains	0.382	0.401	0.527	0.621	73	Daly Basin	0.453	0.492	0.623	0.760
31	Gawler	0.298	0.322	0.506	0.626	74	South Eastern Queensland	0.439	0.476	0.615	0.751
32	Great Victoria Desert	0.331	0.359	0.500	0.611	75	Pine Creek	0.451	0.488	0.614	0.741
33	Nullarbor	0.294	0.331	0.496	0.570	76	Brigalow Belt South	0.357	0.392	0.554	0.713
34	Hampton	0.344	0.368	0.547	0.592	77	Central Arnhem	0.337	0.380	0.521	0.678
35	Eyre Yorke Block	0.318	0.349	0.529	0.663	78	Victorian Midlands	0.296	0.319	0.490	0.667
36	Flinders Lofty Block	0.325	0.355	0.561	0.670	79	Darwin Coastal	0.468	0.506	0.628	0.762
37	Kanmantoo	0.361	0.391	0.558	0.719	80	Tasmanian Northern Slopes	0.271	0.290	0.439	0.580
38	Mount Isa Inlier	0.528	0.566	0.669	0.797	81	Arnhem Coast	0.355	0.383	0.501	0.660
39	Gulf Plains	0.486	0.525	0.665	0.776	82	Arnhem Plateau	0.454	0.491	0.594	0.735
40	Cape York Peninsula	0.386	0.424	0.553	0.678	83	Tiwi Cobourg	0.414	0.455	0.587	0.721
41	Mitchell Grass Downs	0.462	0.500	0.626	0.750	84	Davenport Murchison Ranges	0.541	0.558	0.649	0.751
42	Wet Tropics	0.422	0.452	0.602	0.777	85	King	0.328	0.353	0.487	0.619

## 4.2 Disappearing and novel environments

All of the remaining analyses described in this report were performed only for the vascular plant group and the 2070 scenarios.

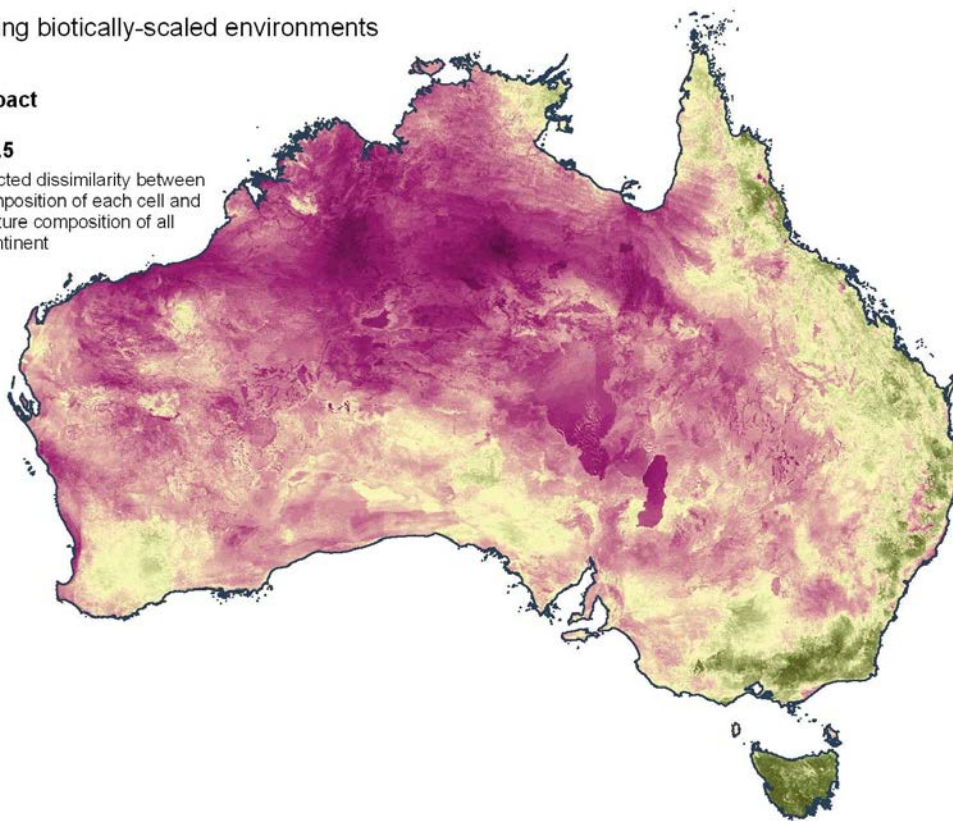
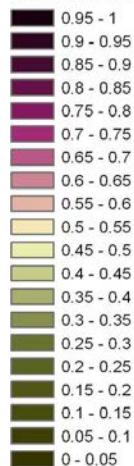
The minimum predicted dissimilarity between the current vascular plant composition of each cell and the potential future composition of all cells on the continent under a given climate scenario was generated as an indicator of 'disappearing [biotically scaled] environments' (as per Williams et al. 2007). This was repeated for both the 2070 medium-impact and 2070 high-impact scenarios (Figure 13). Higher values (dark pinks) indicate environments that are less likely to be found anywhere on the continent under the scenario, while low values (greens) indicate environments that are most likely to exist somewhere on the continent.

Conversely, the minimum predicted dissimilarity between the future composition of each cell under a given scenario and the current composition of all cells on the continent was generated as an indicator of 'novel or no-analogue [biotically scaled] environments' (as per Williams et al. 2007). Again, this was repeated for the 2070 medium-impact and high-impact scenarios (Figure 14). Higher values (dark pinks) indicate potential locations of future environments for which no analogue currently exists anywhere on the continent.

Disappearing biotically-scaled environments

**2070**  
**medium impact**  
**A1B**  
**CSIRO mk3.5**

Minimum predicted dissimilarity between the current composition of each cell and the potential future composition of all cells on the continent



Disappearing biotically-scaled environments

**2070**  
**high impact**  
**A1FI**  
**CSIRO mk3.5**

Minimum predicted dissimilarity between the current composition of each cell and the potential future composition of all cells on the continent

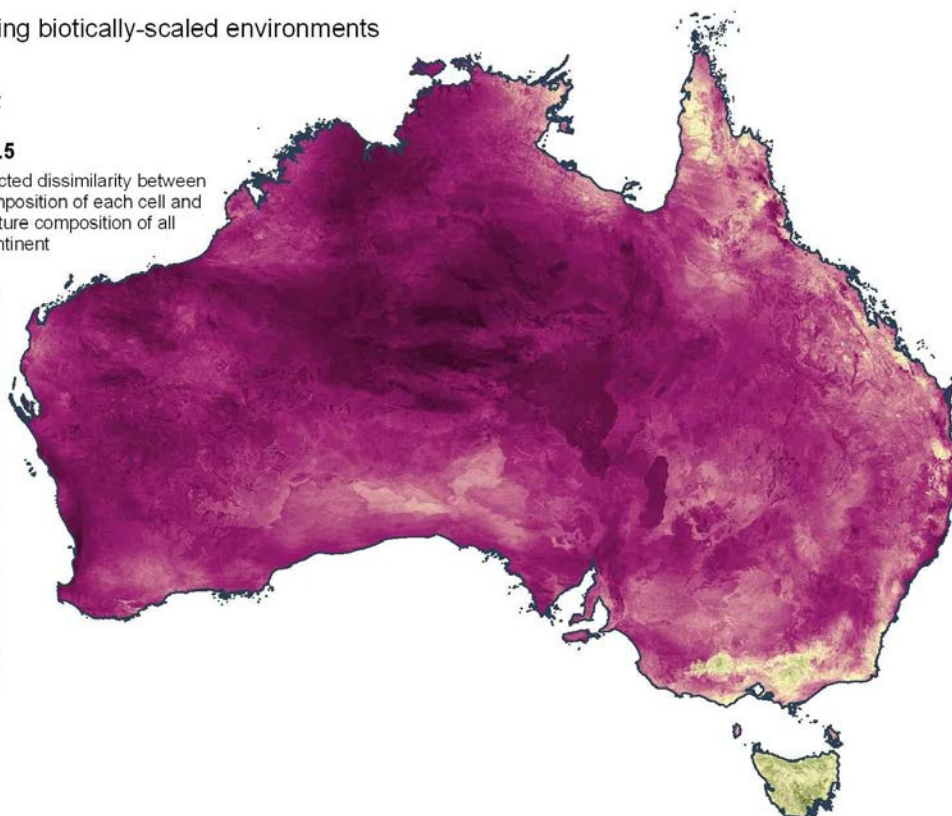
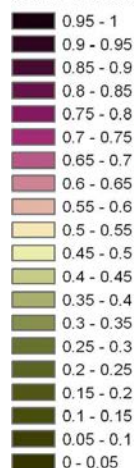
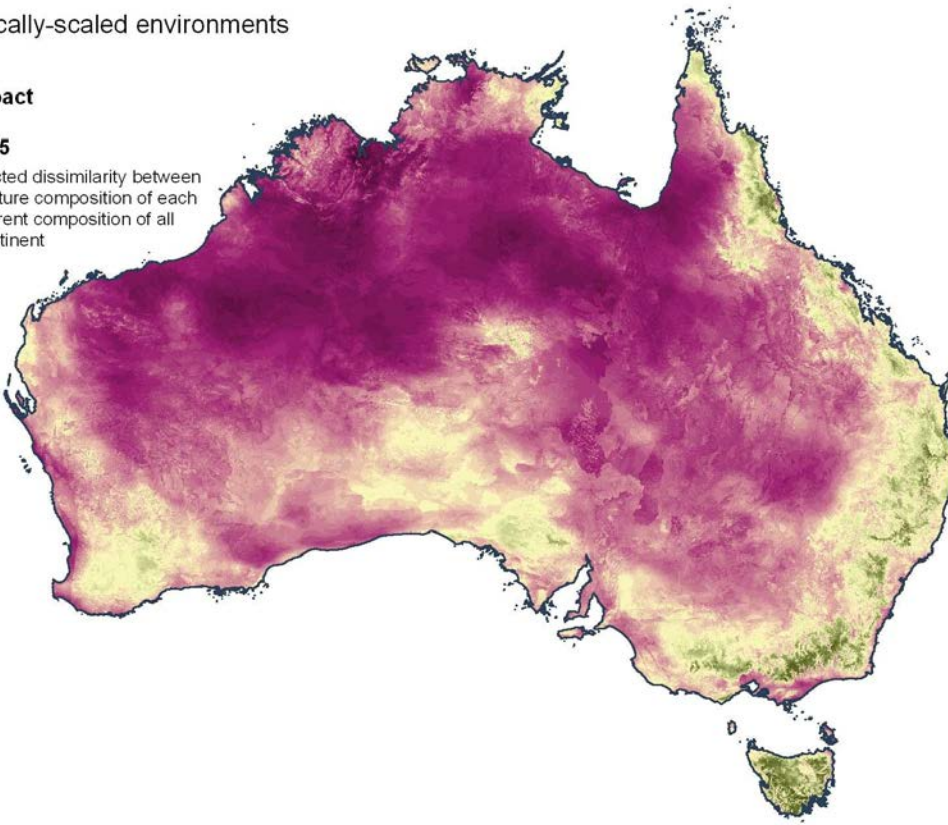
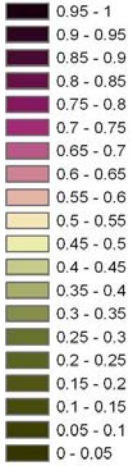


**Figure 13** Disappearing biotically scaled environments under 2070 medium-impact and high-impact scenarios, based on the vascular plant GDM. The colours depict different levels of minimum predicted dissimilarity between the current composition of each cell and the potential future composition of all cells on the continent for this scenario

Novel biotically-scaled environments

2070  
medium impact  
A1B  
CSIRO mk3.5

Minimum predicted dissimilarity between the potential future composition of each cell and the current composition of all cells on the continent



Novel biotically-scaled environments

2070  
high impact  
A1FI  
CSIRO mk3.5

Minimum predicted dissimilarity between the potential future composition of each cell and the current composition of all cells on the continent

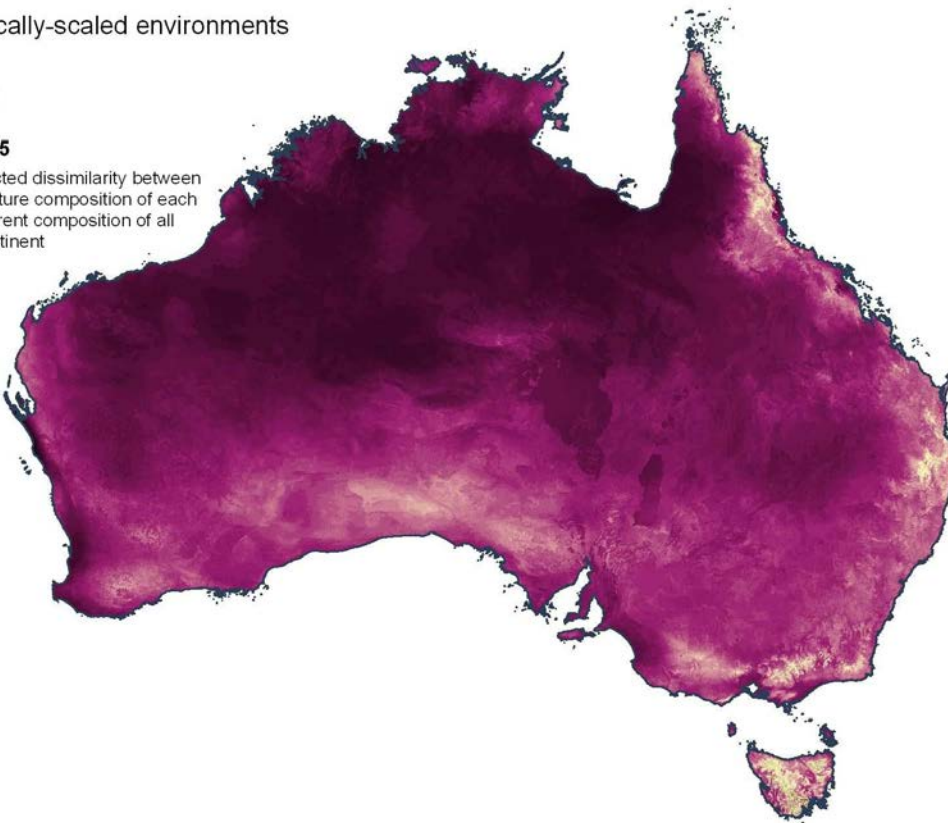
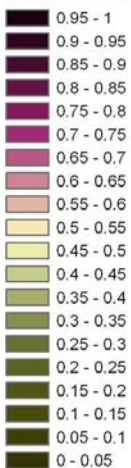


Figure 14 Novel biotically scaled environments under 2070 medium-impact and high-impact scenarios, based on the vascular plant GDM. The colours depict different levels of minimum predicted dissimilarity between the potential future composition of each cell and the current composition of all cells on the continent for this scenario

### 4.3 Potential for landscape buffering

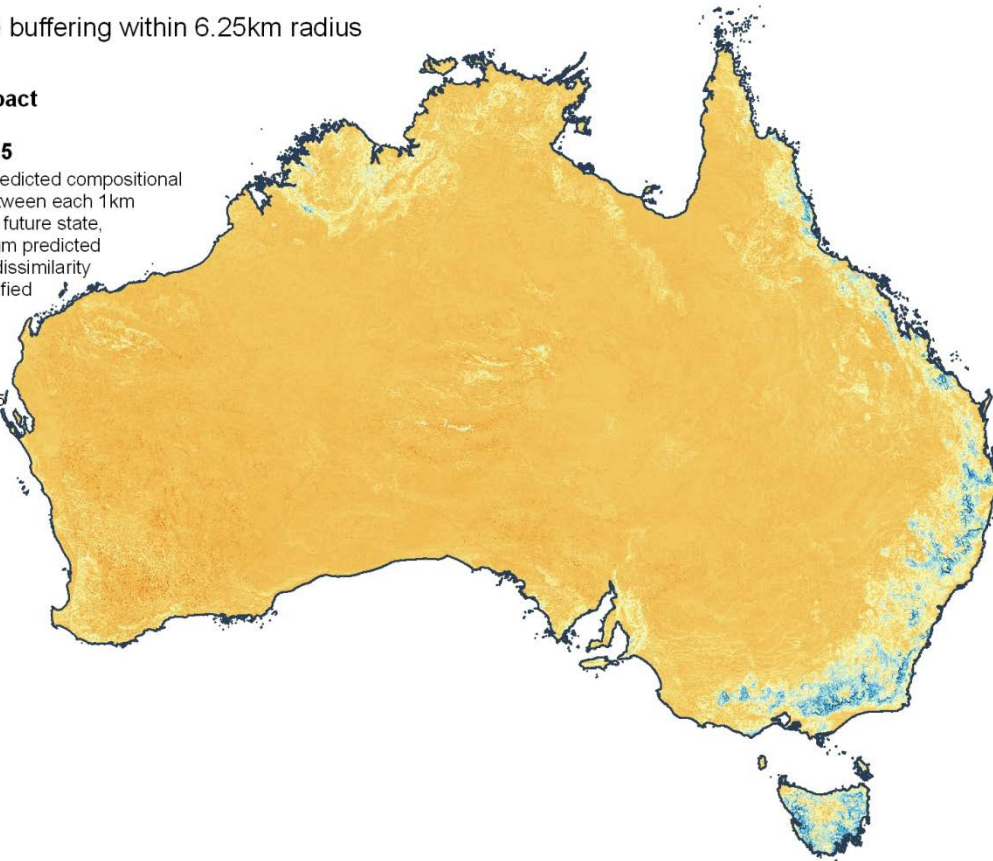
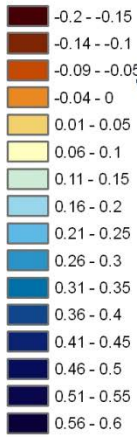
The presence of environmental diversity (heterogeneity) across a landscape may play a key role in ameliorating, or buffering, the effects of climate change on retention of compositional diversity within that landscape (Dunlop and Brown 2008). We therefore derived an index of the potential buffering effect of environmental heterogeneity in the landscape surrounding any given grid cell. This was calculated as the predicted dissimilarity between the current and future composition of the cell (from Section 4.1 above), minus the minimum predicted dissimilarity between the current composition of this cell and the future composition of any other cell within a specified radius. We derived this index using predictions from the vascular plant GDM for the 2070 medium-impact and high-impact scenarios, and using the following radii: 750 m, 1.5625 km, 3.125 km, 6.25 km, 12.5 km, 25 km, 50 km and 100 km.

Results for a representative selection of these combinations are presented in Figures 15–18 below, shown for radii of 6.25 km, 12.5 km, 50 km and 100 km. Note that a high value, which indicates good buffering, does not have any implications for the total area that provides the buffering within the radius. The high value refers only to the most similar 1 km<sup>2</sup> grid cell within the radius. Neutral colours indicate areas where the predicted future composition in the surrounding landscape is similar to the future composition of the focal cell. This will often be the case in topographically homogenous areas, where the landscape has a less heterogeneous mesoclimate. Darker browns indicate areas where the focal cell itself is the most similar cell under future conditions. Landscape buffering is shown in blues. Here some of the predicted future composition of the surrounding area is more similar to the present composition than the focal cell itself in the future. This is often the case for cells that have nearby cells with greater elevation, where a future increase in altitude can compensate for elevated temperature. The blue colour therefore tends to highlight the valley bottoms and hillsides. The tops of mountains cannot take advantage of this so are often poorly buffered. This effect is shown in more detail in Figure 19. Blue doughnut-shaped rings, particularly in the 25 km radius maps, tend to indicate situations where a large number of cells (the blue cells in the ring) are all looking to a specific elevated area for buffering.

Landscape buffering within 6.25km radius

**2070  
medium impact  
A1B  
CSIRO mk3.5**

Difference in predicted compositional dissimilarity between each 1km grid cell and its future state, and the minimum predicted compositional dissimilarity within the specified radius



Landscape buffering within 6.25km radius

**2070  
high impact  
A1FI  
CSIRO mk3.5**

Difference in predicted compositional dissimilarity between each 1km grid cell and its future state, and the minimum predicted compositional dissimilarity within the specified radius

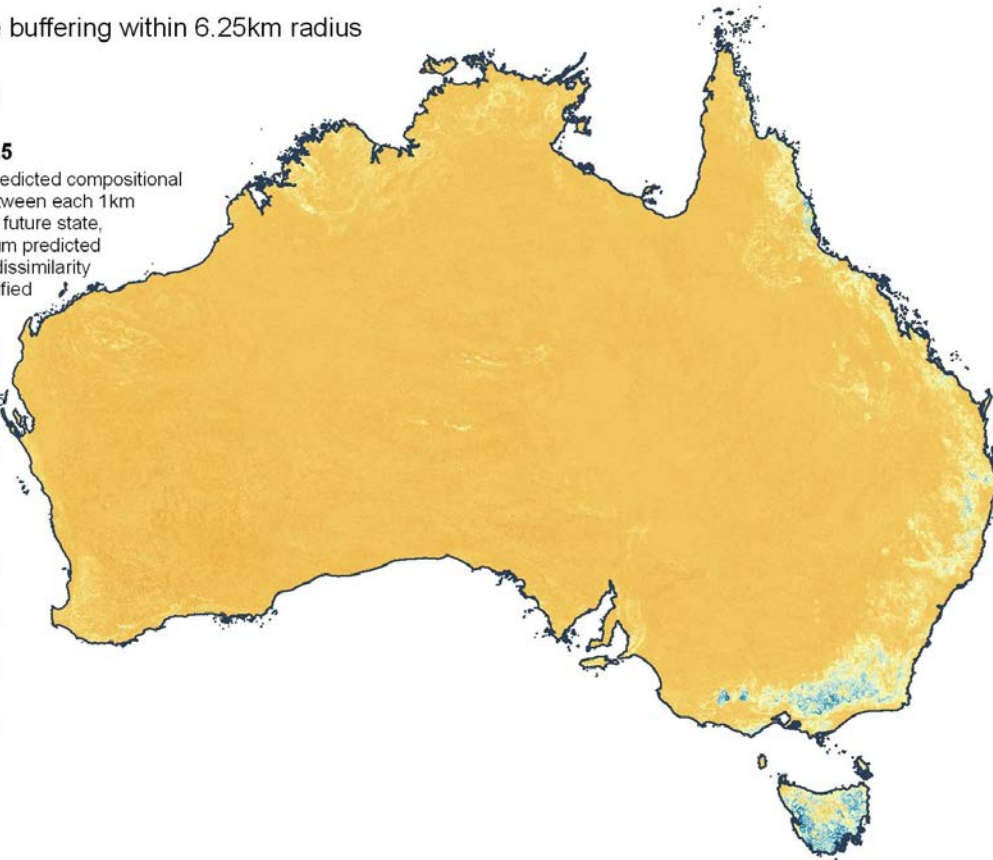
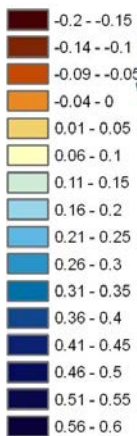
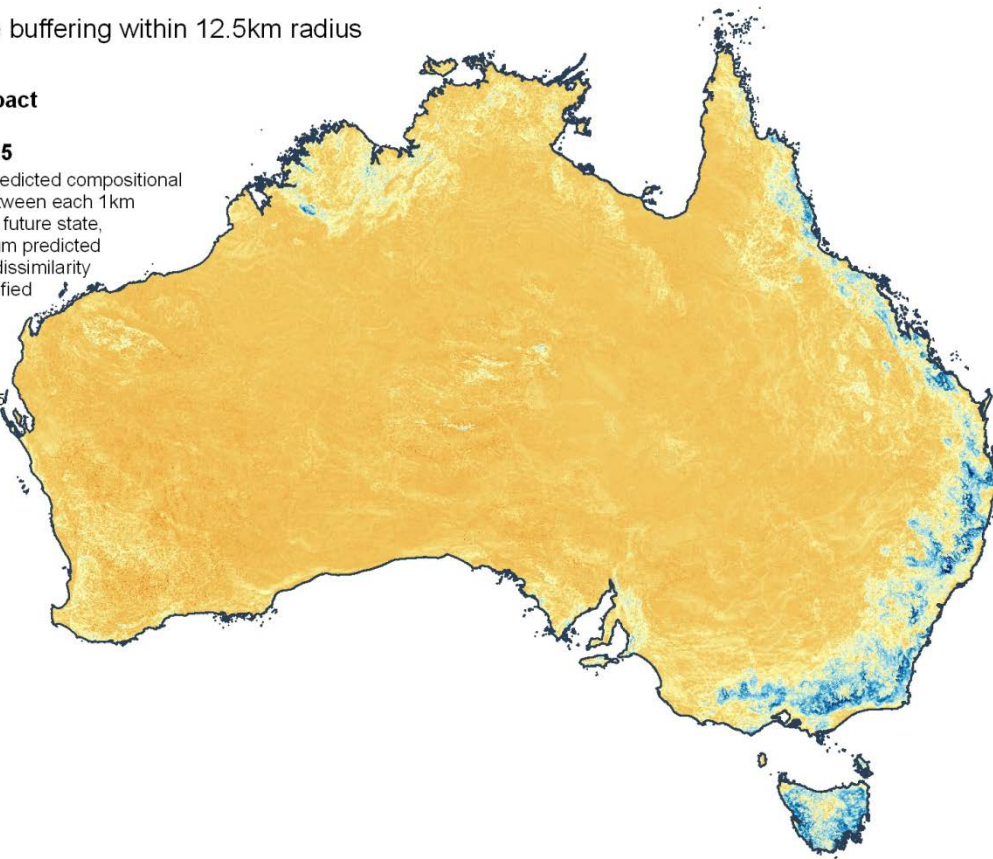
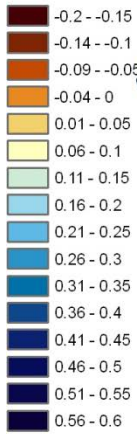


**Figure 15 Potential buffering of environmental heterogeneity in the landscape within 6.25 km under 2070 medium-impact and high-impact scenarios, based on the vascular plant GDM**

Landscape buffering within 12.5km radius

**2070**  
**medium impact**  
**A1B**  
**CSIRO mk3.5**

Difference in predicted compositional dissimilarity between each 1km grid cell and its future state, and the minimum predicted compositional dissimilarity within the specified radius



Landscape buffering within 12.5km radius

**2070**  
**high impact**  
**A1FI**  
**CSIRO mk3.5**

Difference in predicted compositional dissimilarity between each 1km grid cell and its future state, and the minimum predicted compositional dissimilarity within the specified radius

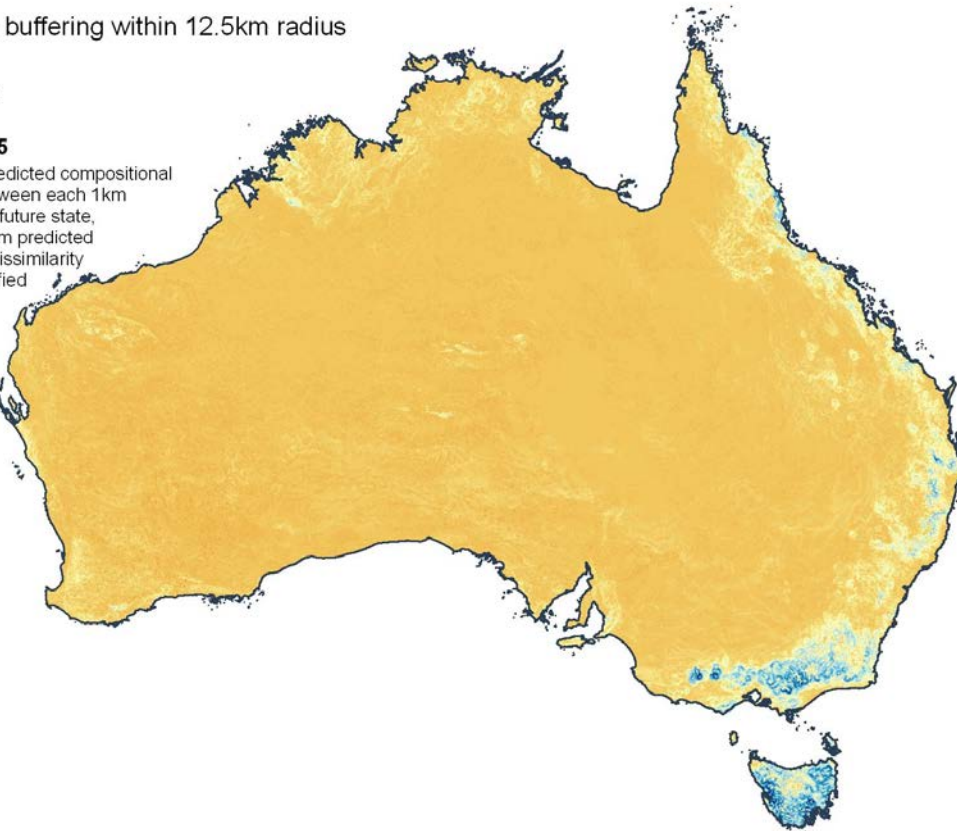
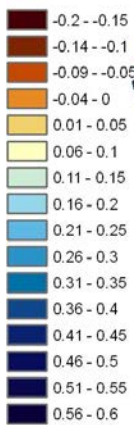
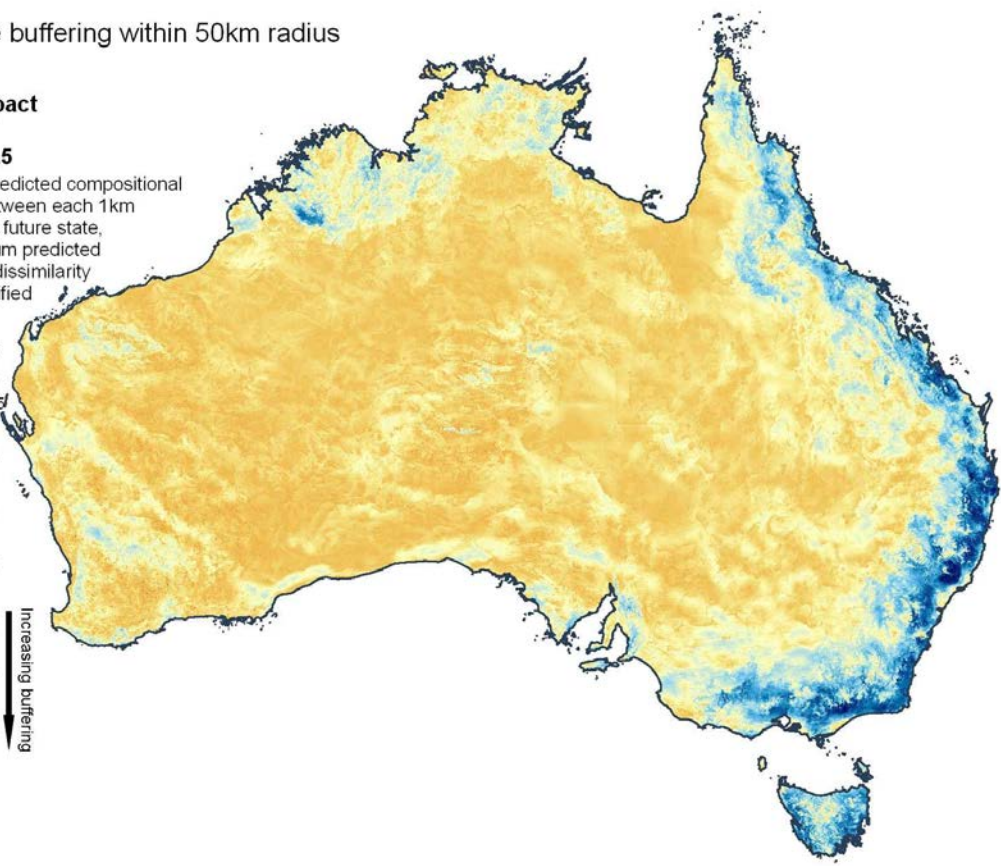
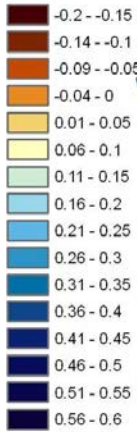


**Figure 16 Potential buffering of environmental heterogeneity in the landscape within 12.5 km under 2070 medium-impact and high-impact scenarios, based on the vascular plant GDM**

Landscape buffering within 50km radius

**2070**  
**medium impact**  
**A1B**  
**CSIRO mk3.5**

Difference in predicted compositional dissimilarity between each 1km grid cell and its future state, and the minimum predicted compositional dissimilarity within the specified radius



Landscape buffering within 50km radius

**2070**  
**high impact**  
**A1FI**  
**CSIRO mk3.5**

Difference in predicted compositional dissimilarity between each 1km grid cell and its future state, and the minimum predicted compositional dissimilarity within the specified radius

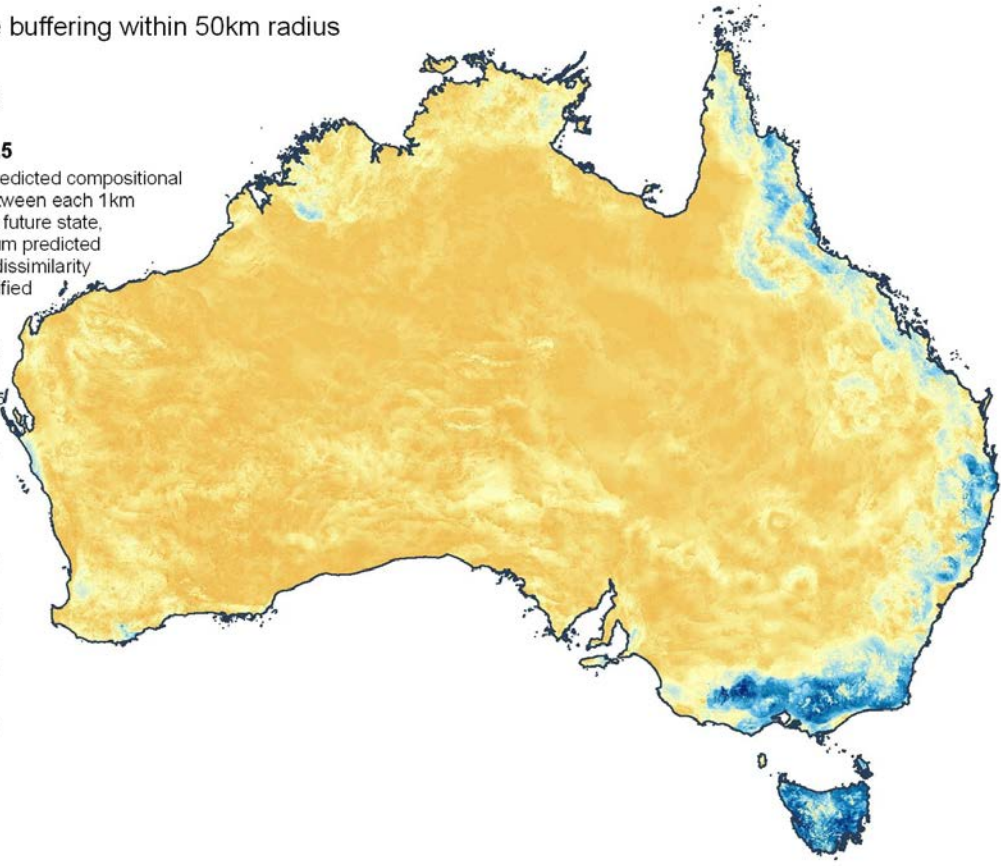
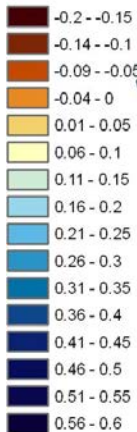
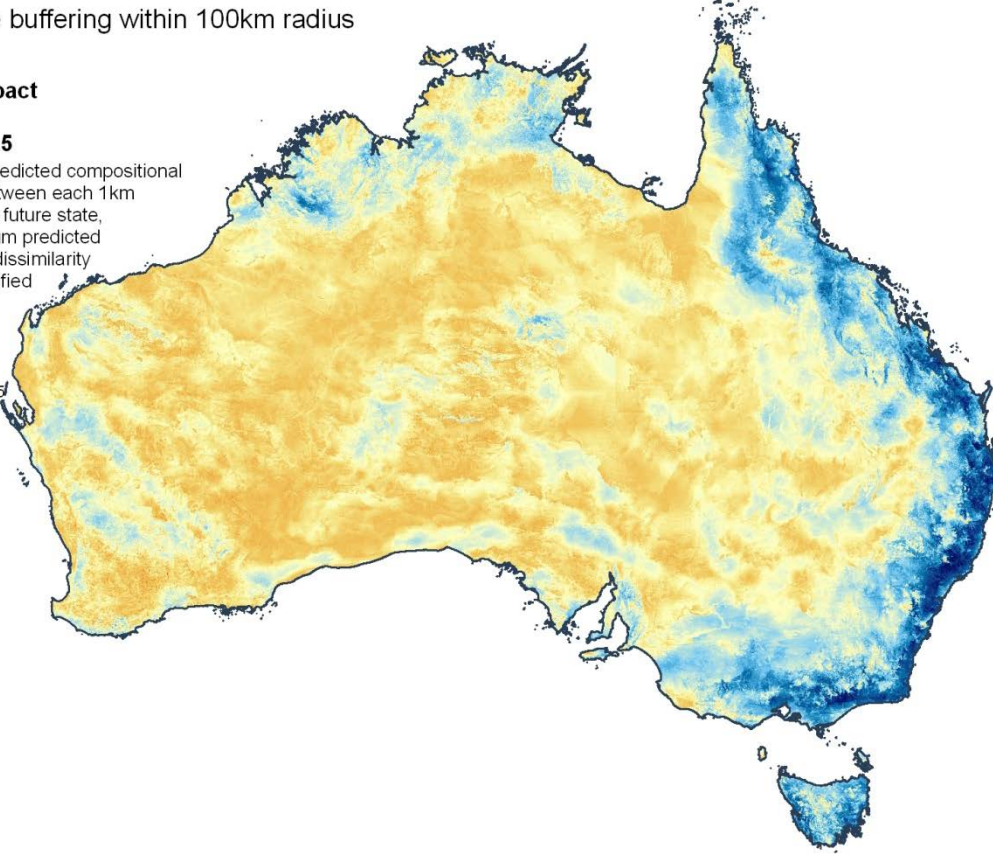
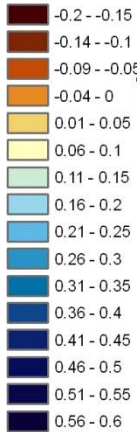


**Figure 17 Potential buffering of environmental heterogeneity in the landscape within 50 km under 2070 medium-impact and high-impact scenarios, based on the vascular plant GDM**

Landscape buffering within 100km radius

**2070**  
**medium impact**  
**A1B**  
**CSIRO mk3.5**

Difference in predicted compositional dissimilarity between each 1km grid cell and its future state, and the minimum predicted compositional dissimilarity within the specified radius



Landscape buffering within 100km radius

**2070**  
**high impact**  
**A1FI**  
**CSIRO mk3.5**

Difference in predicted compositional dissimilarity between each 1km grid cell and its future state, and the minimum predicted compositional dissimilarity within the specified radius

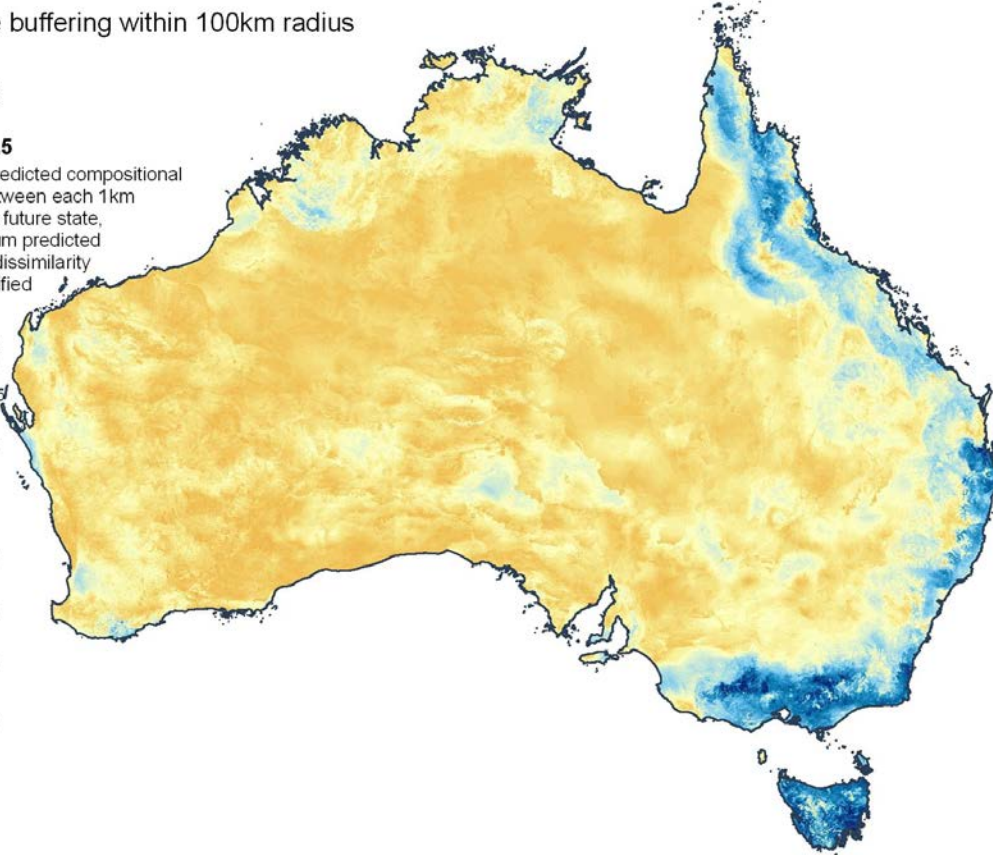
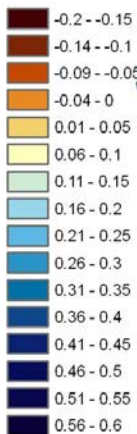
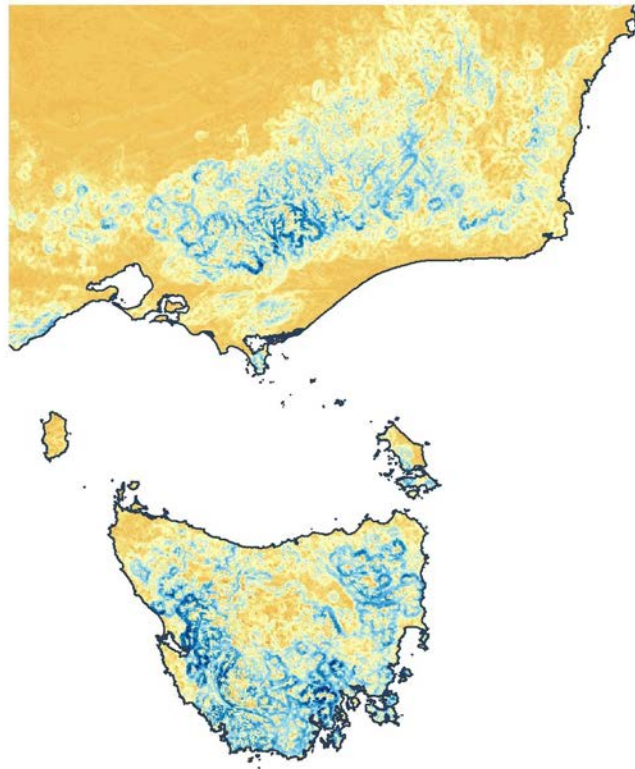
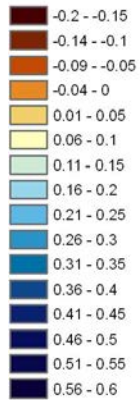


**Figure 18 Potential buffering of environmental heterogeneity in the landscape within 100 km under 2070 medium-impact and high-impact scenarios, based on the vascular plant GDM**

Landscape buffering  
within 6.25km  
radius

2070  
high impact  
A1FI  
CSIRO mk3.5



Landscape buffering  
within 25km  
radius

2070  
high impact  
A1FI  
CSIRO mk3.5

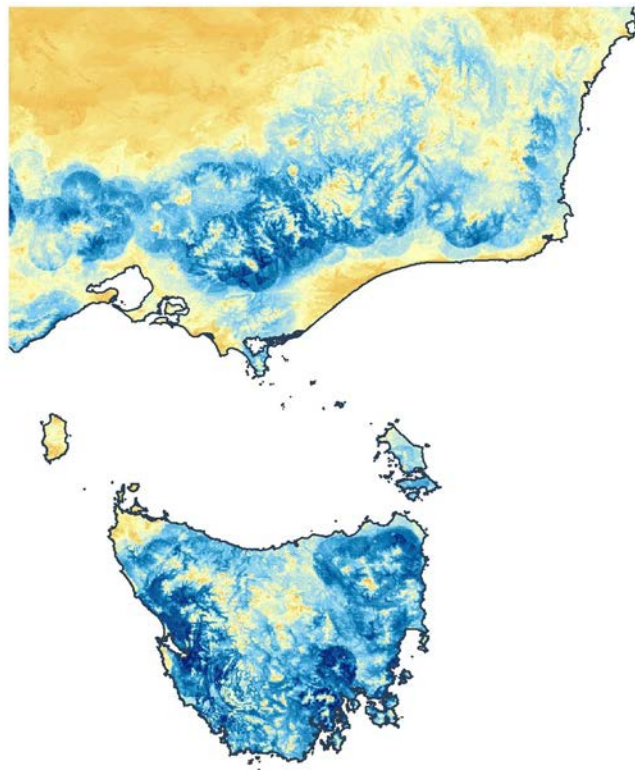
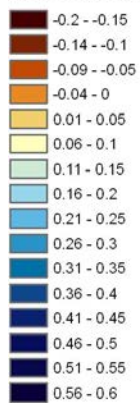


**Figure 19 Potential buffering effects of environmental heterogeneity in the landscape within 6.25 km and 25 km under 2070 high-impact scenario based on the vascular plant GDM. Close up of the south-eastern corner of mainland Australia and of Tasmania, illustrating topographic buffering effects**

## 4.4 Potential change in ‘effective habitat area’

To integrate the effects of potential cell-by-cell changes in composition (from Section 4.1) with the potential for landscape buffering (from Section 4.3) we estimated the proportional change in effective habitat area for each grid cell under a given climate scenario. In this analysis the ‘effective habitat area’ for a given focal cell under present climatic conditions is simply a weighted sum of the areas of all cells within a specified radius, where each of these cells is weighted according to the predicted similarity  $s_{ij} = (1-d_{ij})$  between this cell and the focal cell (see Ferrier et al. 2004, and Allnutt et al. 2008 for a detailed explanation of this concept). The effective habitat area for this same focal cell under a changed climate is derived by replacing the values of  $s_{ij}$  used in this calculation with predicted levels of similarity between the future composition of surrounding cells and the current composition of the focal cell. This future effective habitat area is then expressed as a proportion of the current effective habitat area.

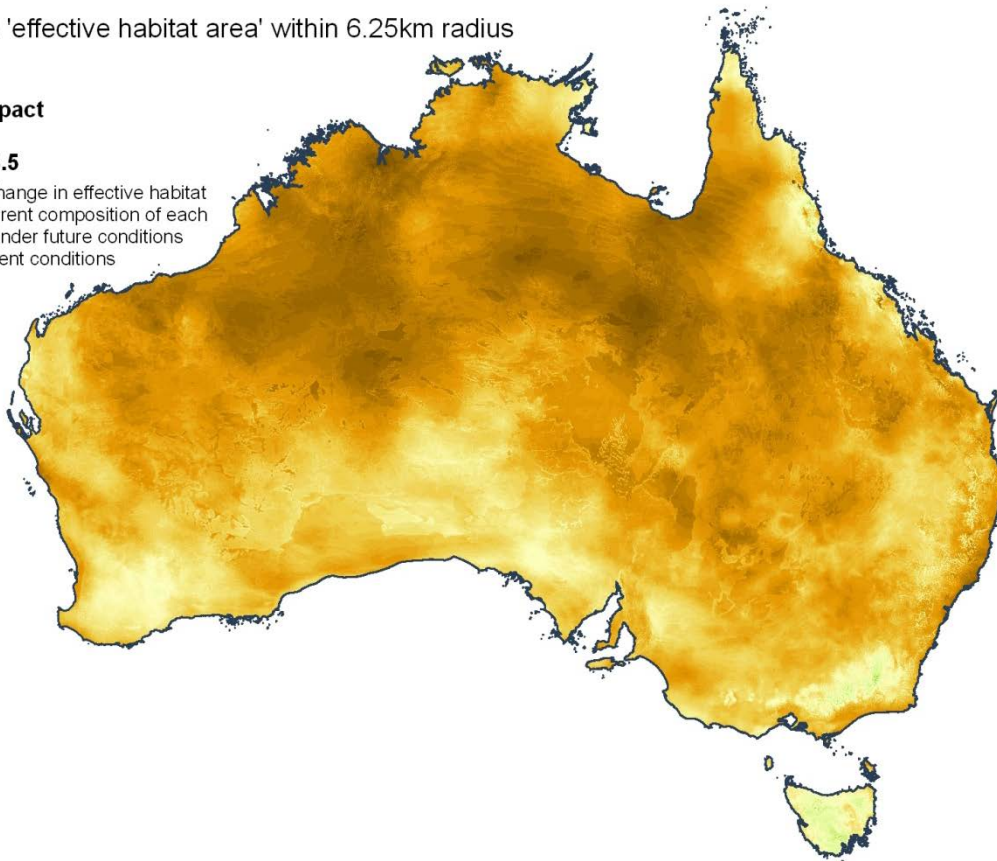
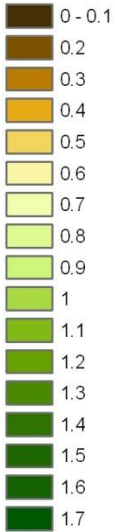
As for the index of landscape buffering (Section 4.3), this proportional change in effective habitat area was calculated using predictions from the vascular plant GDM for the 2070 medium-impact and high-impact scenarios, and using the following radii: 750 m, 1.5625 km, 3.125 km, 6.25 km, 12.5 km, 25 km, 50 km and 100 km. Results for a representative selection of these combinations are presented in Figures 20–22, for radii of 6.25 km, 12.5 km and 100 km. Figures for 50 km can be seen in section 4.5 in Figures 25 and 26. A zoomed-in area comparable to that in Figure 19 for landscape buffering is shown in Figure 23 for radii 6.25 km and 25 km.

Note that unlike the landscape buffering index (Section 4.3), proportional change in effective habitat area is a measure of the properties of the whole area within a radius. Consequently, while increasing the radius (and therefore the area measured) may increase the probability of finding similar habitats in the future, this may be offset by the inclusion of less similar cells. In most cases, the brown colouring indicates a reduction in the effective habitat area under changing climate, consistent with the predicted compositional dissimilarities. Only the elevated regions of south-eastern Australia show areas where the effective habitat area is relatively unchanged (pale greens) under the medium-impact scenario.

Change in 'effective habitat area' within 6.25km radius

**2070  
medium impact  
A1B  
CSIRO mk3.5**

Proportional change in effective habitat area of the current composition of each 1km grid cell under future conditions relative to current conditions



Change in 'effective habitat area' within 6.25km radius

**2070  
high impact  
A1FI  
CSIRO mk3.5**

Proportional change in effective habitat area of the current composition of each 1km grid cell under future conditions relative to current conditions

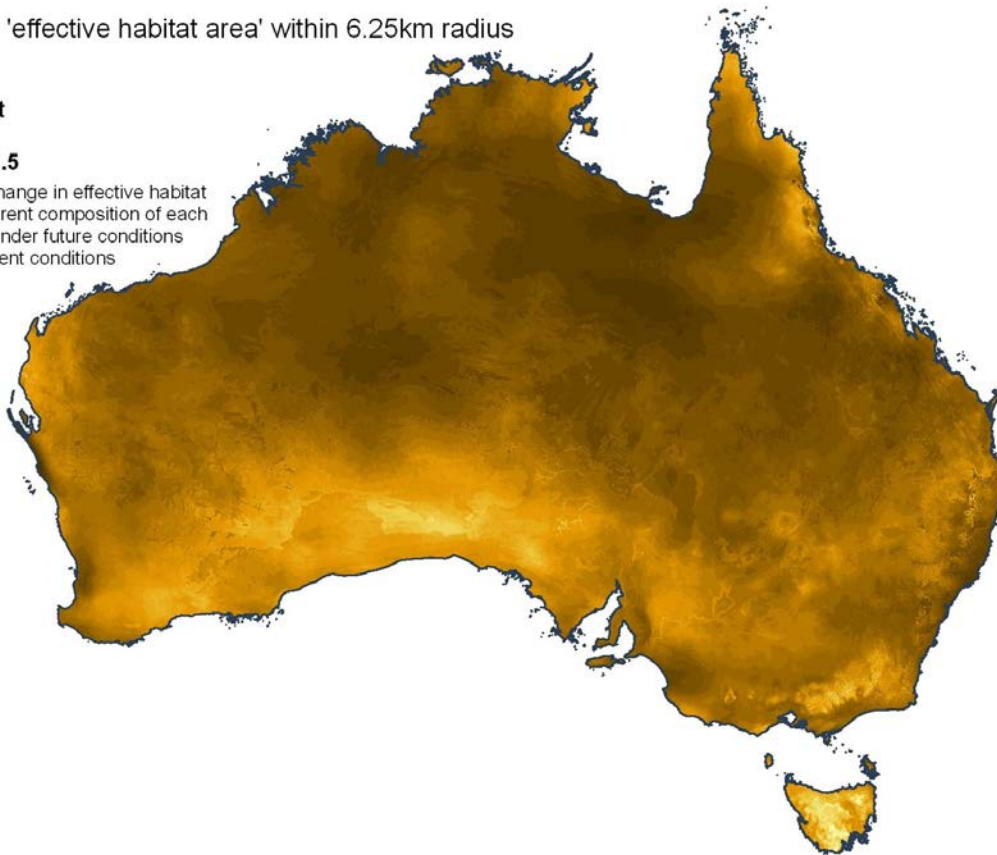
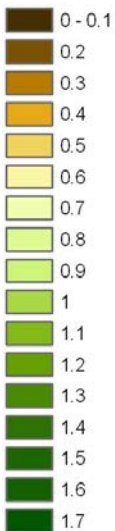
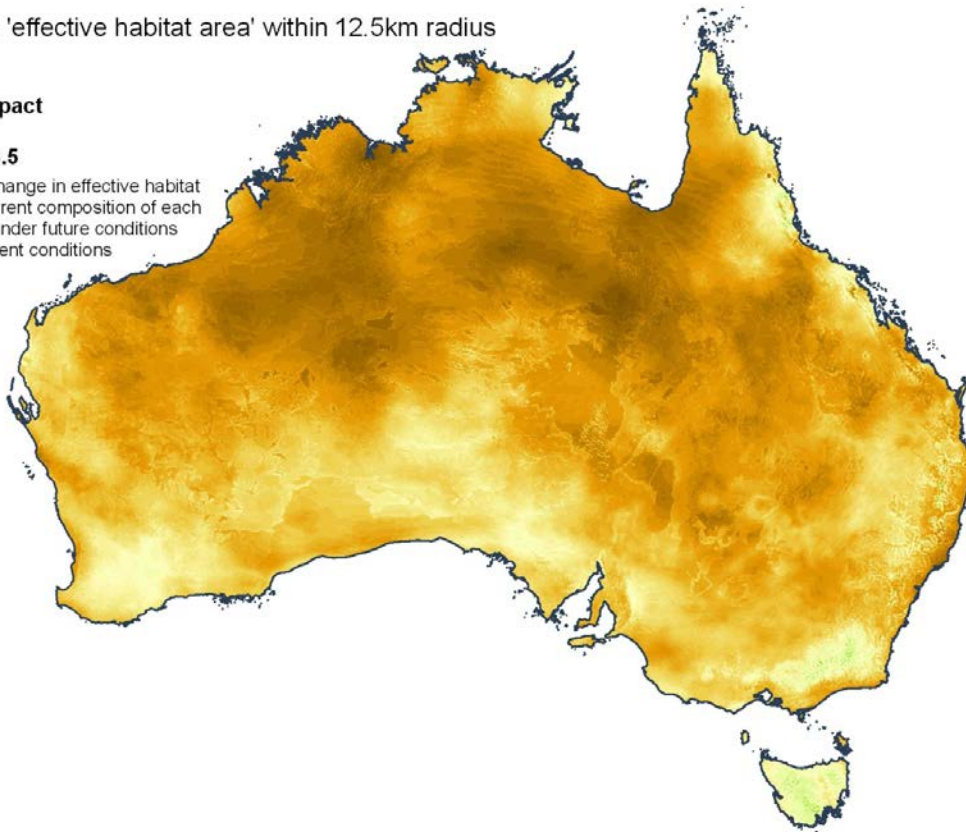
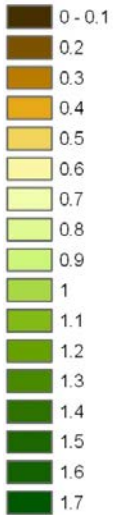


Figure 20 Change in the effective habitat area within 6.25 km for both 2070 medium-impact and high-impact scenarios based on the vascular plants GDM. Browns indicate a reduction, pale green (value of 1 in the legend) indicates no change, and darker greens an increase in effective habitat area

Change in 'effective habitat area' within 12.5km radius

**2070**  
**medium impact**  
**A1B**  
**CSIRO mk3.5**

Proportional change in effective habitat area of the current composition of each 1km grid cell under future conditions relative to current conditions



Change in 'effective habitat area' within 12.5km radius

**2070**  
**high impact**  
**A1FI**  
**CSIRO mk3.5**

Proportional change in effective habitat area of the current composition of each 1km grid cell under future conditions relative to current conditions

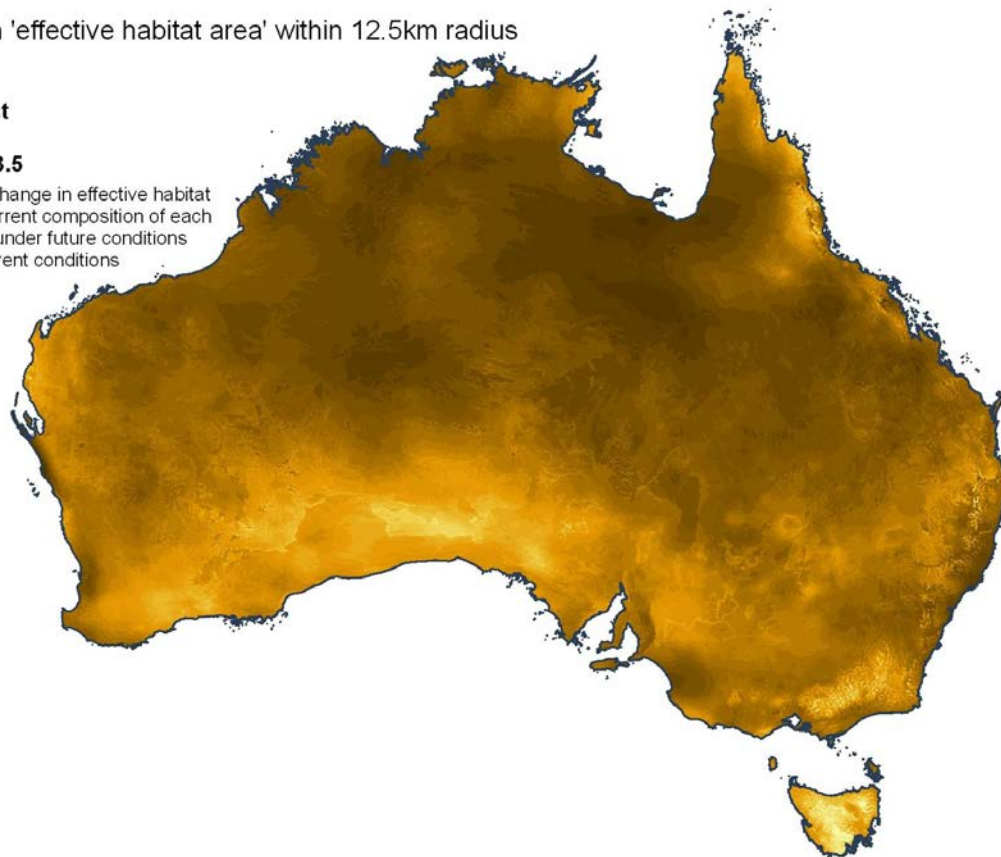
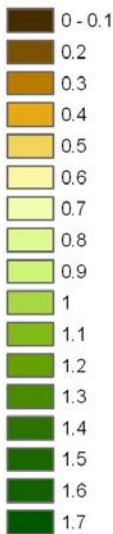
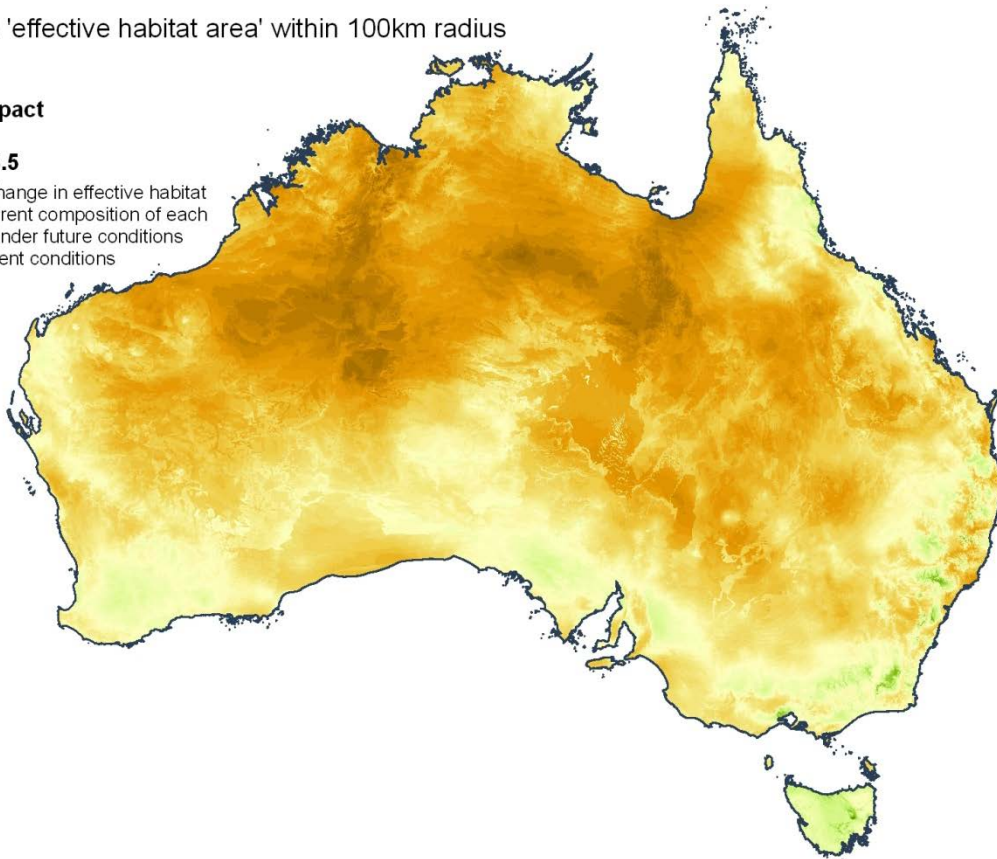
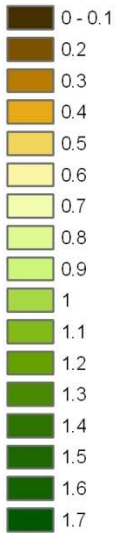


Figure 21 Change in the effective habitat area within 12.5 km for both 2070 medium-impact and high-impact scenarios based on the vascular plants GDM. Browns indicate a reduction, pale green (value of 1 in the legend) indicates no change, and darker greens an increase in effective habitat area

Change in 'effective habitat area' within 100km radius

**2070**  
**medium impact**  
**A1B**  
**CSIRO mk3.5**

Proportional change in effective habitat area of the current composition of each 1km grid cell under future conditions relative to current conditions



Change in 'effective habitat area' within 100km radius

**2070**  
**high impact**  
**A1FI**  
**CSIRO mk3.5**

Proportional change in effective habitat area of the current composition of each 1km grid cell under future conditions relative to current conditions

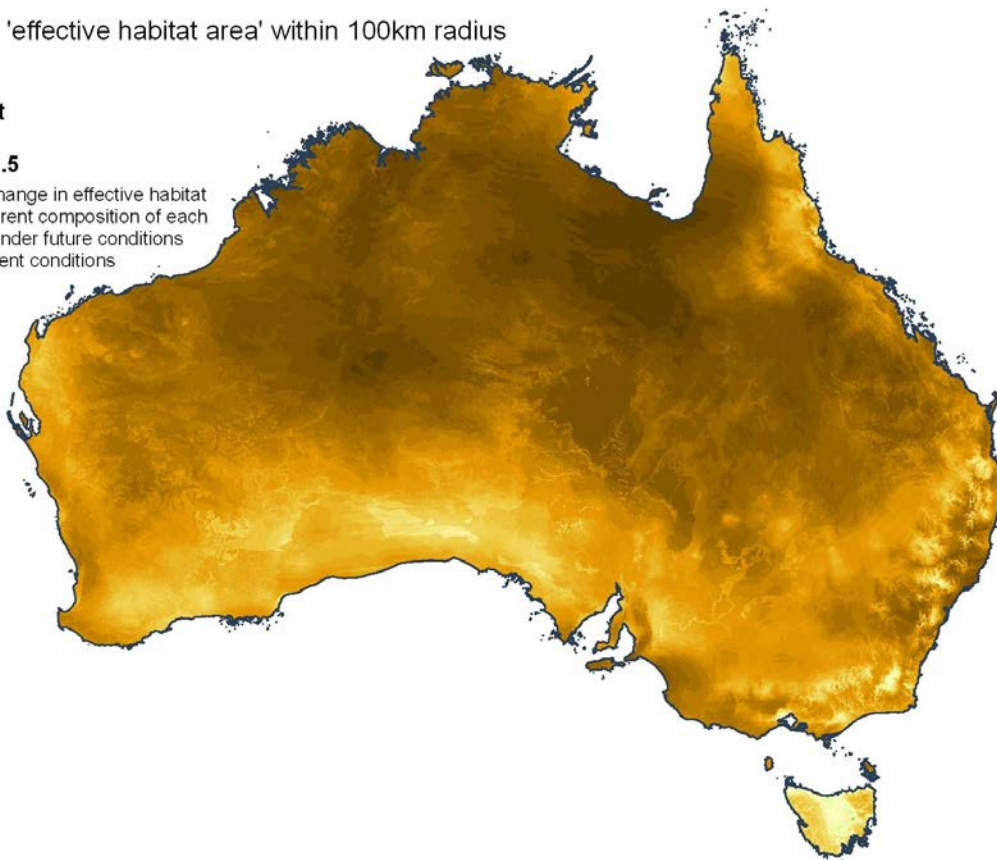
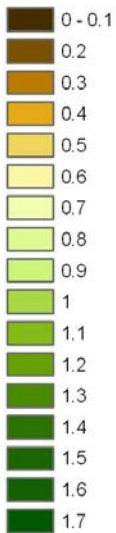


**Figure 22** Change in the effective habitat area within 100 km for both 2070 medium-impact and high-impact scenarios based on the vascular plants GDM. Browns indicate a reduction, pale green (value of 1 in the legend) indicates no change, and darker greens an increase in effective habitat area

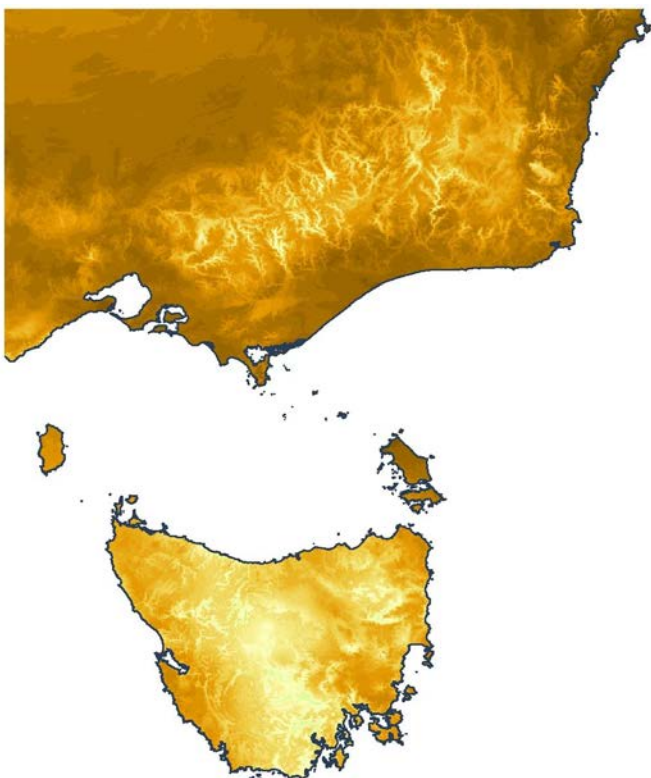
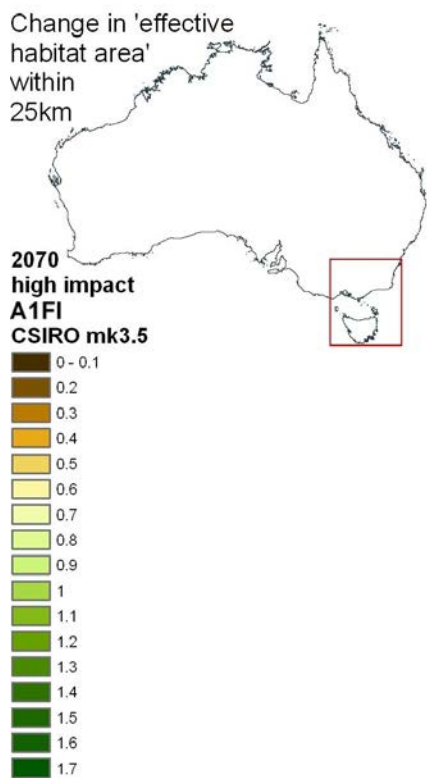
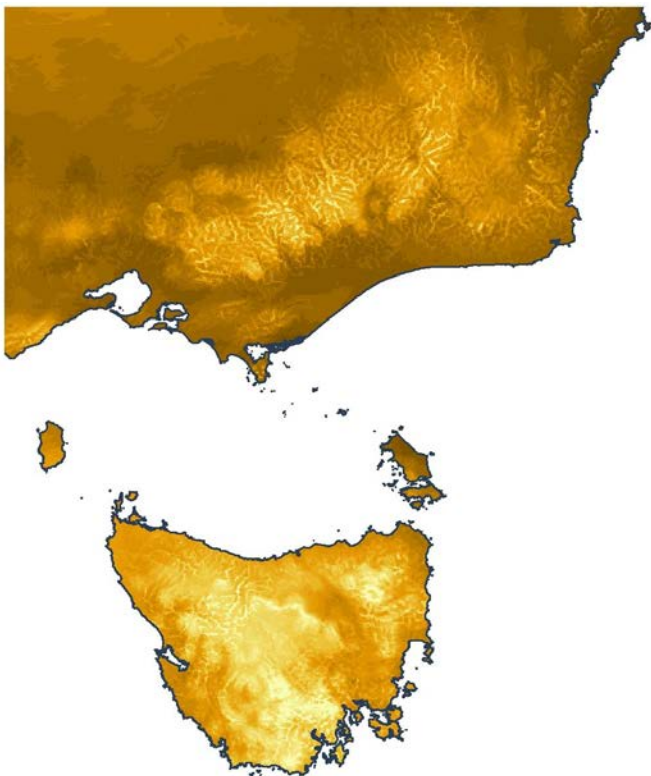
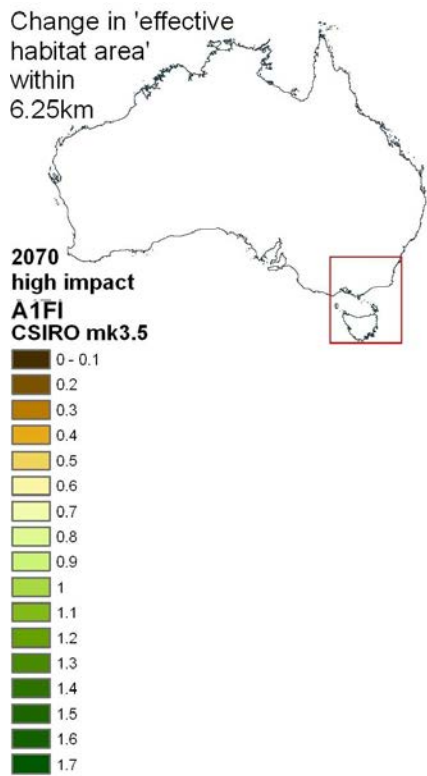


Figure 23 Change in effective habitat area in the landscape within 6.25 km and 25 km under 2070 high-impact scenario based on the vascular plants GDM. Close up of the south-eastern corner of mainland Australia and of Tasmania, illustrating topographic buffering effects

## 4.5 Added effects of habitat loss and fragmentation

The analysis of proportional change in effective habitat area under climate change (Section 4.4) was further extended to consider the added effect of past habitat loss (and fragmentation). Data on the current (extant) distribution of native vegetation in Australia (Figure 24) were derived from the National Vegetation Information System (NVIS) version 3.1 (see Williams et al. 2010 for details). The calculation of 'future effective habitat area' (from section 4.4) was then adjusted such that only grid cells containing extant native vegetation in the specified radius around a focal cell contributed to effective area calculated for that cell. This revised future effective habitat area was then used to derive a 'proportional change in effective habitat area' measure incorporating the effects of both climate change and habitat loss. Results for this are shown in Figures 25 and 26, mapped against the same scenarios with pristine vegetation. The difference between this and the original measure derived in Section 4.4 (climate effects only) was also calculated, and the resultant maps, highlighting areas where restoration might have maximum benefit in terms of biotically scaled environment, are shown in Figure 27.

### Current extant vegetation mask

Binary classification of each 1km grid cell as either degraded (cleared) or pristine

- Degraded
- Pristine

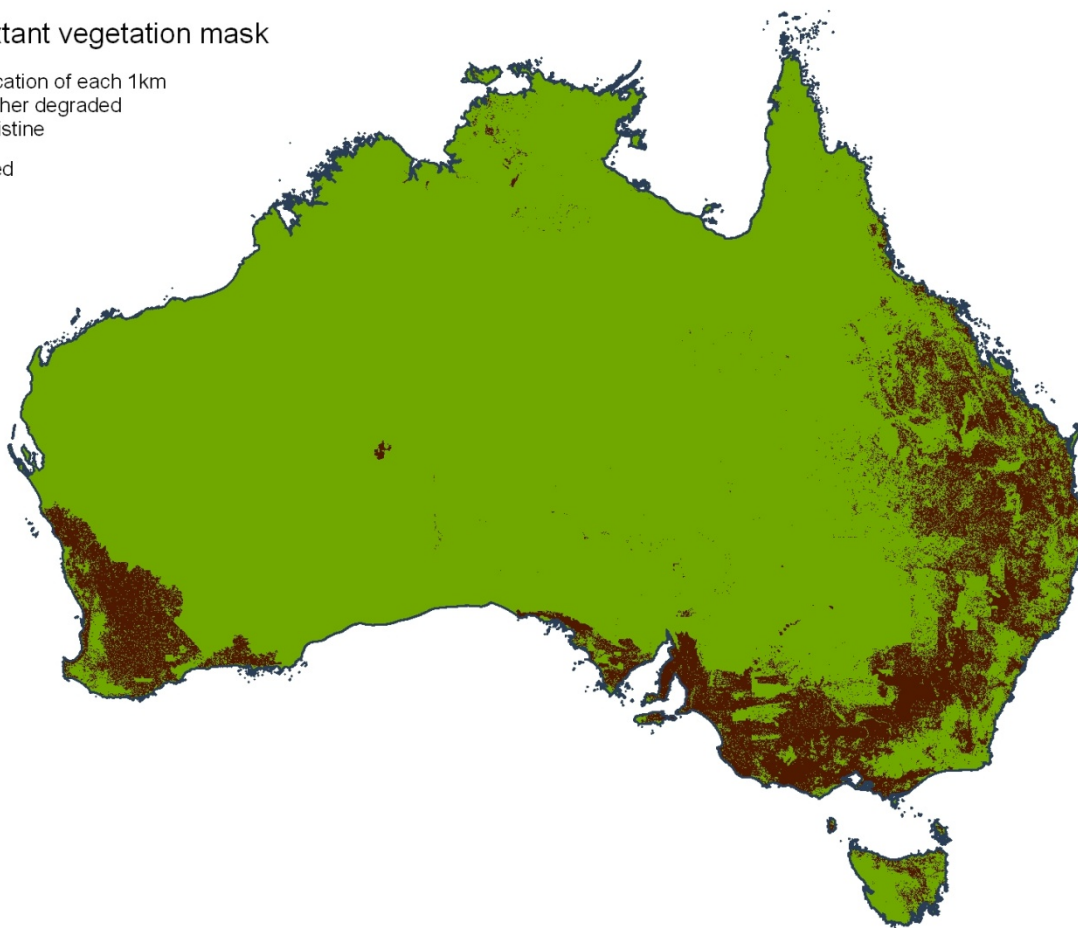
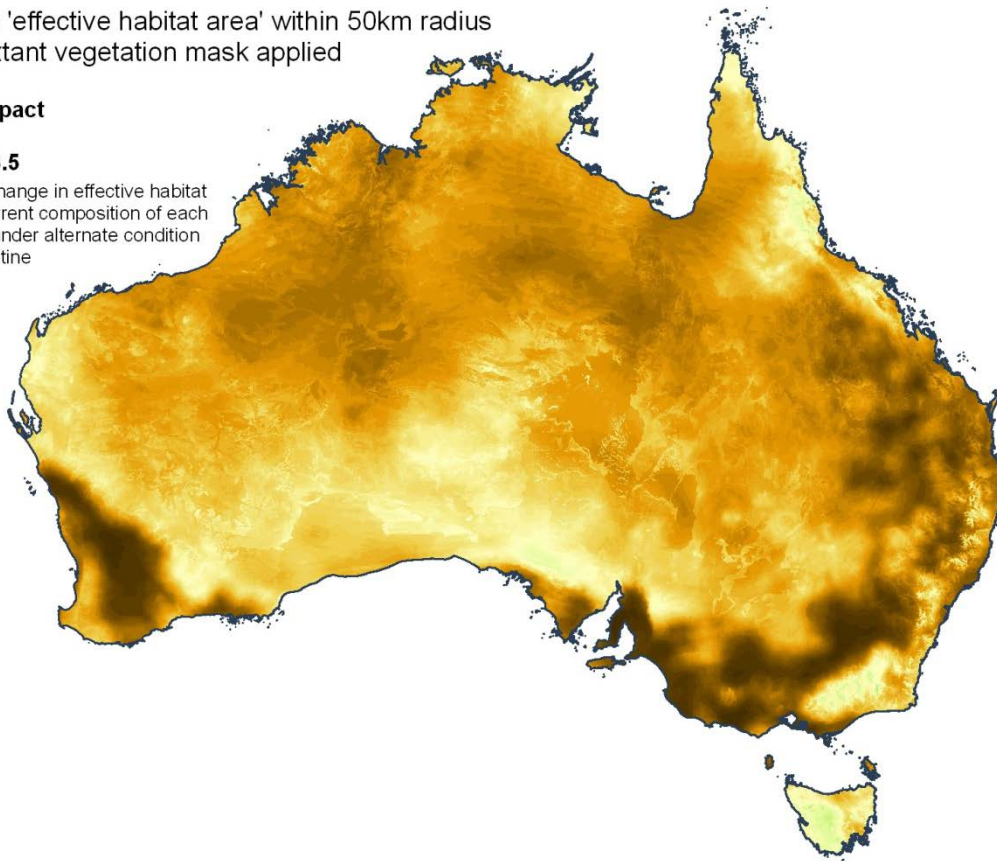
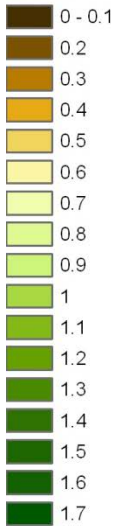


**Figure 24** Current (extant) distribution of native vegetation in Australia derived from the National Vegetation Information System (NVIS) version 3.1 (Williams et al. 2010) as used in subsequent analyses

Change in 'effective habitat area' within 50km radius  
Current extant vegetation mask applied

**2070**  
**medium impact**  
**A1B**  
**CSIRO mk3.5**

Proportional change in effective habitat area of the current composition of each 1km grid cell under alternate condition relative to pristine condition



Change in 'effective habitat area' within 50km radius

**2070**  
**medium impact**  
**A1B**  
**CSIRO mk3.5**

Proportional change in effective habitat area of the current composition of each 1km grid cell under future conditions relative to current conditions

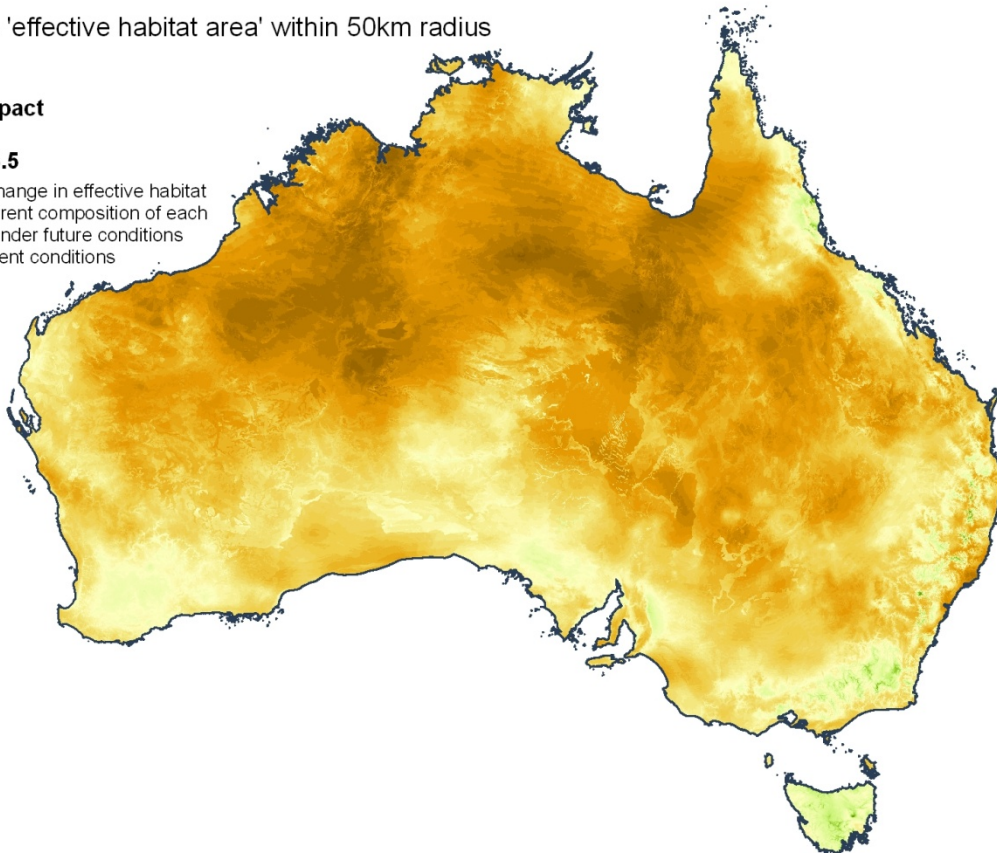
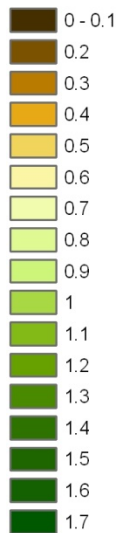
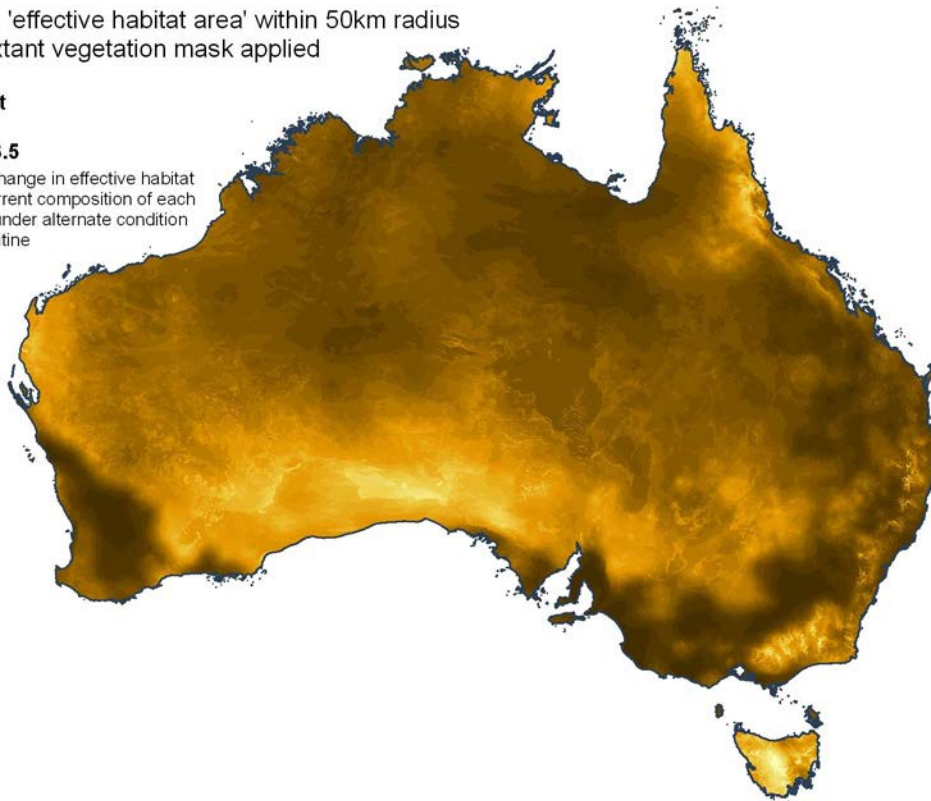
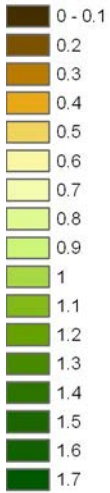


**Figure 25** Change in effective habitat area within a 50 km radius under 2070 medium-impact scenario, based on the vascular plant GDM, with (top) and without (bottom) the effects of habitat loss applied

Change in 'effective habitat area' within 50km radius  
 Current extant vegetation mask applied

**2070**  
**high impact**  
**A1FI**  
**CSIRO mk3.5**

Proportional change in effective habitat area of the current composition of each 1km grid cell under alternate condition relative to pristine condition



Change in 'effective habitat area' within 50km radius

**2070**  
**high impact**  
**A1FI**  
**CSIRO mk3.5**

Proportional change in effective habitat area of the current composition of each 1km grid cell under future conditions relative to current conditions

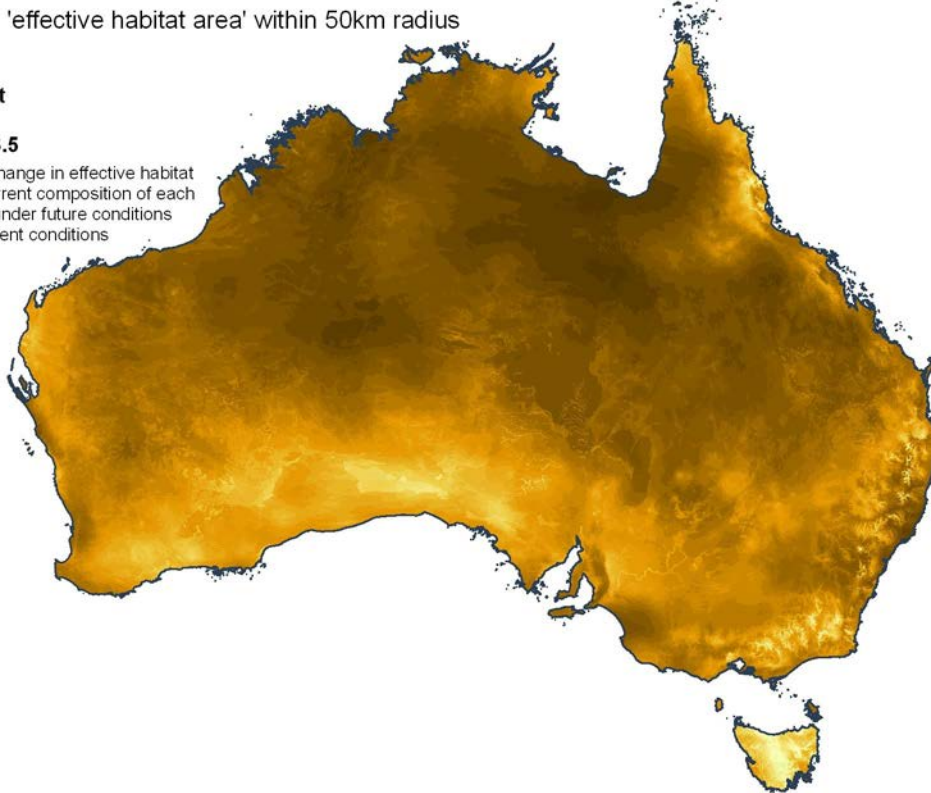
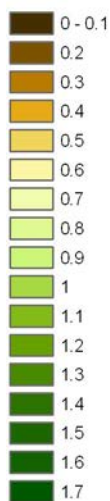
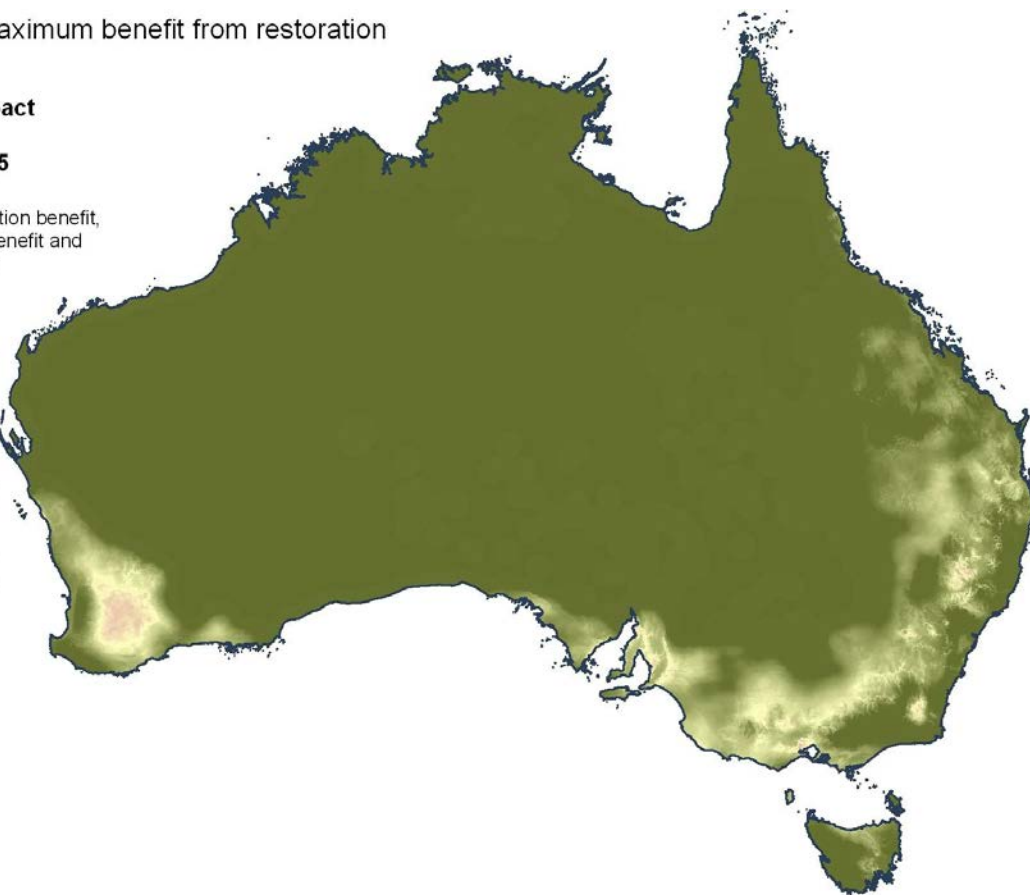
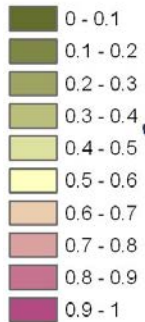


**Figure 26** Change in effective habitat area within a 50 km radius under 2070 high-impact scenario, based on the vascular plant GDM, with (top) and without (bottom) the effects of habitat loss applied

Areas of maximum benefit from restoration

**2070**  
**medium impact**  
**A1B**  
**CSIRO mk3.5**

Index of restoration benefit,  
where 0 is no benefit and  
1 is high benefit



Areas of maximum benefit from restoration

**2070**  
**high impact**  
**A1FI**  
**CSIRO mk3.5**

Index of restoration benefit,  
where 0 is no benefit and  
1 is high benefit

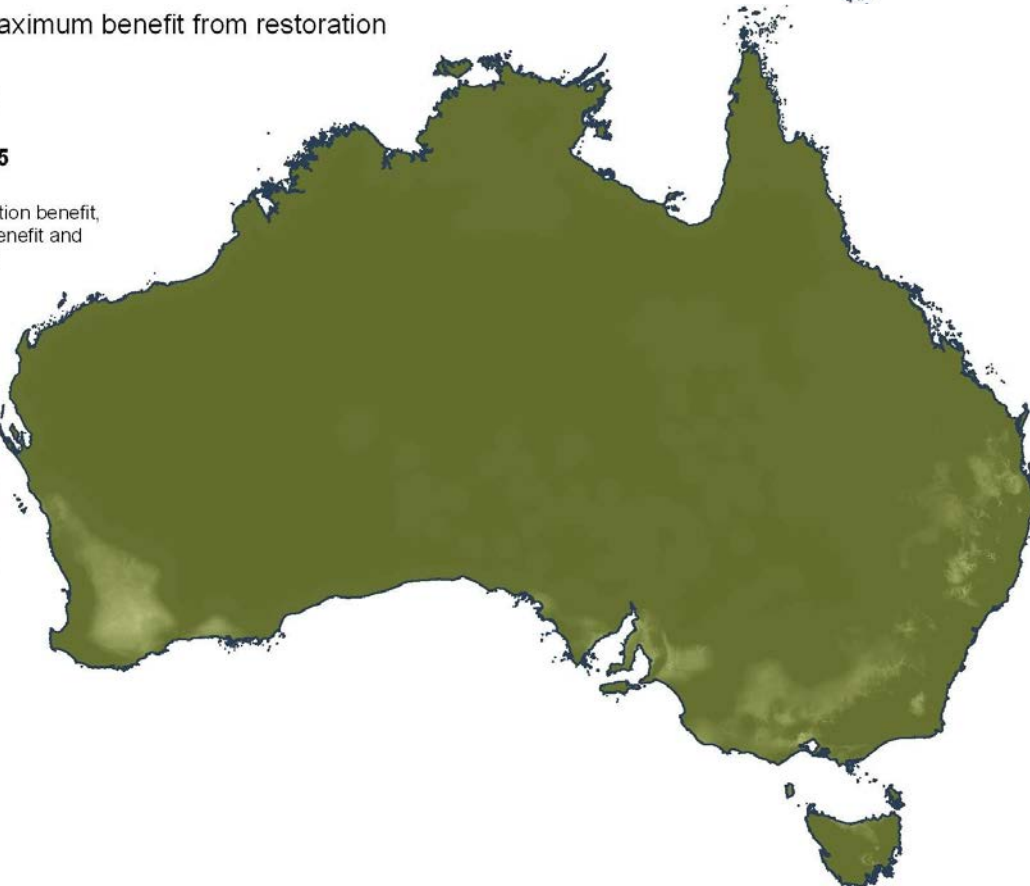
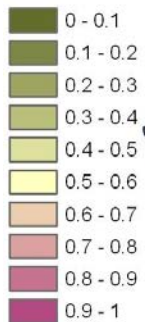


**Figure 27** Areas where restoration would enhance the effective habitat area of present biotically scaled environments under future climate for the vascular plant GDM. Greens indicate little benefit to restoration, and largely show land in good condition. Pinks indicate maximum benefit. Note that these are fewer in the high-impact scenario, due to the generally less suitable habitat

## 5 Analysis of NRS representativeness under climate change

Past analyses of the representativeness of the NRS have been based largely on discrete classes such as bioregions or vegetation types. In those analyses each location (grid cell) is a member of a particular class (e.g. a bioregion or a vegetation type), and all cells in a given class are therefore viewed as having the same level of proportional representation in reserves. In other words, the proportion assigned to a given cell does not reflect whether that particular cell is itself reserved but rather the overall proportion of cells in the same class (e.g. bioregion) that are reserved.

To couch this traditional approach in terms of the language of this report: cells occurring within the same class are treated as having a compositional dissimilarity of 0 (i.e. they are identical biologically) while cells in different classes are treated as having a dissimilarity of 1 (i.e. they are totally distinct biologically). In the GDM-based approach adopted here, the dissimilarity between pairs of cells is allowed to vary continuously across the landscape, and the estimation of proportional representation in reserves has been adapted to reflect this. The logic behind this approach, and examples of its previous application, are provided by Ferrier et al. (2004) and Allnutt et al. (2008).

In the Caring for Our Country project (Williams et al. 2010) this GDM-based approach was used to assess the representativeness of the NRS under current climatic conditions. This assessment was based on NRS data from the collaborative Australia protected area database (CAPAD), version 2006. In this analysis the proportional representation of any given grid cell  $i$  – that is, the proportion of cells (anywhere on the continent) similar to that cell that are included in the NRS – was calculated as:

$$\frac{\sum_{j=1}^n s_{ij} r_j}{\sum_{j=1}^n s_{ij}}$$

where  $s_{ij}$  is the predicted compositional similarity between the focal cell ( $i$ ) and each ( $j$ ) of the  $n$  cells on the continent, and  $r_j$  is the reservation status of cell  $j$ , that is, 0 = unreserved, 1 = reserved.

The resulting map of proportional NRS representation based on the vascular plant GDM is reproduced here in Figure 28.

## Representation of present biotically-scaled environments in present reserves

### Current climate

Index of representation by reserve areas where 0 is no representation and increasing values indicate better representation

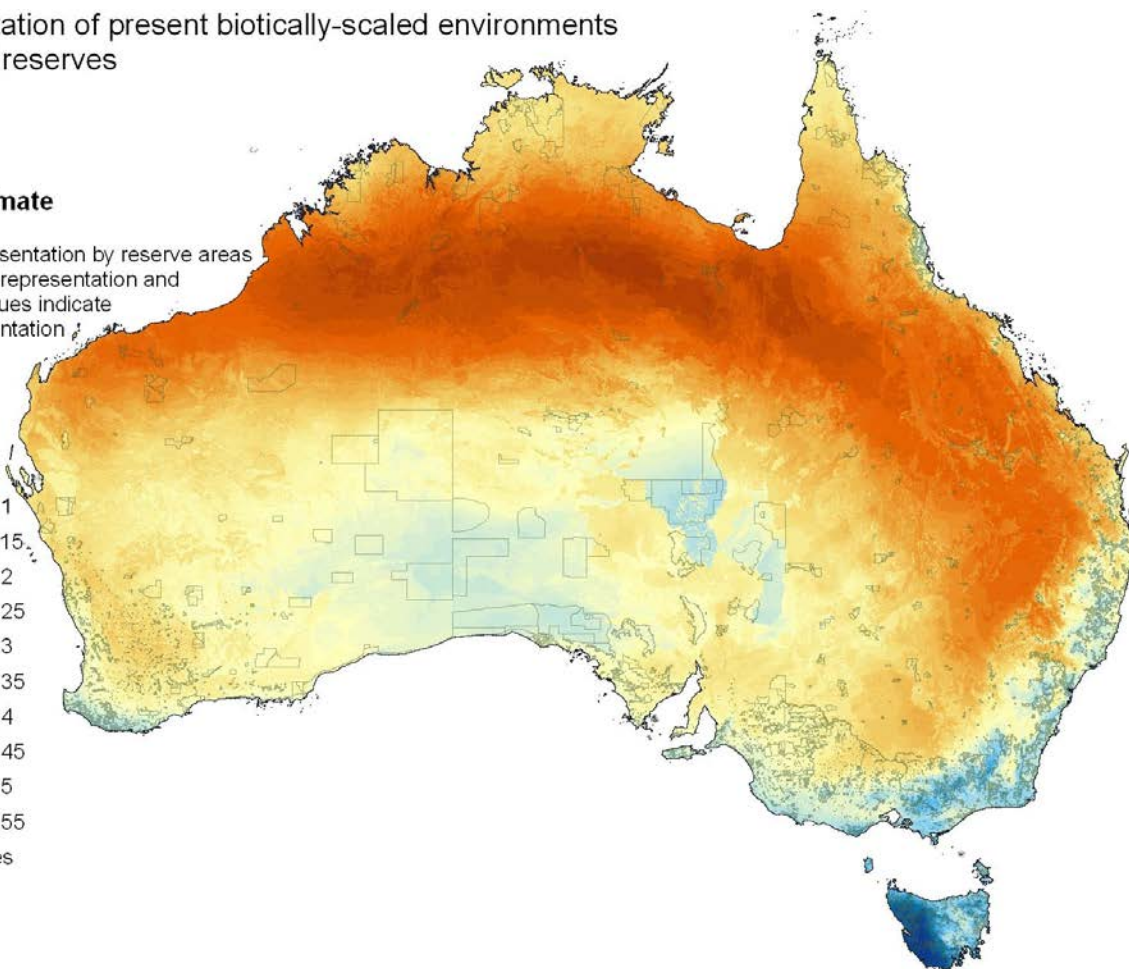
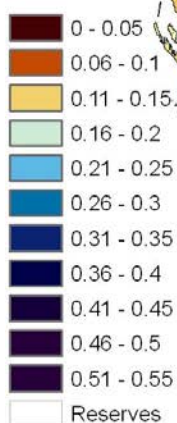


**Figure 28** The extent to which the reserve system (CAPAD 2006) is representative of the present environment based on the vascular plant GDM. The index shows the proportion of the present continental distribution of each biotically scaled environment which is covered by the reserve system. Orange colours indicate poor representation, and blues better representation

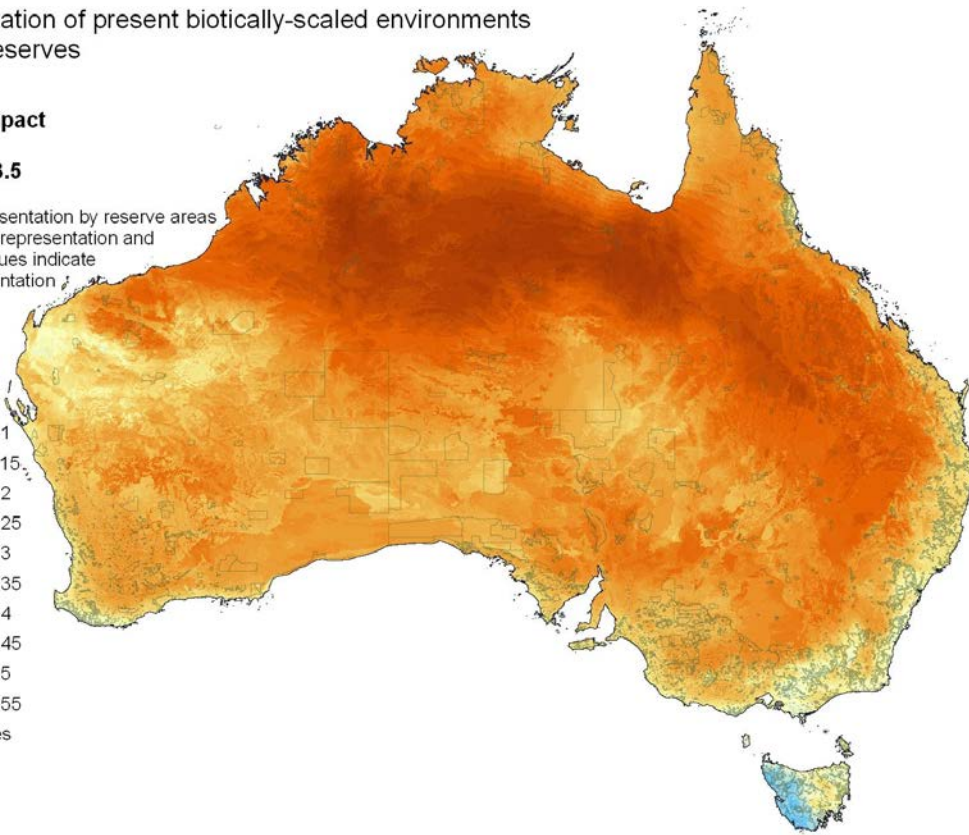
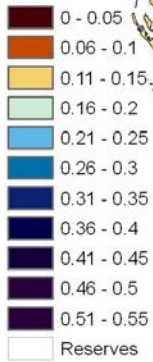
This approach to assessing and mapping representativeness of reserves has never before been extended to consider the potential effects of climate change. As part of the NRS2 project we experimented with two variations of the original analysis to account for potential climate-change effects. In the first of these, the value for  $s_{ij}$  used in the numerator of the above equation is replaced by the predicted similarity between the current composition of the focal cell ( $i$ ) and the potential future composition (after climate change) of cell  $j$  (the denominator of the equation is left unchanged). The result of applying this modified analysis using the vascular plant GDM is presented in Figure 29. This map therefore indicates the extent to which present biotically scaled environments will continue to be represented within the NRS (assuming current reserve boundaries) under climate change.

In the second variation of this analysis, the values of  $s_{ij}$  used in both the numerator and denominator of the above equation are replaced by the predicted similarity between the future composition of both cells  $i$  and  $j$ . This map (Figure 30) therefore indicates the extent to which future biotically scaled environments will be represented within the NRS (again assuming current boundaries).

Representation of present biotically-scaled environments  
in future reserves

**2070**  
**medium impact**  
**A1B**  
**CSIRO mk3.5**

Index of representation by reserve areas  
where 0 is no representation and  
increasing values indicate  
better representation



Representation of present biotically-scaled environments  
in future reserves

**2070**  
**high impact**  
**A1FI**  
**CSIRO mk3.5**

Index of representation by reserve areas  
where 0 is no representation and  
increasing values indicate  
better representation

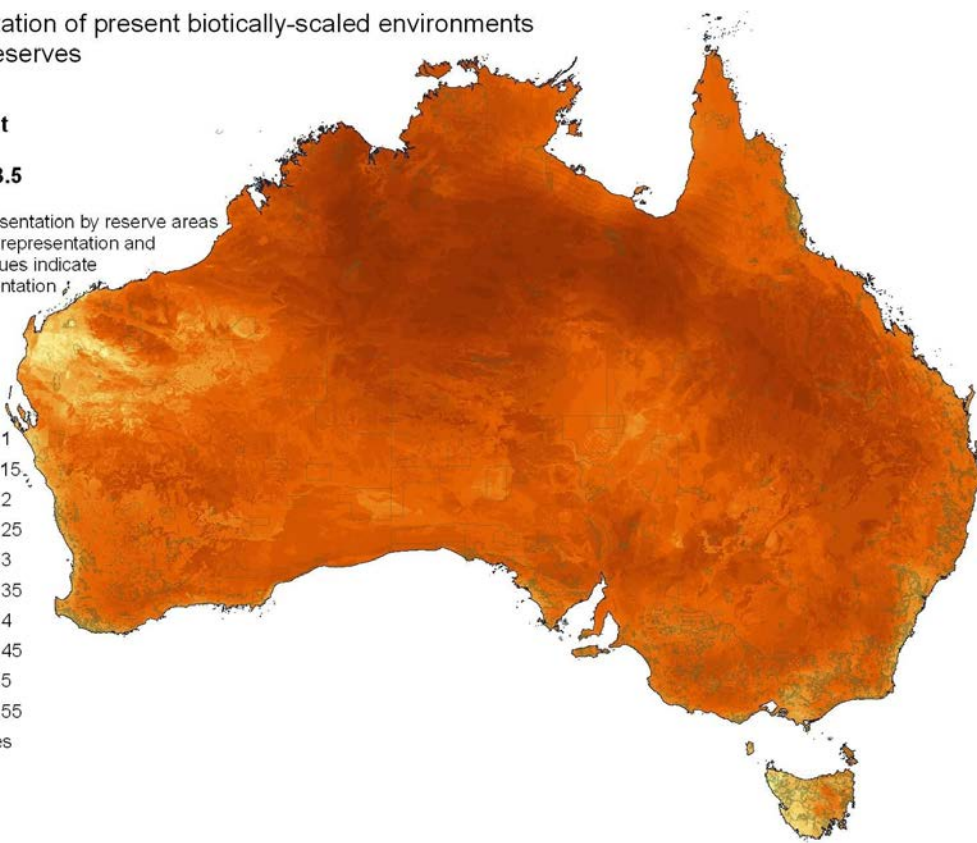
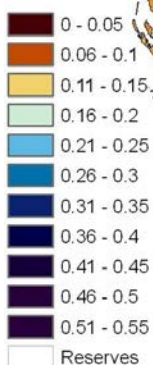
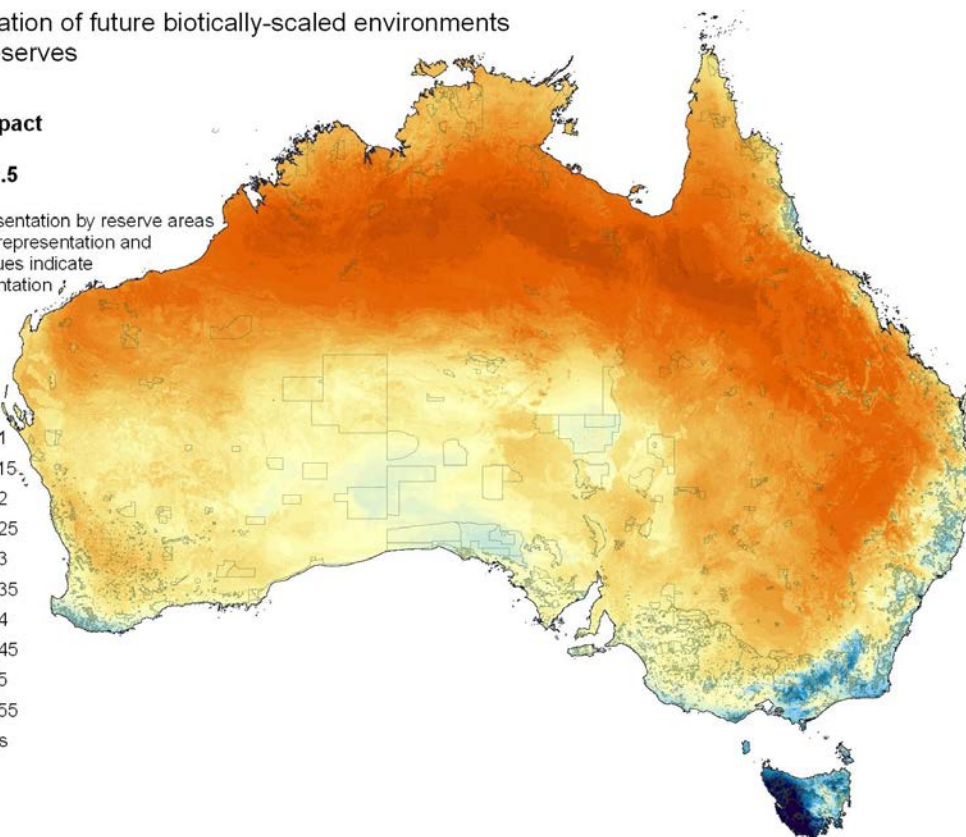
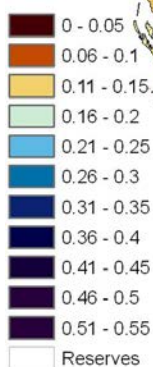


**Figure 29** The extent to which the NRS under future climate scenarios is representative of the present environment based on the vascular plant GDM. The index shows the proportion of the present continental distribution of each biotically scaled environment that is covered by the NRS under future climate

Representation of future biotically-scaled environments  
in future reserves

**2070**  
**medium impact**  
**A1B**  
**CSIRO mk3.5**

Index of representation by reserve areas  
where 0 is no representation and  
increasing values indicate  
better representation



Representation of future biotically-scaled environments  
in future reserves

**2070**  
**high impact**  
**A1FI**  
**CSIRO mk3.5**

Index of representation by reserve areas  
where 0 is no representation and  
increasing values indicate  
better representation

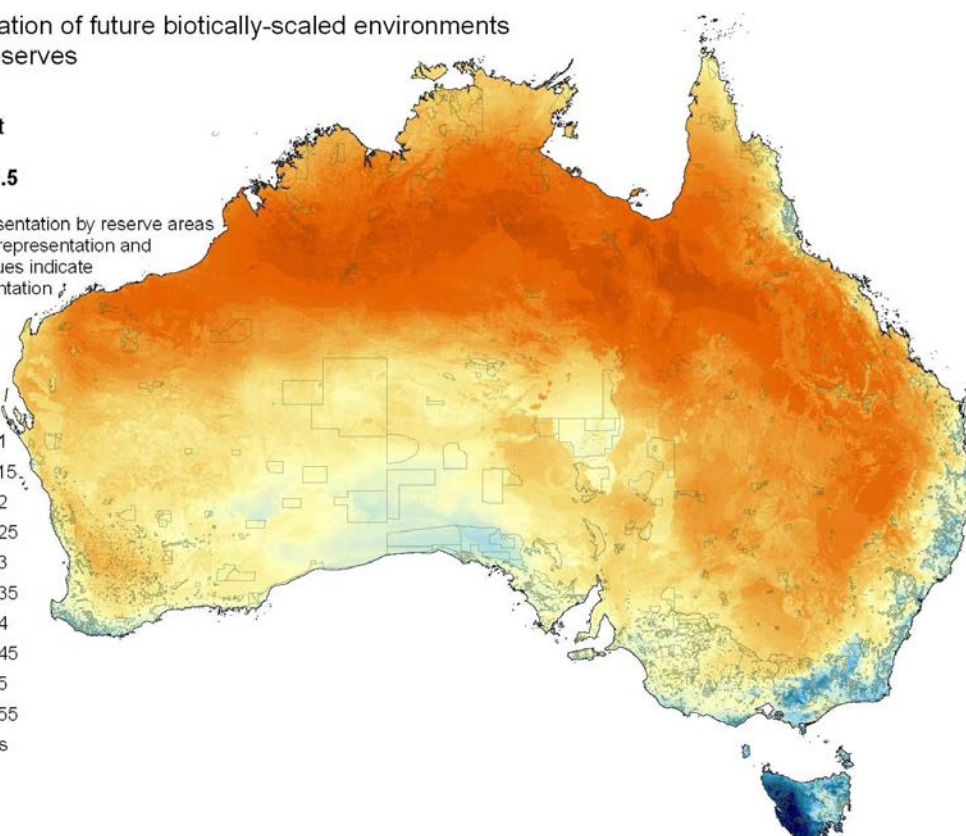
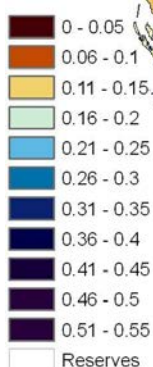


**Figure 30** The extent to which the NRS under future climate scenarios is representative of the future environment based on the vascular plant GDM. The index shows the proportion of the future continental distribution of each biotically scaled environment that is covered by the NRS under future climate

## 6 Conclusion

This study used GDM of compositional turnover in six species groups across the Australian continent, combined with climate change scenarios, to develop indicators of potential future environmental stress arising from climate change by 2030 and 2070. These indicators reflect only the *potential* for change. The actual change in biological composition resulting from climate change will be shaped by many factors, and associated sources of uncertainty, beyond those considered in this modelling. More detailed analysis using the models developed for vascular plants and the 2070 medium and high impact climate scenarios explored the extent to which environmental variation at continental to local scales might mitigate the ecological impact of environmental change at individual locations.

The study found levels of environmental stress, using the vascular plant models and the chosen climate change scenarios, could start soon (by 2030) and be very significant and widespread by 2070. Environmental change is likely to be variable across the country, and many factors will influence how environmental change will translate into ecological change. The study showed that ecological change may be mitigated to some moderate extent in areas with significant altitudinal variation. The analysis also showed very clearly that ecological impacts are likely to be much more significant under higher emissions scenarios.

# References

- Allnutt TF, Ferrier S, Manion G, Powell GVN, Ricketts TH, Fisher BL, Harper GJ, Irwin ME, Kremen C, Labat J-N, Lees DC, Pearch TA and Rakotondrainibe F (2008) A method for quantifying biodiversity loss in and its application to a 50-year record of deforestation across Madagascar. *Conservation Letters* 1(4), 173–181.
- Busby JR (1986) *Bioclimate Prediction System (BIOCLIM) User's Manual*. Version 2.0. Bureau of Flora and Fauna, Canberra.
- CAPAD (2006) *CAPAD: protected area data*. Australian Government Department of Sustainability, Environment, Water, Population and Communities, Canberra.  
<http://www.environment.gov.au/parks/nrs/science/capad/2006/index.html>.
- CSIRO (2012) *OzClim. Exploring climate change scenarios for Australia*. <http://www.csiro.au/ozclim>.
- Department of Sustainability, Environment, Water, Population and Communities (2012) Australian Natural Heritage Assessment Tool (ANHAT). <http://www.environment.gov.au/heritage/anhata/>.
- Dunlop M and Brown PR (2008) *Implications of Climate Change for Australia's National Reserve System: A Preliminary Assessment*. Report to the Department of Climate Change. Department of Climate Change, Canberra. <http://www.climatechange.gov.au/impacts/publications/nrs-report.html>.
- Dunlop M, Hilbert DW, Ferrier S, House A, Liedloff A, Prober SM, Smyth A, Martin TG, Harwood T, Williams KJ, Fletcher C and Murphy H (2012) *The Implications of Climate Change for Biodiversity Conservation and the National Reserve System: Final Synthesis*. A report prepared for the Department of Sustainability, Environment, Water, Population and Communities, and the Department of Climate Change and Energy Efficiency. CSIRO Climate Adaptation Flagship, Canberra.
- Fenner School of Environment and Society (2012) *Software & datasets*. ANU College of Medicine, Biology & Environment. Australian National University, Canberra.  
<http://fennerschool.anu.edu.au/research/software-datasets>.
- Ferrier S (2002) Mapping spatial pattern in biodiversity for regional conservation planning: where to from here? *Systematic Biology* 51(2), 331–363.
- Ferrier S and Guisan A (2006) Spatial modelling of biodiversity at the community level. *Journal of Applied Ecology* 43(3), 393–404.
- Ferrier S, Drielsma M, Manion G and Watson G (2002) Extended statistical approaches to modelling spatial pattern in biodiversity in north-east New South Wales. II. Community-level modelling. *Biodiversity and Conservation* 11, 2309–2338.
- Ferrier S, Manion G, Elith J and Richardson K (2007) Using generalized dissimilarity modelling to analyse and predict patterns of beta-diversity in regional biodiversity assessment. *Diversity and Distributions* 13(3), 252–264.
- Ferrier S, Powell GVN, Richardson KS, Manion G, Overton JM, Allnutt TF, Cameron SE, Mantle K, Burgess ND, Faith DP, Lamoreux JF, Kier G, Hijmans RJ, Funk VA, Cassis GA, Fisher BL, Flemons P, Lees D, Lovett JC and Van Rompaey RSAR (2004) Mapping more of terrestrial biodiversity for global conservation assessment. *BioScience* 54(12), 1101–1109.
- Gordon HB, Rotstayn LD, McGregor JL, Dix MR, Kowalczyk EA, O'Farrell SP, Waterman LJ, Hirst AC, Wilson SG, Collier MA, Watterson IG and Elliott TI (2002) *The CSIRO Mk3 Climate System Model* [Electronic publication]. CSIRO Atmospheric Research technical paper; no. 60. CSIRO Atmospheric Research. Aspendale. [http://www.dar.csiro.au/publications/gordon\\_2002a.pdf](http://www.dar.csiro.au/publications/gordon_2002a.pdf).

- Harwood T and Williams KJ (2009) CSIRO OzConverter: Edit 0.25° OzClim \*.asc output files. <http://www.csiro.au/products/OzConverter-Software.html>.
- Harwood T, Williams KJ and Ferrier S (2012) *Generation of spatially downscaled climate change predictions for Australia*. CSIRO Climate Adaptation Flagship Working Paper No. 13F. <http://www.csiro.au/en/Organisation-Structure/Flagships/Climate-Adaptation-Flagship/CAF-working-papers.aspx>.
- Houlder DJ, Hutchinson MF, Nix HA and McMahon JP (2000) *ANUCLIM User Guide, Version 5.1*. Centre for Resource and Environmental Studies, Australian National University, Canberra. <http://www.fennerschool.anu.edu.au/publications/software/anuclim.php>.
- House APN, Hilbert DW, Ferrier S, Martin TG, Dunlop M, Harwood T, Williams KJ, Fletcher CS, Murphy H and Gobbett D (2012) *The implications of climate change for biodiversity conservation and the National Reserve System: sclerophyll forests of south-eastern Australia*. CSIRO Climate Adaptation Flagship Working Paper No. 13A. <http://www.csiro.au/en/Organisation-Structure/Flagships/Climate-Adaptation-Flagship/CAF-working-papers.aspx>.
- IPCC (2000) *Emissions Scenarios. Special Report of the Intergovernmental Panel on Climate Change*. Eds. Nakicenovic N and Swart R. Cambridge University Press Cambridge, UK.
- Liedloff AC, Williams RJ, Hilbert DW, Ferrier S, Dunlop M, Harwood T, Williams KJ and Fletcher CS (2012) *The implications of climate change for biodiversity conservation and the National Reserve System: the tropical savanna woodlands and grasslands*. CSIRO Climate Adaptation Flagship Working Paper No. 13B. <http://www.csiro.au/en/Organisation-Structure/Flagships/Climate-Adaptation-Flagship/CAF-working-papers.aspx>.
- Prober SM, Hilbert DW, Ferrier S, Dunlop M, Harwood T, Williams KJ, Fletcher CS and Gobbett D (2012) *The implications of climate change for biodiversity conservation and the National Reserve System: temperate grasslands and grassy woodlands*. CSIRO Climate Adaptation Flagship Working Paper No. 13C. <http://www.csiro.au/en/Organisation-Structure/Flagships/Climate-Adaptation-Flagship/CAF-working-papers.aspx>.
- Smyth AK, Hilbert DW, Ferrier S, Dunlop M, Harwood T, Williams KJ, Fletcher CS and Gobbett D (2012) *The implications of climate change for biodiversity conservation and the National Reserve System: hummock grasslands biome*. CSIRO Climate Adaptation Flagship Working Paper No. 13D. <http://www.csiro.au/en/Organisation-Structure/Flagships/Climate-Adaptation-Flagship/CAF-working-papers.aspx>.
- Suppiah R, Hennessy KJ, Whetton PH, McInnes K, Macadam I, Bathols J, Ricketts J and Page CJ (2007) Australian Climate change projections derived from simulations performed for the IPCC 4th Assessment Report. *Australian Meteorological Magazine* 56(3), 131–152.
- Williams JW, Jackson ST and Kutzbach JE (2007) Projected distributions of novel and disappearing climates by 2100 AD. *PNAS* 104, 5738–5742.
- Williams KJ, Belbin L, Austin MP, Stein J and Ferrier S (2012) Which environmental variables should I use in my biodiversity model? *International Journal of Geographic Information Sciences* 26(11), 2009–2047.
- Williams KJ, Ferrier S, Rosauer D, Yeates D, Manion G, Harwood T, Stein J, Faith DP, Laity T and Whalen A (2010) *Harnessing continent-wide biodiversity datasets for prioritising national conservation investment*. A report to the Department of Environment, Water, Heritage and the Arts. CSIRO, Canberra.

# Appendix A GDM models used in the NRS2 project

This project employed a set of GDM models already derived for the Australian continent by a separate (then) DEWHA-funded Caring for Our Country Open Grants project performed by CSIRO in collaboration with DEWHA and the ANU Fenner School of Environment and Society. The following description of these models is adapted from material presented in the report for the Caring for Our Country project (Williams et al. 2010). Readers interested in further detail are encouraged to access the full report.

## A.1 Biological data

### A.1.1 ANHAT DATABASE

Biological data for GDM analysis were derived in July 2009 from the Australian Natural Heritage Assessment Tool (ANHAT) Database (Department of Sustainability, Environment, Water, Population and Communities 2012). ANHAT compiled over 32 million records on locations where species were observed or collected in Australia. The records are managed by a wide range of institutions and individuals. All species information used in ANHAT is checked to ensure it refers to a valid species by its currently accepted name.

### A.1.2 DATA FILTERING

Biological data often contain significant errors of location and taxonomic identification. Some of these errors were addressed by custodians before data were incorporated into ANHAT. We also developed additional filters for inclusion/exclusion of records to improve data quality based on georeference precision, where known, and to exclude exotic or marine taxa from the analysis of terrestrial biodiversity, with some exceptions, as follows:

- Species classified as marine/aquatic were excluded (i.e. `terrestrialmarine=2`).
- Exotic species – weeds and ferals – were excluded.
- Undefined species names at the genus level ‘sp.’ were excluded (i.e. `taxonlevelid <= 2`).
- Taxon levels below species (e.g. subspecies, infraspecies, variety) were ignored by grouping at the species level.

The resulting number of records, sites summarised within grid cells, and species in each of the biological groups used in the NRS2 project are summarised in Table 1.

Additional filters were developed for spatial precision by reviewing the spread of data in IBRA bioregions and classes of spatial precision (i.e. +/- radius from a point of 1–1000 m, 1001–2000 m, 2001–5000 m, 5001–10,000 m, 10,001–20,000 m, null or 0). Although a reasonable upper limit of spatial precision for the analysis of 1000 m<sup>2</sup> grid cells (0.01 geographic degrees) would be around 1000 m, it was necessary to accept all available data for some biological groups in sparsely sampled regions (Table 2). In this case an upper limit of 20,000 m was used. The resulting numbers of records for GDM analysis are listed in Table 2 by biological group in contrast with the unfiltered number of records in Table 1. The geographic pattern of sites within each bioregion for each biological group for GDM analysis is presented in Figures A.1–A.6. Sites for some groups are dominated by ‘singletons’ where only one species has been recorded (Table 1). In all cases, data are more intensely collected near human population centres and along accessible roads.

For GDM analysis, sites were summarised within 0.01 geographic degrees of latitude and longitude (grid cells). Species recorded multiple times within a grid cell (including with different sub-taxa) were represented by a single record.

**Apx Table A.1 Summary of ANHAT data available for the biological groups used in the NRS2 project**

TARGET TAXA GROUP	UNFILTERED*			#SPECIES	FILTERED	
	# SPECIES	# SITES†	# RECORDS: SPECIES BY SITES†		#SITES† WITH SINGLE SPECIES	TOTAL #SITES†
Vascular plants	12,881	465,592	2,995,841	12,660	152,803	374,640
Mammals	298	134,989	331,890	294	53,265	100,369
Birds	690	257,544	4,046,352	673	63,456	242,814
Reptiles	819	104,642	312,437	805	41,131	83,661
Frogs	218	54,852	135,617	218	53,077	100,143
Land Snails	2,774	20,321	52,715	2,550	10,173	19,118

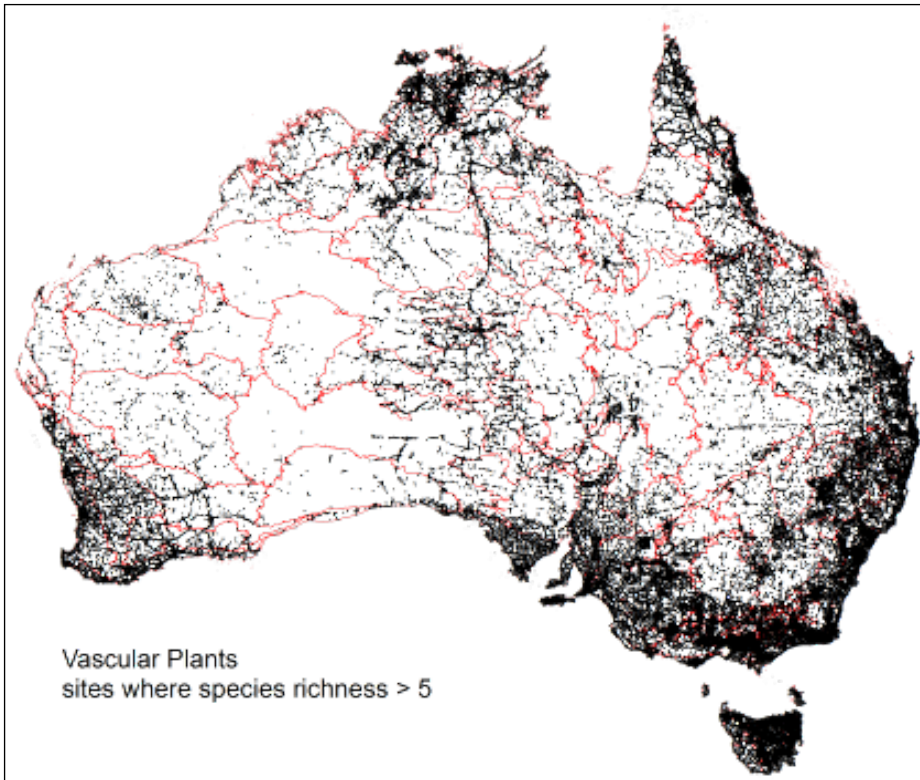
\* Unfiltered numbers based on SQL queries for all records with precision ≤ 20,000 or null, species-level taxon, excluding undefined species labelled 'sp.', not marine

† sites are 0.01° geographic grid cells

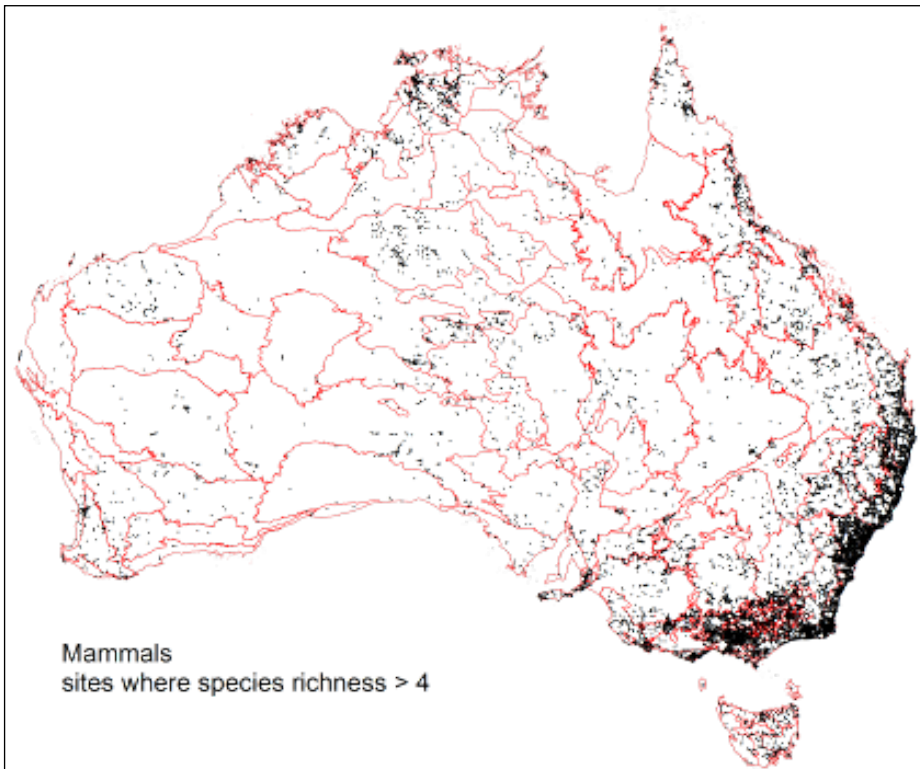
**Apx Table A.2 Filters used to customise queries by spatial precision and IBRA region for each biological group**

TARGET BIOLOGICAL GROUP	BROAD DESCRIPTION OF FILTER	RECORDS†	% RECORDS EXTRACTED
Vascular plants	Customise by region, set precision limits, mostly ≤2000 m, drop null in some cases	2,340,886	78.1
Mammals	Customise by region, set precision limits, mostly ≤1000 m or ≤5000 m with null, drop null in some cases	257,510	77.6
Birds	Use precision ≤5000 m and null	3,912,192	96.7
Reptiles	Use precision ≤2000 m and null, drop null in selected regions dominated by precise records (consider using precision ≤5000 m with null as there may be many imprecise null records)	249,169	79.8
Frogs	Many regions could be sampled with 5000 m precision, and some with 2000 m precision or better, with scope to drop null in a few cases where sampling density is very high	115,175	84.9
Land snails	many regions could be sampled with precision ≤10,000 m and null, and in some regions ≤20,000 m and null, or ≤5000 m and null	50,749	96.3

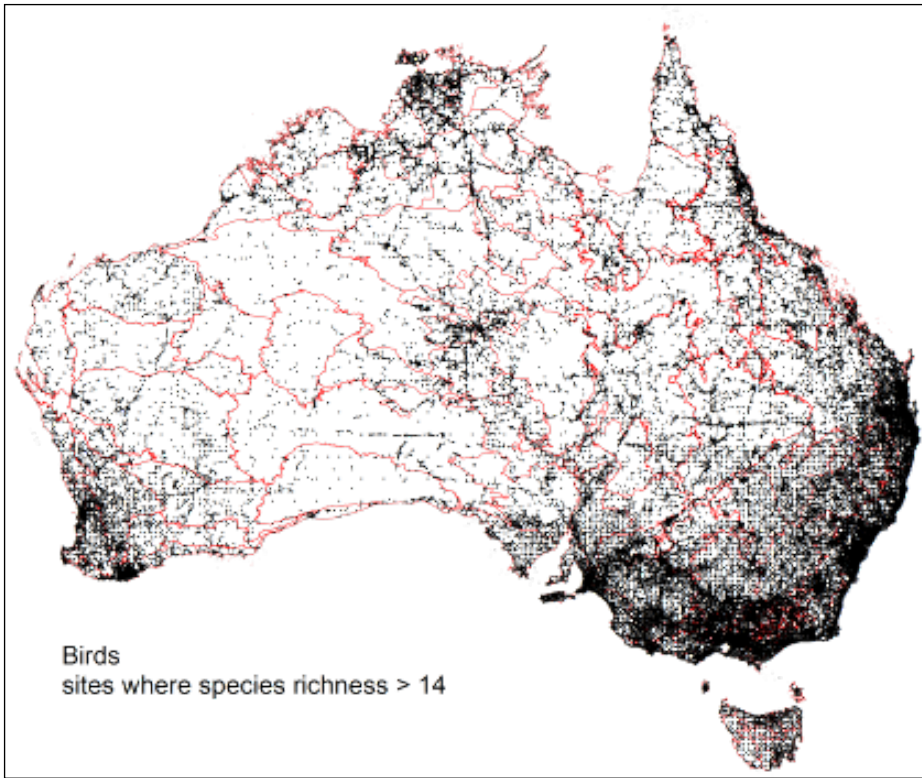
\* records are combinations of sites (0.01° grid cells) by species



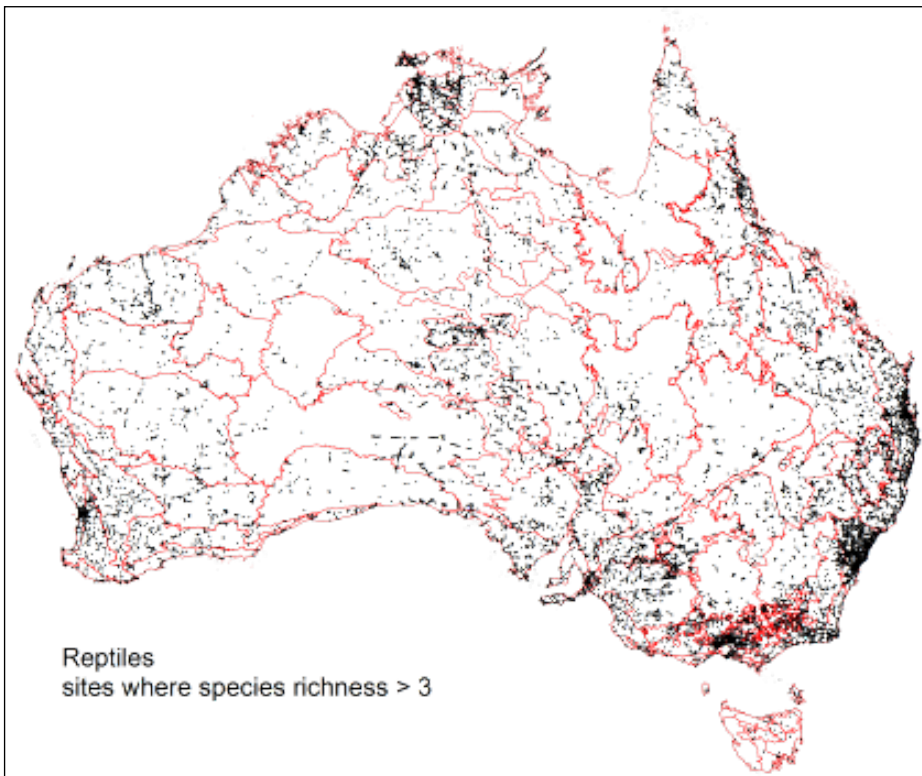
Apx Figure A.1 Location of vascular plant sites (0.01° grids) used for GDM analysis showing bioregion boundaries (IBRA 6.1)



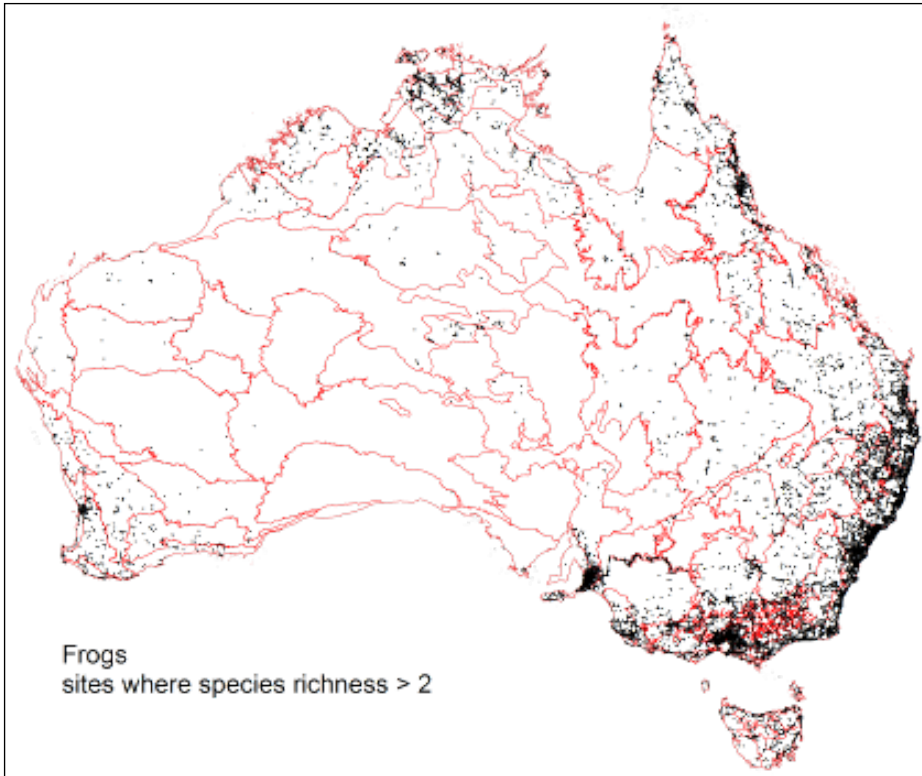
Apx Figure A.2: Location of mammal sites (0.01° grids) used for GDM analysis showing bioregion boundaries (IBRA 6.1)



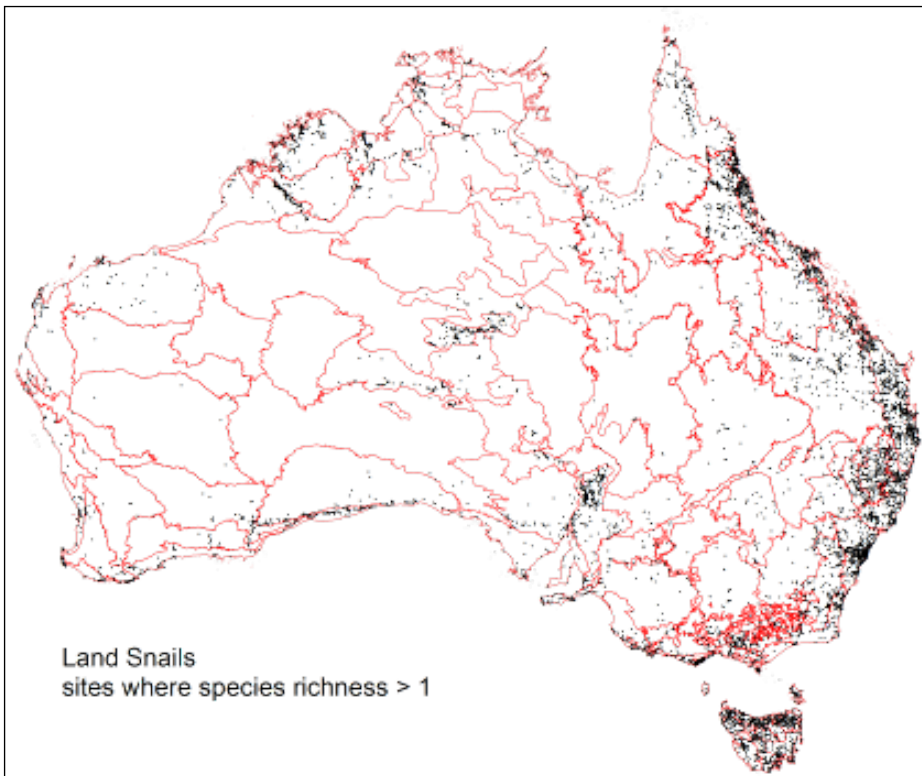
Apx Figure A.3 Location of birds sites (0.01° grids) used for GDM analysis showing bioregion boundaries (IBRA 6.1)



Apx Figure A.4 Location of reptile sites (0.01° grids) used for GDM analysis showing bioregion boundaries (IBRA 6.1)



**Apx Figure A.5 Location of frog sites (0.01° grids) used for GDM analysis showing bioregion boundaries (IBRA 6.1)**



**Apx Figure A.6 Location of land snail sites (0.01° grids) used for GDM analysis showing bioregion boundaries (IBRA 6.1)**

### A.1.3 UNDER-SAMPLING COVARIATES

False absences of species in sampled sites, resulting from incomplete sampling of those cells, may result in inflated estimates of compositional dissimilarity between sites. We addressed this effect through inclusion of a measure of under-sampling as a covariate predictor in the GDM models. For each taxonomic group the number of species recorded in each grid cell was treated as an approximate indicator of the sampling effort expended within that cell. For each biological group the under-sampling covariate was calculated as the normalised inverse of the logarithm of number of species recorded:

$$-1 \times \left[ \frac{1}{\max(\log_{10}(spp + 1))} \right] \times \log_{10}(spp + 1) + 1$$

where *spp* is the number of species recorded in the 0.01° grid cell.

## A.2 Environmental predictors

As part of the Caring for Our Country project an existing set of 54 climate, soil and terrain predictor variables (compiled by Janet Stein, ANU Fenner School) was expanded significantly to include a number of new soil attributes; new climatic variables relating to rainfall seasonality, relative humidity, and water balance; and a suite of biotic attributes derived from NVIS vegetation mapping. In total 74 abiotic and 26 biotic variables were assembled, at 1 km<sup>2</sup> grid resolution for the entire continent, and covering most of the major known environmental drivers of distribution patterns in terrestrial biodiversity. These variables are listed in Tables 3, 4 and 5 below. For further details see Williams et al. (2010) and Williams et al. (2012).

**Apx Table A.3 Substrate and terrain attributes**

ATTRIBUTE (PREDICTOR)	DESCRIPTION
DATASUPT	Data levels supporting soil property interpretations (index)
SOLDEPTH	Solum depth (surface and subsoil layers) (metres)
SOLPAWHC	Plant-available soil water holding capacity (mm)
LOGKSAT	Solum average median horizon saturated hydraulic conductivity (mm/h), log <sub>10</sub> transformed
CALCRETE	Calcrete in or below soil profile (presence)
PEDALITY	Grade of soil pedal structure (grade)
CLAY	Solum average median clay content (%)
NUTRIENTS	Gross nutrient status (rating)
CORG0	Pre-European estimate of mean annual store of soil organic carbon (COrg0.Base) (kgC ha <sup>-1</sup> )
NMNL0	Pre-European estimate of mean annual store of mineral nitrogen (NMnl0.Base) (kgN ha <sup>-1</sup> )
NMNLCONC0	Pre-European estimate of mean annual concentration of mineral nitrogen in soil water (NMnlConc0.Base) (mgN kgH <sub>2</sub> O <sup>-1</sup> )
NTOT0	Pre-European estimate of mean annual store of total plant-available soil nitrogen (NTot0.Base) (kgN ha <sup>-1</sup> )
PMNL0	Pre-European estimate of mean annual store of plant-available mineral phosphorus (PMnl0.Base) (kgP ha <sup>-1</sup> )
PMNLCONC0	Pre-European estimate of mean annual concentration of dissolved phosphorus in soil water (PMnlConc0.Base) (mgP kgH <sub>2</sub> O <sup>-1</sup> )
PTOT0	Pre-European estimate of mean annual store of total plant-available soil phosphorus (PTot0.Base) (kgP ha <sup>-1</sup> )
FERT	Inherent rock fertility (rating)
GEOLLMEANAGE	Geological age (log <sub>10</sub> ) mean (Log <sub>10</sub> M years)
GEOLLRNGEAGE	Geological age (log <sub>10</sub> ) range (Log <sub>10</sub> M years)
GRAVITY	Bouguer gravity anomalies (acceleration, Gal)
MAGNETICS	Magnetic anomalies (nanoTesla, nT)
SLOPE	Terrain slope (%)
RELIEF	Terrain relief (metres)

ATTRIBUTE (PREDICTOR)	DESCRIPTION
ROUGHNESS	Terrain roughness (%)
TWI	Topographic wetness index (index)
MRVBF	Valley Bottom Flatness (index)
MRRTF	Ridgetop Flatness (index)
VALLEYBOTTOM	Proportion Valley bottoms (%)
RIDGETOPFLAT	Proportion Ridge tops (%)
EROSIONAL	Proportion Erosional surfaces (%)
DISTNONPERMW	Weighted distance to non-permanent water features (index)
DISTPERMWAT	Weighted distance to permanent water features (index)
DISTANYWATER	Weighted distance to any water features (index)

**Apx Table A.4 Climate attributes**

ATTRIBUTE (PREDICTOR)	DESCRIPTION
C4GI	Mean annual growth index C <sub>4</sub> megatherm plants
MEGAGI	Mean annual growth index C <sub>3</sub> macrotherm plants
MESOGI	Mean annual growth index C <sub>3</sub> mesotherm plants
MICROGI	Mean annual growth index C <sub>3</sub> microtherm plants
RHU215_I	Minimum month relative humidity at 3pm (%)
RHU215_X	Maximum month relative humidity at 3pm (%)
ADEFI	Maximum month precipitation deficit (mm)
ADEFX	Minimum month precipitation deficit (mm)
ARID_MAX	Minimum month aridity index
ARID_MIN	Maximum month aridity index
EVAPI	Minimum month evaporation (mm)
EVAPX	Maximum month evaporation (mm)
RAINI	Precipitation of the driest month (mm)
RAINX	Precipitation of the wettest month (mm)
RPREC_MAX	Greatest rainfall difference between successive months (mm/day)
RPREC_MIN	Least rainfall difference between successive months (mm/day)
SRAIN0	Annual rainfall seasonality index
SRAIN1	Summer or winter rainfall season
SRAIN2	Spring or autumn rainfall season
EAE0_MAX	Maximum month crop factor
EAE0_MIN	Minimum month crop factor
PWAT_MAX	Maximum month soil water stress index (%)
PWAT_MIN	Minimum month soil water stress index (%)
SPLS_MAX	Maximum month soil water surplus (mm)
SPLS_MIN	Minimum month soil water surplus (mm)
WDEF_MAX	Maximum month soil water deficit (mm)
WDEF_MIN	Minimum month soil water deficit (mm)
WPOT_MAX	Maximum month soil water potential (MPa)
WPOT_MIN	Minimum month soil water potential (MPa)
RADNI	Minimum month rainfall-modified solar radiation (MJ/m <sup>2</sup> /day)
RADNX	Maximum month rainfall-modified solar radiation (MJ/m <sup>2</sup> /day)
MAXTI	Maximum temperature coolest month (°C)
MAXTX	Maximum temperature hottest month (°C)
MINTI	Minimum temperature coldest month (°C)
MINTX	Minimum temperature warmest month (°C)
RTIMAX	Maximum difference in minimum temperatures (°C/day)

ATTRIBUTE (PREDICTOR)	DESCRIPTION
RTIMIN	Minimum difference in minimum temperatures (°C/day)
RTXMAX	Maximum difference in maximum temperatures (°C/day)
RTXMIN	Minimum difference in maximum temperatures (°C/day)
TRNGA	Annual Range Temperature (°C)
TRNGI	Minimum month diurnal temperature range (°C)
TRNGX	Maximum month diurnal temperature range (°C)

**Apx Table A.5 Vegetation attributes**

VEGETATION ATTRIBUTE	DESCRIPTION
Median Height (MVS31_HTMF)	The median height in metres of the tallest stratum (U, M, G) derived from the indicative height range implied by the description
Range Height (MVS31_HTRF)	The height range in metres of the tallest stratum (U, M, G) derived from the height range implied by the description
Cover Median (MVS31_CCMF)	The median canopy cover in percent of the tallest stratum (U, M, G) derived from the indicative canopy cover range for the description
Cover Range (MVS31_CCRF)	The canopy cover range in percent of the tallest stratum (U, M, G) derived from the canopy cover range implied by the description
Eucalypt-dominated (MVS31_EUCF)	The presence of eucalypts (=1) as a dominant or characteristic of the tallest stratum
Acacia-dominated (MVS31_ACAF)	The presence of acacia (=1) as a dominant or characteristic of the tallest stratum
Banksia and undefined heath or shrub lands (MVS31_BKAF)	The likely presence of banksia or other undefined heath or shrubland (=1) as a dominant or characteristic of the tallest stratum (NVIS ID: 16, 30, 32, 50, 97)
Other Myrtaceae (MVS31_MYRF)	The likely presence of Melaleuca or Leptospermum (=1) as a dominant or characteristic of the tallest stratum
Grassy2 (MVS31_GS2F)	The presence of grasses (=1) other than tussock and hummock grasses, as a dominant feature or characteristic of the ground stratum
Grassy (MVS31_GSYF)	The presence of grasses (=1) including tussock and hummock grasses, as a dominant feature or characteristic of the ground stratum
Shrubby (MVS31_SBYF)	The presence of shrubs (=1) as a dominant feature or characteristic of the middle stratum
Tussocky (MVS31_TSYF)	The presence of tussock grasses (=1) as a dominant feature or characteristic of the ground stratum
Hummocky (MVS31_HMYF)	The presence of hummock grasses (=1) as a dominant feature or characteristic of the ground stratum
Rainforest (MVS31_RFTF)	The presence of rainforest or wet forest (=1) as a dominant feature or characteristic of the tallest stratum
Chenopods (MVS31_CPDF)	The presence of chenopods or samphire (=1) as a dominant feature or characteristic of the middle or ground stratum
Bare (MVS31_BREF)	The presence of bare rock, sand, mudflats, salt lakes, or alpine fjeldmark (=1) as a dominant feature or characteristic of the ground stratum
Saline (MVS31_SLEF)	The presence of saline habitats (=1) including salt marshes, mangroves and estuarine areas as a dominant feature or characteristic of the ground stratum
Freshwater aquatic (MVS31_AQAF)	The presence of freshwater habitats (=1) including lakes, wetlands and marshes as a dominant feature or characteristic of the ground stratum
Vegetation structure index (MVS31_XX1F)	A multiplicative combination of vegetation height and cover variables (Median Height x Median Cover)
Vegetation formation complexity (MVS31_XX2F)	An additive combination of vegetation 'presence' attributes: eucalypt-dominated + acacia-dominated + banksia + grassy2 + shrubby + tussocky + hummocky + rainforest + chenopods + bare + saline + freshwater aquatic
Vegetation complexity (MVS31SO)	Vegetation complexity from tropical rainforest (=1) to arid grasslands (=60), based on the variable sort order defined for the pre-European major vegetation subgroups in NVIS 3.1

## A.3 Fitted models

GDM models were fitted to the biological and environmental data described above using a stepwise variable selection strategy, detailed in Williams et al. (2010). Table 6 gives the sum of the fitted coefficients for each environmental predictor included in the resulting model for each biological group. These values indicate the relative importance of each predictor in ‘explaining’ patterns of community composition in the group concerned; see Williams et al. (2010) for details.

**Apx Table A.6 Predictor variables and summed fitted coefficients for final models for each taxa group**

PREDICTOR VARIABLE	BIRDS	FROGS	MAMMALS	PLANTS	REPTILES	SNAILS
RADNI	0.44	1.69	0.77	1.92	2.59	2.75
SRAIN1		3.55	0.64	4.99	0.74	3.26
RTIMIN		0.59	0.38	1.26	0.27	0.97
MESOGI		1.27	0.51	0.94	0.38	2.62
DISTPERMWAT	0.27	2.02	0.44		0.48	1.46
RPRECMAX	0.91	1.28	0.39	3.67	3.91	1.04
MICROGI	0.34	1.00		1.55	0.60	
RADNX		0.62	1.14	1.81	0.86	1.46
RPRECMIN	0.51	1.19	0.38	1.17		0.85
PEDALITY	0.23		0.47	0.86	0.22	0.71
MAGNETICS			1.21	2.18	1.44	
MEGAGI			0.61	1.41		
SRAIN2	0.42				0.23	1.78
MAXTX	0.28		0.35	0.99	1.52	0.95
GRAVITY		0.51		1.27	0.64	0.97
MINTI	0.36	0.33	0.28			1.64
ADEFI	0.38			0.86	0.48	0.72
RELIEF		0.29	0.36			0.71
MINTX				0.89		0.85
NMNLCONCO	0.17					1.02
PWAT_MIN	0.22		0.24		0.99	
RTXMAX	0.15	0.22		0.69	0.25	
DISTNONPERMW			0.86			
RAINI				0.63		1.12
GEOLLRNGEAGE				0.95	0.23	0.55
C4GI	0.54	0.46			0.63	
NMNLO		0.43			0.50	0.57
EVAPX			0.67			
PMNLO	0.29		0.49			
SOLDEPTH		0.29				0.85
RHU215_I		0.39				
LOGKSAT				0.53	0.23	
RTIMAX	0.19				0.34	
FERT			0.29			
MAXTI			0.65	1.38		
ROUGHNESS	0.45			0.78		
EVAPI		0.57				
PTOTO			0.39			

PREDICTOR VARIABLE	BIRDS	FROGS	MAMMALS	PLANTS	REPTILES	SNAILS
SLOPE		0.51				
ADEFX	0.17				0.23	
SCOVARMAMMS			1.49			
SCOVARSNAILS						1.42
SCOVARREPTS					0.82	
RAINX				0.73		
TRNGA			0.68			
SCOVARBIRDS	0.57					
WDEF_MIN				0.55		
NTOTO		0.44				
SCOVARFROGS		0.33				
MRVBF	0.24					
SCOVARDRAGS						
MVS31_XX2F		0.20				
CLAY	0.17					
TRNGX	0.15					



#### CONTACT US

**t** 1300 363 400  
+61 3 9545 2176  
**e** [enquiries@csiro.au](mailto:enquiries@csiro.au)  
**w** [www.csiro.au](http://www.csiro.au)

#### YOUR CSIRO

Australia is founding its future on science and innovation. Its national science agency, CSIRO, is a powerhouse of ideas, technologies and skills for building prosperity, growth, health and sustainability. It serves governments, industries, business and communities across the nation.

#### FOR FURTHER INFORMATION

**Ecosystem Sciences**  
Simon Ferrier  
**t** +61 2 6246 4191  
**e** [simon.ferrier@csiro.au](mailto:simon.ferrier@csiro.au)  
**w** [www.csiro.au/people/Simon.Ferrier](http://www.csiro.au/people/Simon.Ferrier)